First Measurement of Muon Neutrino Charged Current Quasielastic (CCQE) Double Differential Cross Section

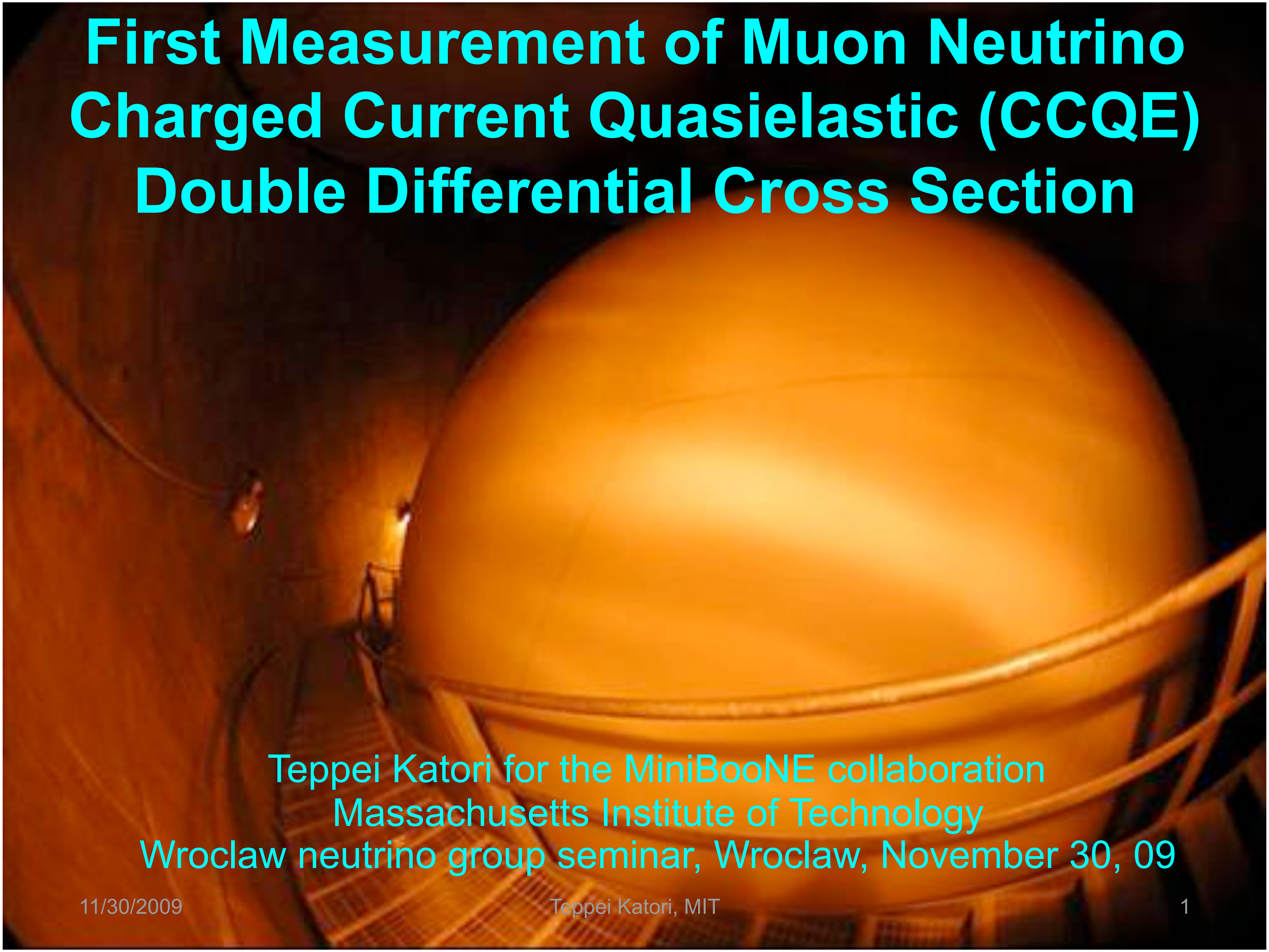

Teppei Katori for the MiniBooNE collaboration
Massachusetts Institute of Technology
Wroclaw neutrino group seminar, Wroclaw, November 30, 09

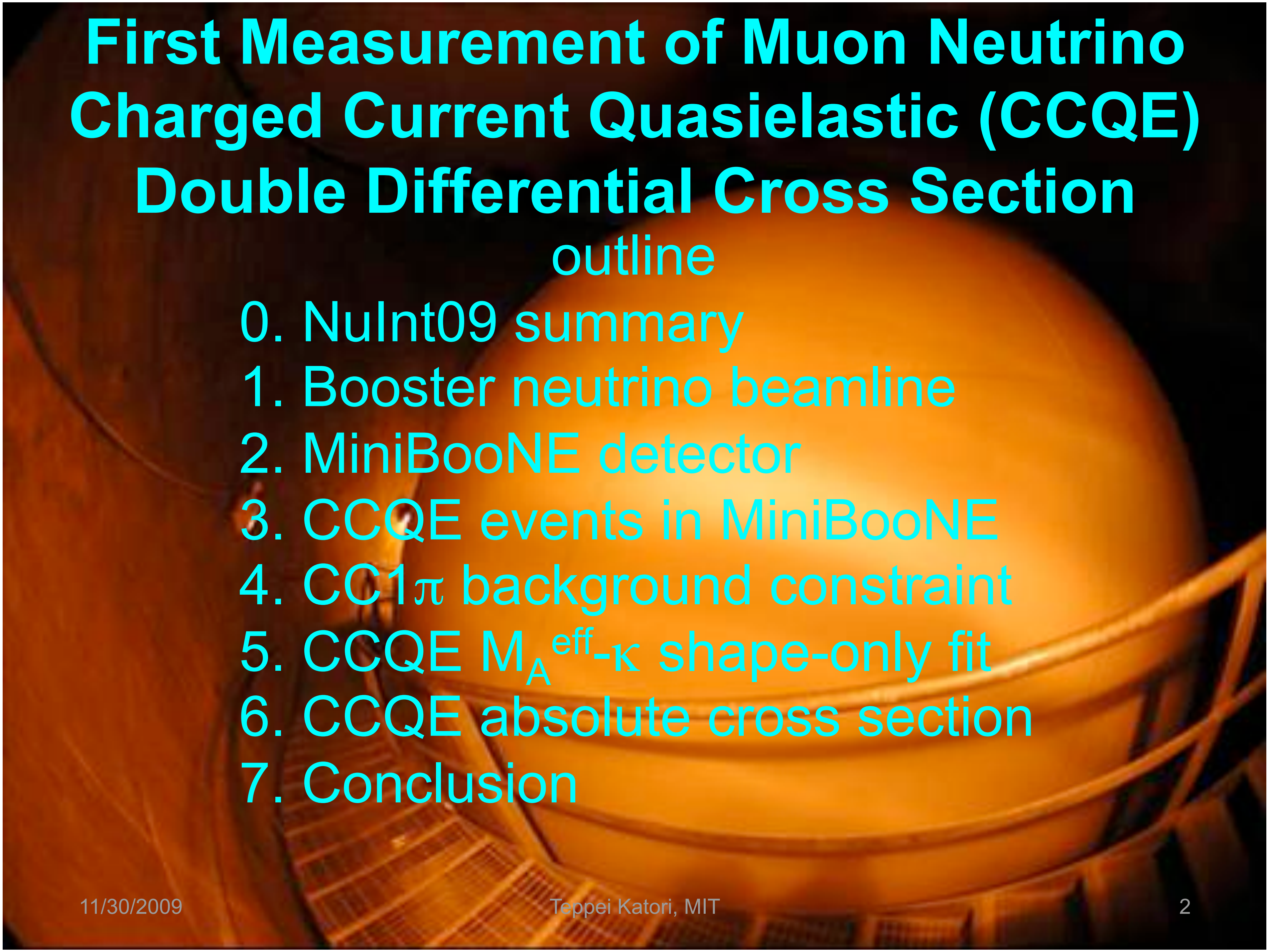

First Measurement of Muon Neutrino Charged Current Quasielastic (CCQE) Double Differential Cross Section

outline

0. NuInt09 summary
1. Booster neutrino beamline
2. MiniBooNE detector
3. CCQE events in MiniBooNE
4. CC1π background constraint
5. CCQE M_A^{eff}-κ shape-only fit
6. CCQE absolute cross section
7. Conclusion

0. NuInt09 summary

NuInt09, May18-22, 2009, Sitges, Spain
This talk is based on the discussions and results presented in NuInt09.

NuInt09 MiniBooNE results
In NuInt09, MiniBooNE had 6 talks and 2 posters

1. charged current quasielastic (CCQE) cross section measurement
   by Teppei Katori
2. neutral current elastic (NCE) cross section measurement
   by Denis Perevalov
3. neutral current π^o production (NCπ^o) cross section measurement (ν and anti-ν)
   by Colin Anderson
4. charged current single pion production (CCπ^+) cross section measurement
   by Mike Wilking
5. charged current single π^o production (CCπ^o) measurement
   by Bob Nelson
6. improved CC1π^+ simulation in NUANCE generator
   by Jarek Novak
7. CCπ^+/CCQE cross section ratio measurement
   by Steve Linden
8. anti-νCCQE measurement
   by Joe Grange

by Teppei Katori

0-1. CCQE cross section in MiniBooNE

Flux-averaged double differential cross section

I will discuss the great detail in this talk later. The main conclusion was,

1. the first measurement of double differential cross section
2. ~30% higher absolute cross section from the recent NOMAD result

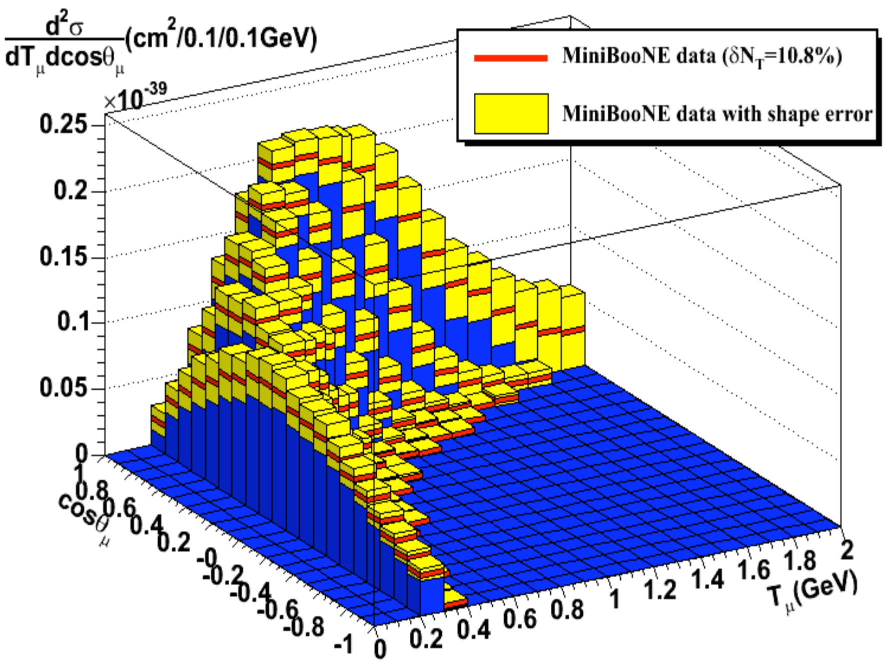

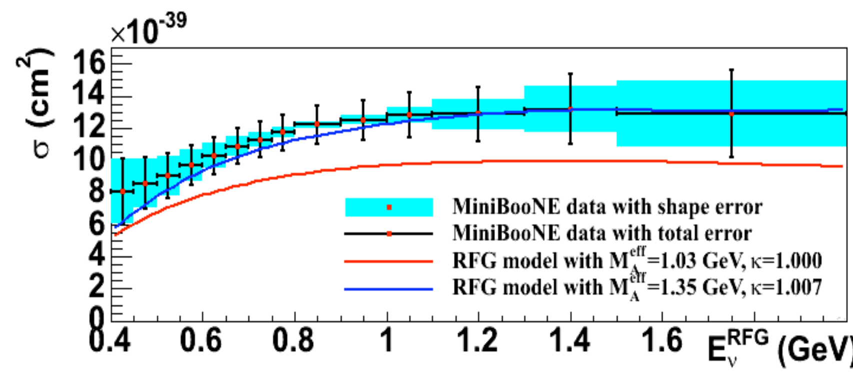

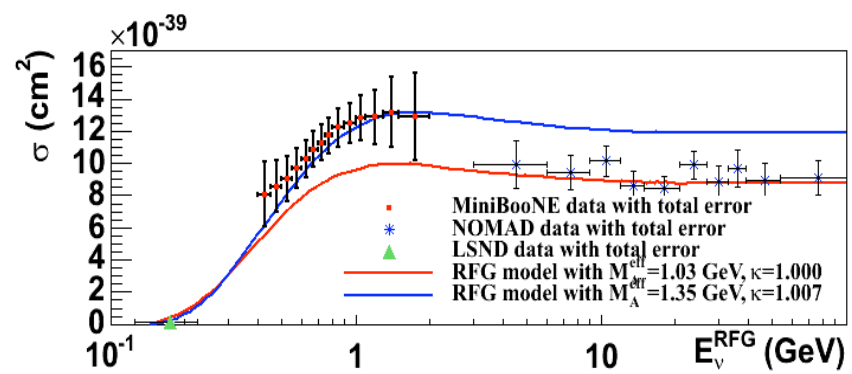

by Denis Perevalov

0-2. NCE cross section in MiniBooNE

$$\nu_\mu + p \rightarrow \nu_\mu + p$$

$$\nu_\mu + n \rightarrow \nu_\mu + n$$

NCE measurement and Δs

By definition, longitudinally polarized quark functions are normalized with axial vector nucleon matrix element.

$$\int_0^1 dx < N | \bar{u}\gamma_\mu\gamma_5 u - \bar{d}\gamma_\mu\gamma_5 d - \bar{s}\gamma_\mu\gamma_5 s | N > = < N | -G_A(Q^2)\gamma_\mu\gamma_5\tau_3 + G_A^s(Q^2)\gamma_\mu\gamma_5 | N >$$

Then, strange quark spin contribution in the nucleon (called Δs) gives simple connection of DIS and elastic scattering world.

$$\int_0^1 dx \Delta s(x) \equiv \Delta s \equiv G_A^s(Q^2 = 0)$$

Since Δs is the Q^2=0 limit of isoscalar axial vector form factor, it can be accessed by NCE scattering measurement.

However, measured Δs in HERMES semi-inclusive DIS measurement (~0) and BNLE734 neutrino NCE measurement (~0.15) don't agree within their errors (so there is a great interest for the precise NCE measurement!).

by Denis Perevalov

0-2. NCE cross section in MiniBooNE

Proton fitter

NCE proton track energy/position/direction are measured by minimizing the charge and time likelihood made from each PMT response. the proton fitter based on the proton scintillation and Cerenkov light profile. This fitter is especially powerful when proton exceeds the Cerenkov threshold (Δx~0.7m, $\Delta\theta$~20^{o}, ΔKE~25%).

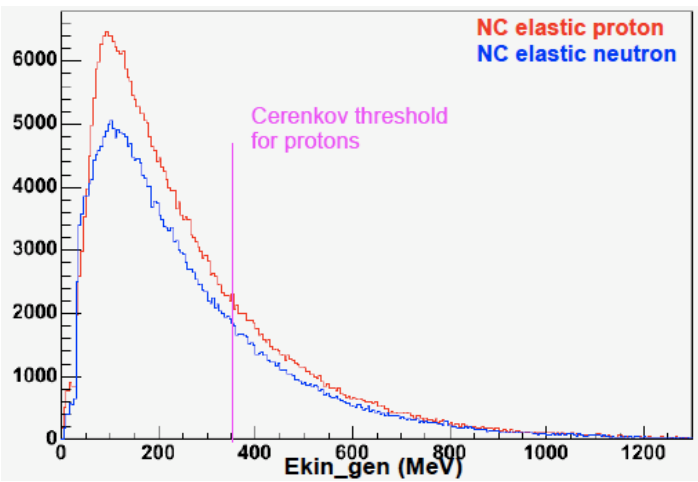

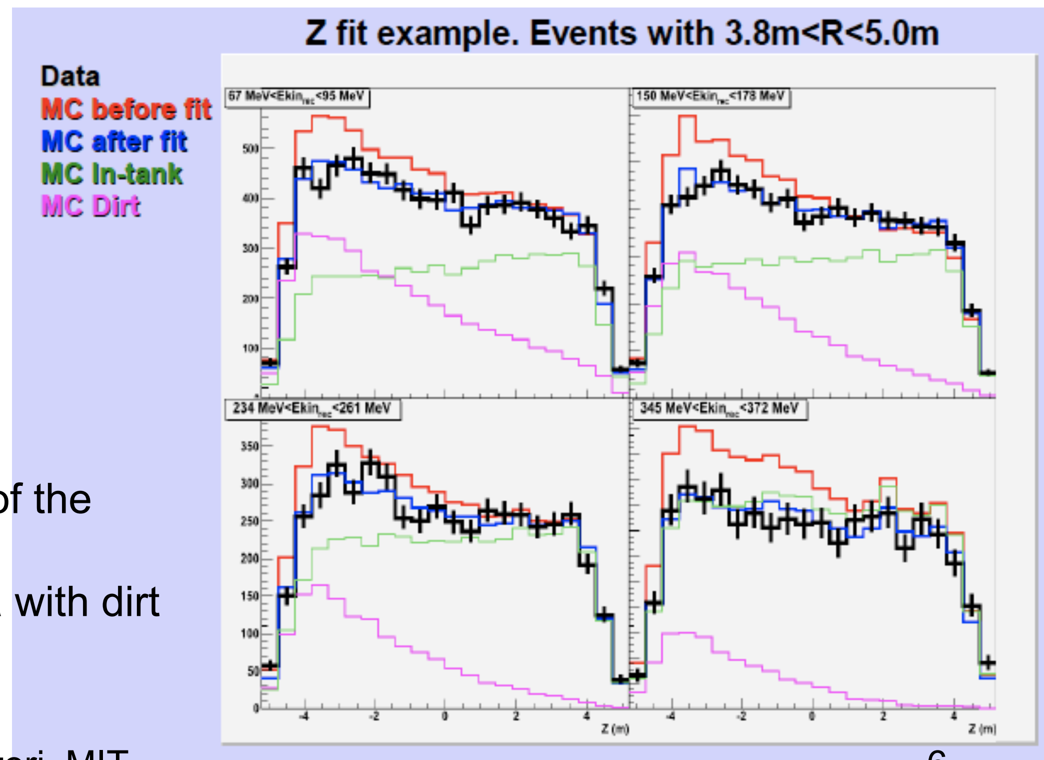

Dirt event constraint

Modeling the neutrino interaction outside of the detector (dirt event) is hard. The dirt event distributions are constrained from the data with dirt enriched sample (~10% error).

by Denis Perevalov

0-2. NCE cross section in MiniBooNE

Flux-averaged NCE p+n differential cross section

Measured cross section agree with BNLE734.

Intrinsic background prediction is also provided.

NCE data also prefer a controversial high M_A value.

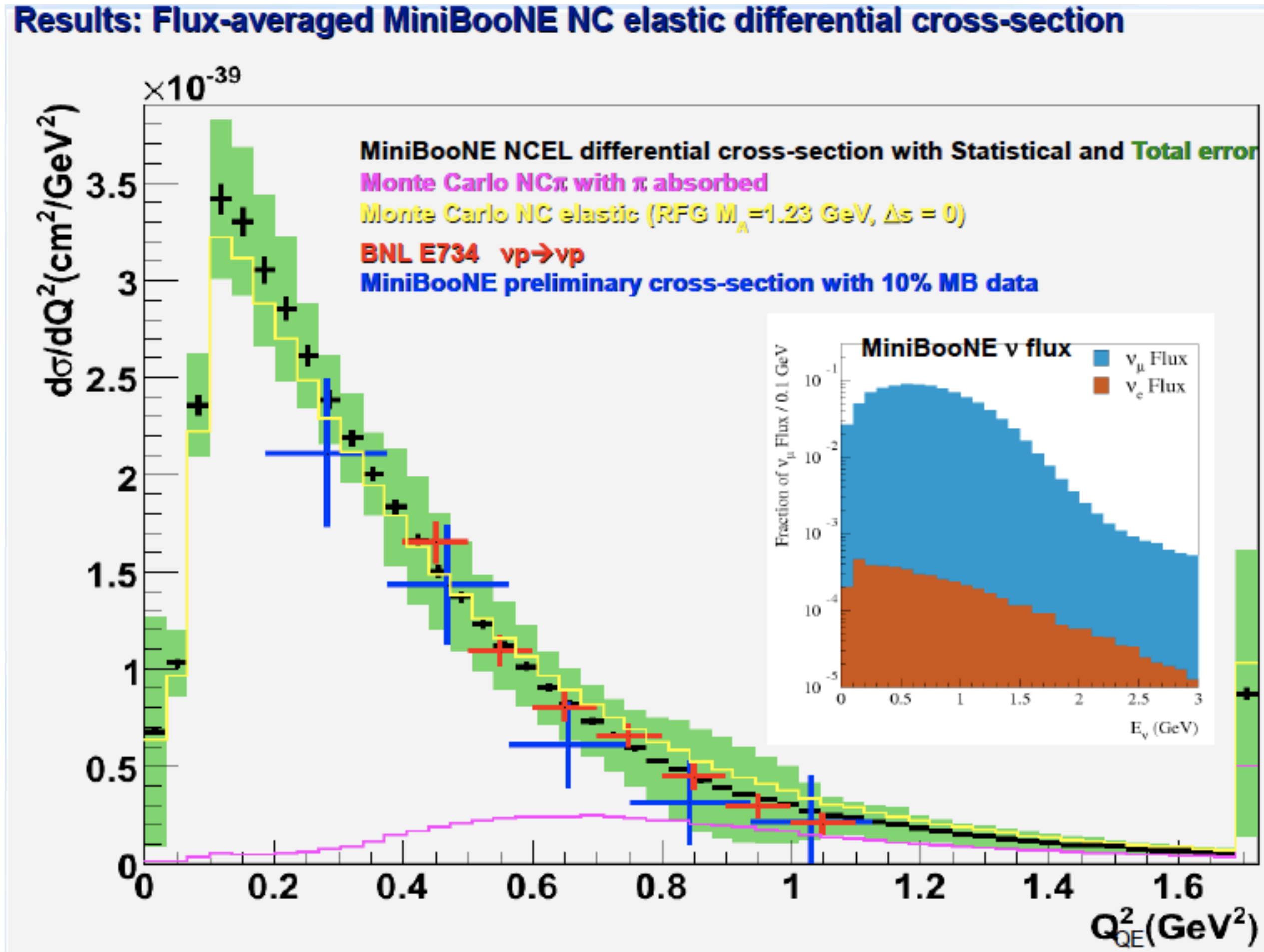

by Denis Perevalov

0-2. NCE cross section in MiniBooNE

NCE proton exclusive measurement

To measure Δs we need a exclusive measurement of NCE proton scattering. The separation is only possible at high energy (above proton Cerenkov threshold).

This is an ongoing analysis.

Reconstructed proton angle

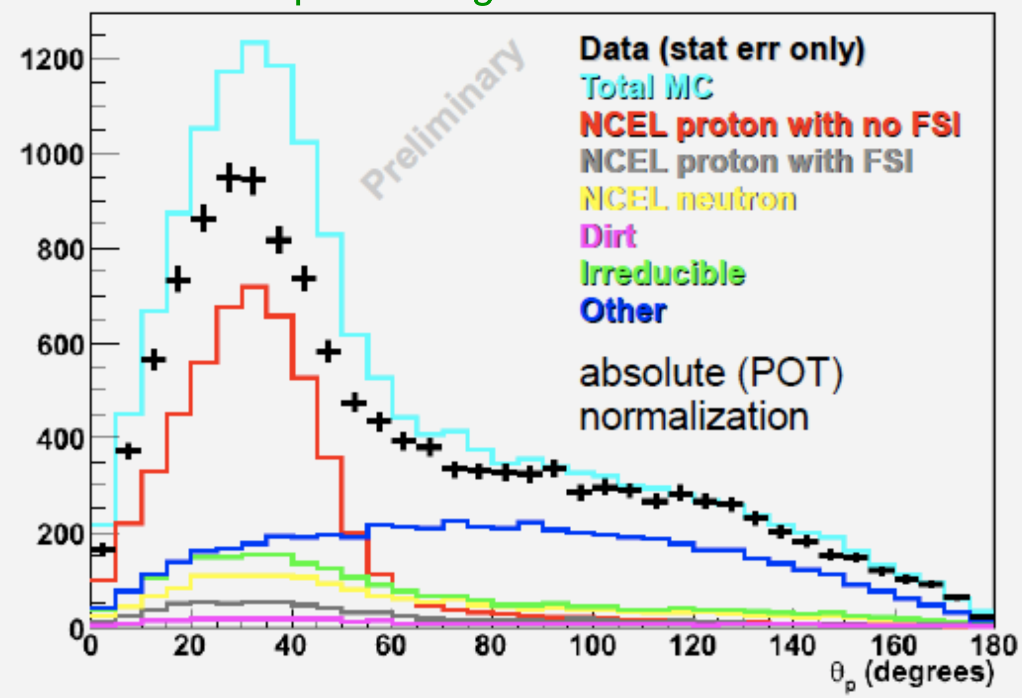

by Colin Anderson

0-3. NCπ^o cross section in MiniBooNE

MiniBooNE collaboration, arXiv:0911.2063

$$\nu_\mu + N \rightarrow \nu_\mu + \Delta^o \rightarrow \nu_\mu + N + \pi^o$$
$$\nu_\mu + A \rightarrow \nu_\mu + A + \pi^o$$

NCπ^o event definition

All pion production channel need to be defined from it's final state. NCπ^o event is defined as NC interaction resulting with one π^o exiting nuclei and no other mesons. Clearly,

- This definition includes π^o production by final state interactions (FSIs).
- This definition excludes NCπ^o interaction when π^o is lost by FSIs.

This is the necessary definition for the theorists to understand final state interactions (FSIs) without biases.

Measurement is done both ν and anti-ν mode.

	Events Passing Cuts	Purity	Efficiency
Neutrino Mode	21542 w/ 6.461E20 POT Data/MC = 1.10	73%	36%
Antineutrino Mode	2305 w/ 3.386E20 POT Data/MC = 0.94	58%	36%

by Colin Anderson

0-3. NCπ^o cross section in MiniBooNE

NCπ^o differential cross section

Unfolding is carefully studied. Different techniques (Tikhonov regularization and iterative Bayesian method) are used depending on the biases of unfolding. Inverse response matrix method is never used.

This is the first measurement of NCπ^o production differential cross section.

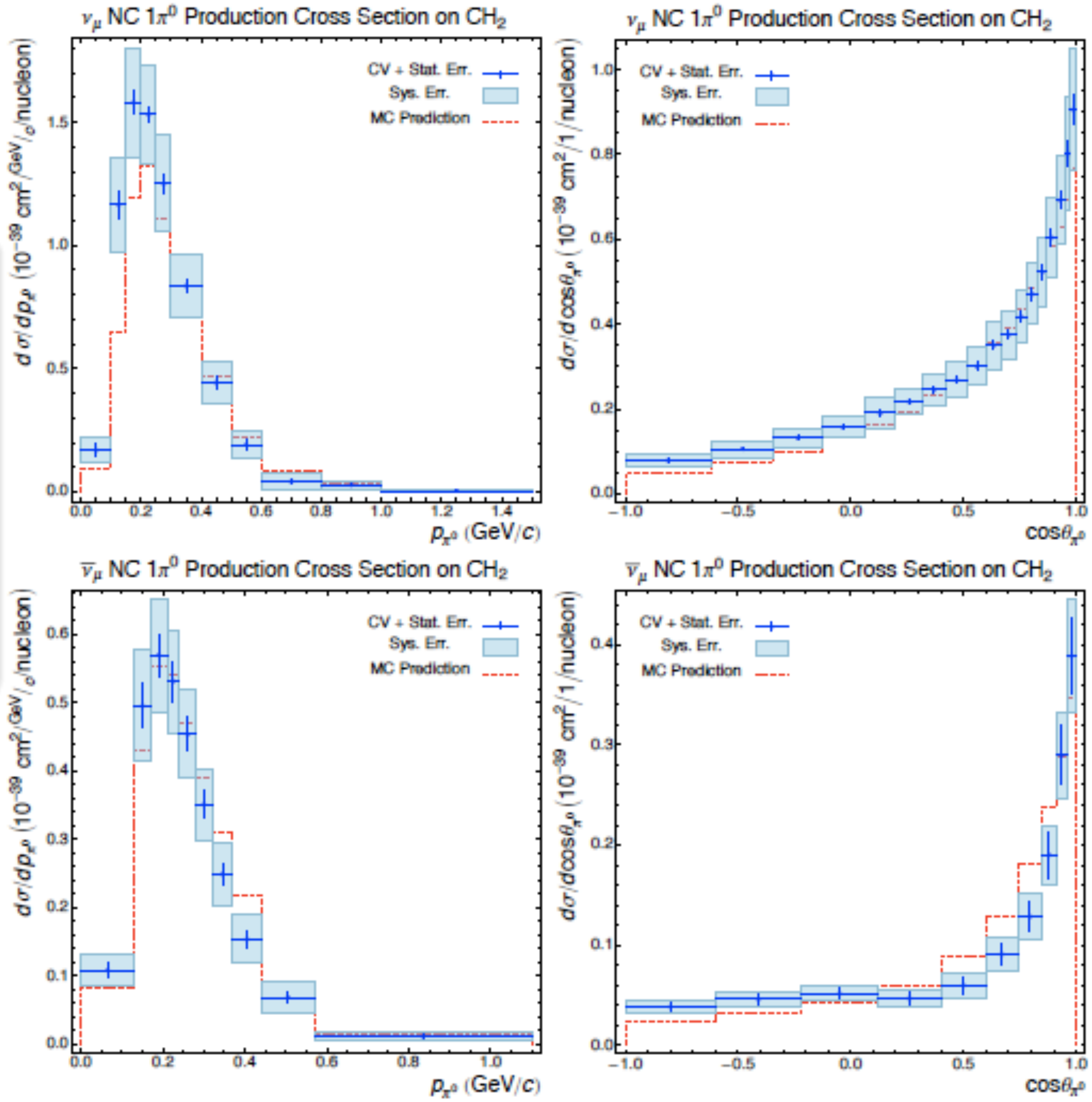

by Colin Anderson

0-3. NCπº cross section in MiniBooNE

NCπº coherent production models

Forward angular distribution is sensitive with coherent πº production.

The measured rates are compared with several theoretical models.

Hernandez et al., arXiv:0903.5285

Alvarez-Ruso et al., PRC76(2007)068501

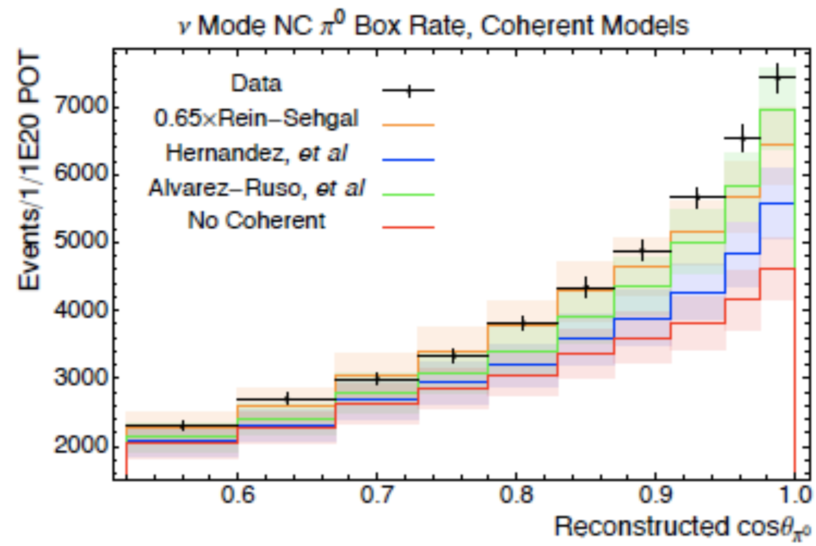

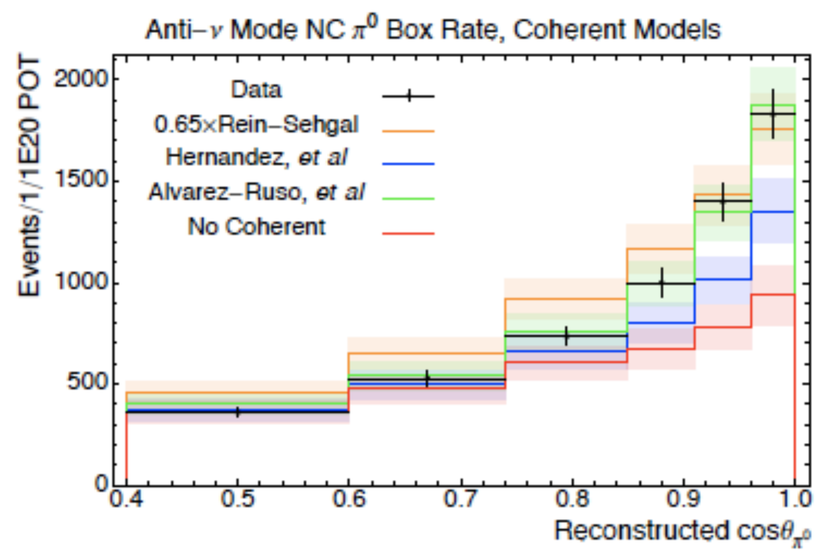

Absolutely Normalized

by Mike Wilking

0-4. CCπ^+ cross section in MiniBooNE

$$\nu_\mu + p(n) \rightarrow \mu + \Delta^{+(+)} \rightarrow \mu + p(n) + \pi^+$$
$$\nu_\mu + A \rightarrow \mu + A + \pi^+$$

CCπ^+ event as a background of CCQE events

CCπ^+ event without pion is the intrinsic background for CCQE in Super-K. Therefore we need a good understanding of CCπ^+ kinematics comparing with CCQE for a better energy reconstruction (= better oscillation measurement).

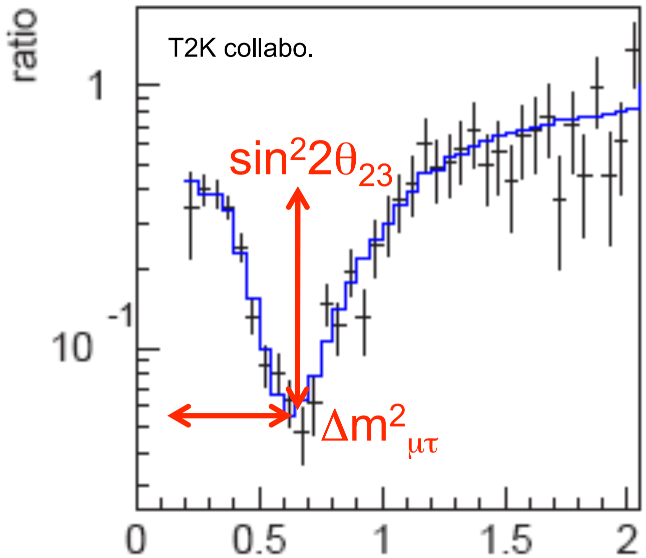

Reconstructed neutrino energy (GeV)

mis-reconstruction of neutrino energy by misunderstanding of CCπ^+ events spoils ν_μ disappearance signals

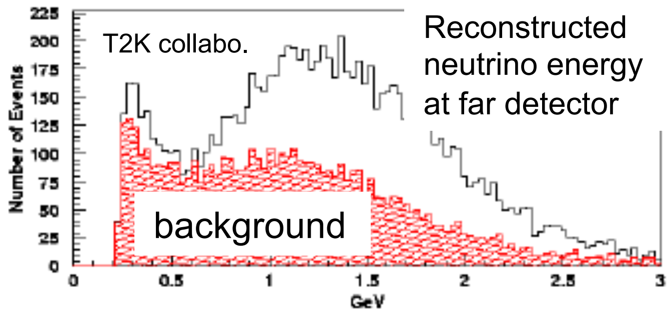

by Mike Wilking

0-4. CCπ^+ cross section in MiniBooNE

CCπ^+ kink fitter

CCπ^+ kink fitter is based on the nature that pion has a hadronic interaction whereas muon doesn't have. Then, pion occasionally shows "kink" in the middle of its track. This kink fitter improves pion energy measurement.

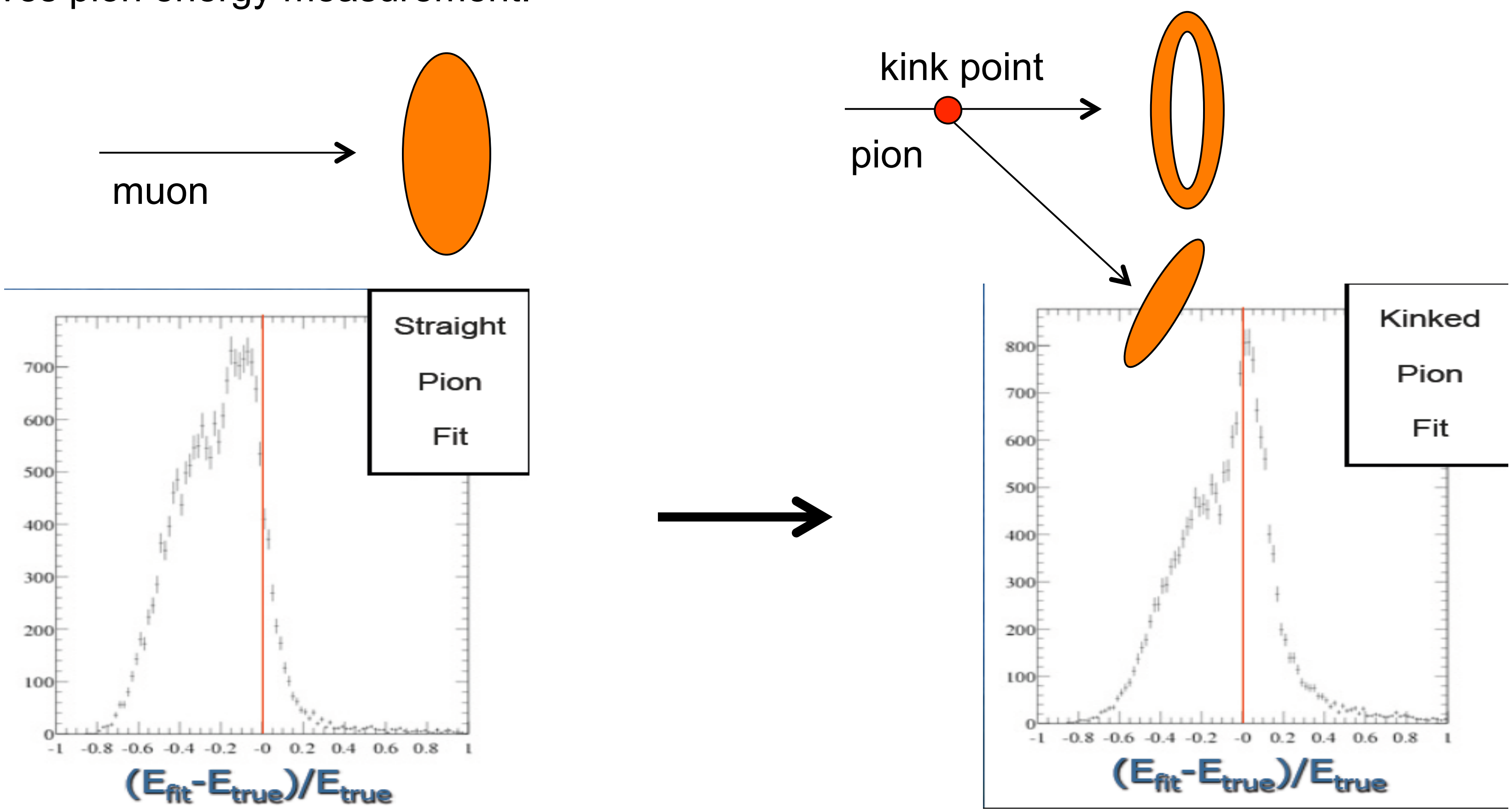

by Mike Wilking

0-4. CCπ^+ cross section in MiniBooNE

CCπ^+ cross section

After the cut, there is ~48,000 events with 90% purity, and correct pion/muon identification rate is 88%.

Following 8 cross sections are measured.

$\sigma(E_\nu)$: total cross section with function of E_ν

$d\sigma/dQ^2$: differential cross section of Q^2

$d^2\sigma/dT_\mu/d\cos\theta_\mu$: double differential cross section of muon kinematics

$d^2\sigma/dT_\pi/d\cos\theta_\pi$: double differential cross section of pion kinematics

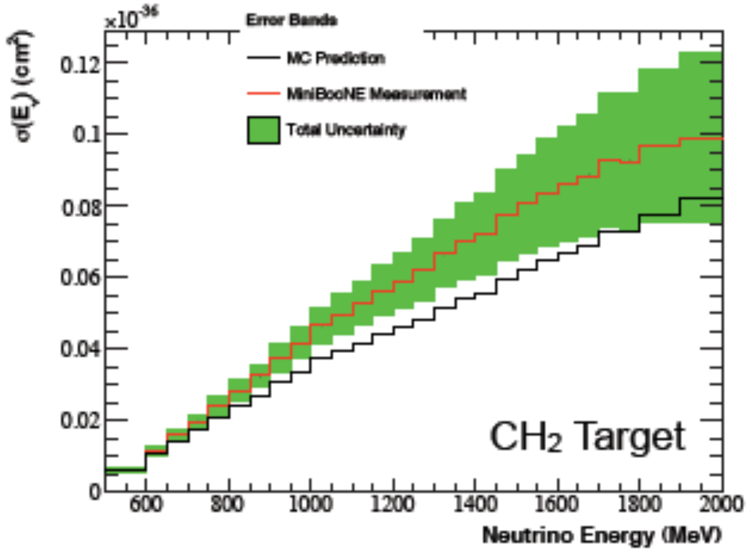

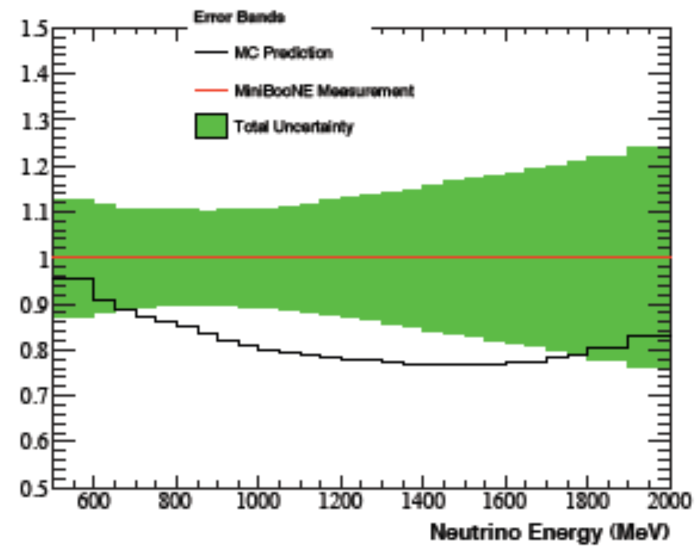

by Bob Nelson

0-5. CCπ^o measurement in MiniBooNE

$$\nu_\mu + n \to \mu + \Delta^+ \to \mu + p + \pi^o$$

CCπ^o event

There is no coherent contribution.
There are only ~5% total and swamped by other CC channels.

CCπ^o fitter (3 tracks fitter)

Probably the most complicated fitter. First primary Cerenkov ring is found, then fitter searches 2 additional rings, then the right combination (1 muon, 2 gammas) is found from 3 possible particle combinations.

78% time muon is correctly found.
Muon angle shows suppression at high $\cos\theta_\mu$.

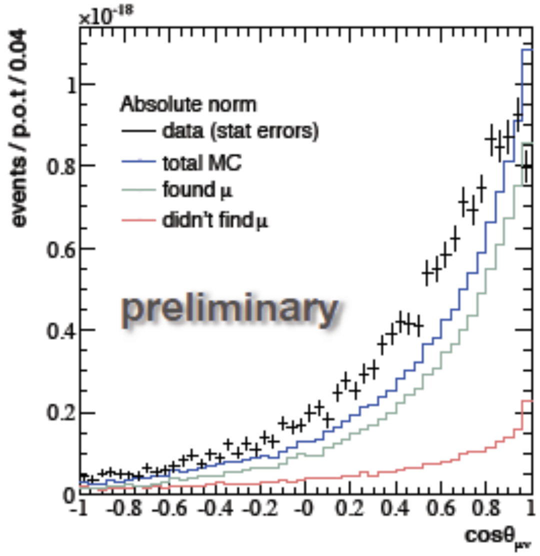

by Bob Nelson

0-5. CCπ^o measurement in MiniBooNE

Kinematics

invariant mass of 2 gammas show π^o mass peak. Muon ID rate is >80% at π^o mass peak.
Reconstructed Q^2 shows suppression at the first bin.
The differential cross sections are coming soon.

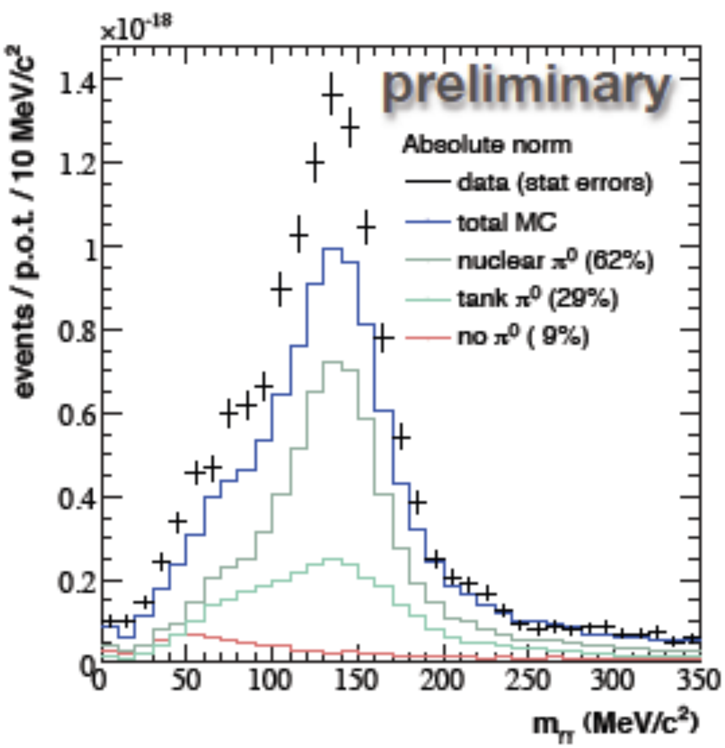

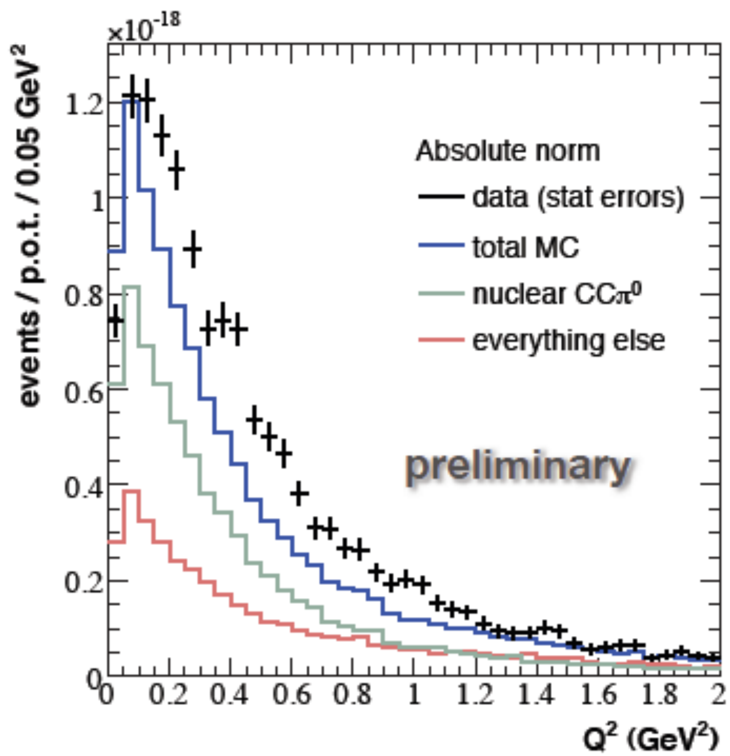

0-6. Improved CCπ^+ simulation

by Jarek Novak

Improved CCπ^+ prediction

All recent improvements are integrated in MiniBooNE simulation, including,
- muon mass correction,
- state-of-arts from factors

$M_A^{1\pi}$ fit with Q^2 distribution

The 3 different fits in Q^2 are performed,
1. $M_A^{1\pi}$ fit with $Q^2>0.2$
2. $M_A^{1\pi}$-coherent fraction simultaneous fit
3. $M_A^{1\pi}$-$C_A^5(0)$ simultaneous fit

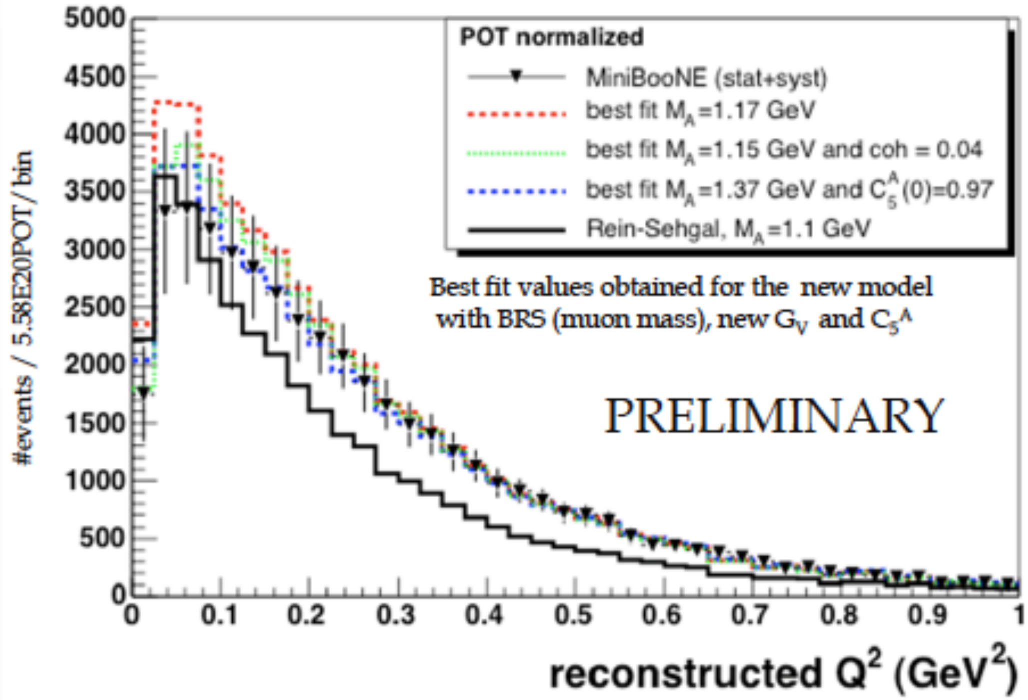

0-7. CCπ^+/CCQE cross section ratio

by Steve Linden

picture wanted

MiniBooNE collaboration,
PRL103(2009)081801

CCπ^+/CCQE cross section ratio measurement

There is a complication for systematic error analysis, because CCQE is the background in CCπ^+ sample, and CCπ^+ is the background in CCQE sample.

Process	Fraction of $CC1\pi^+$-like events (%)	Fraction of CCQE-like events (%)
$CC1\pi^+$ Resonant	86.0	9.4
$CC1\pi^+$ Coherent	6.3	0.2
CCQE	2.4	85.4
Multi-pion	2.5	0.02
$CC1\pi^0$	1.0	2.5
DIS	0.2	< 0.01
Other	1.6	2.5

CCπ^+/CCQE cross section ratio formula

$$\frac{\sigma_{1\pi^+,i}}{\sigma_{QE,i}} = \frac{\epsilon_{QE,i} * \sum_j U_{1\pi^+,ij} * f_{1\pi^+,j} * N_{1\pi^+-cuts,j}}{\epsilon_{1\pi^+,i} * \sum_j U_{QE,ij} * f_{QE,j} * N_{QE-cuts,j}}$$

by Steve Linden

0-7. CCπ^+/CCQE cross section ratio

MiniBooNE collaboration,
PRL103(2009)081801

CCπ^+/CCQE cross section ratio measurement

There is a complication for systematic error analysis, because CCQE is the background in CCπ^+ sample, and CCπ^+ is the background in CCQE sample.

As is same with other pion production analysis, we emphasize that the FSIs are not corrected. We corrected it only when we want to compare with other experimental data.

CCπ^+like/CCQElike cross section ratio

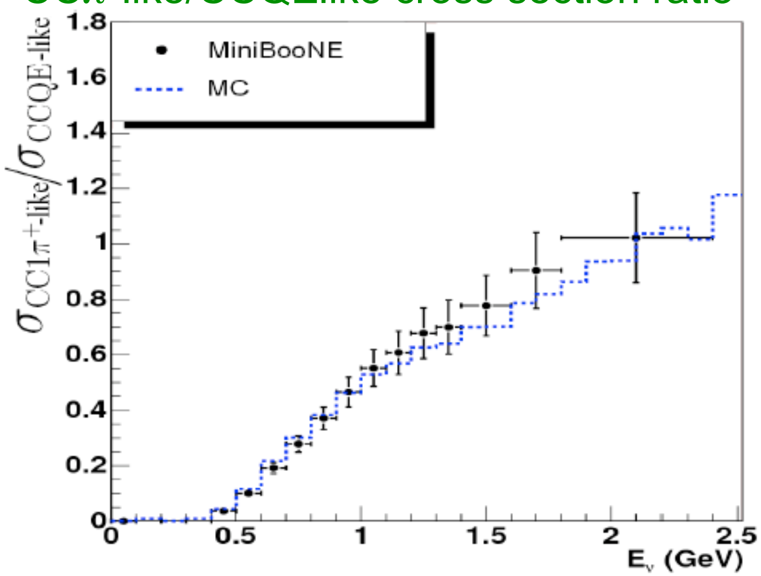

CCπ^+/CCQE cross section ratio

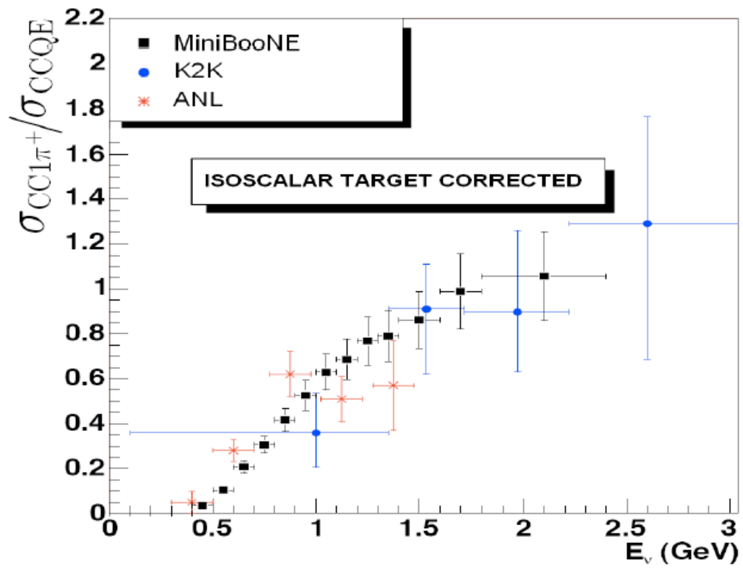

by Joe Grange

0-8. anti-νCCQE measurement

$$\bar{\nu}_\mu + p \rightarrow \mu^+ + n$$

anti-νCCQE measurement is more complicated!

Comparing with νCCQE, anti-νCCQE measurement at least has following difficulties,

1. higher wrong sign background
2. hydrogen scattering
3. no data-based CCπ background tuning is possible (nuclear π^- capture)

After cuts, ~27,000 events with 54% purity.

component	**anti-ν mode**	**ν mode**
right sign CCQE	54%	77%
wrong sign CCQE	22%	2%
QE hydrogen scattering	19%	0%

by Joe Grange

0-8. anti-νCCQE measurement

anti-νCCQE Q^2 distribution

The current analysis is done with quite parallel manner with νCCQE.
The preliminary result also support high M_A value in data-MC Q^2 shape-only comparison.
We are working on the improvement of this analysis.

anti-νCCQE Q^2 plot with world averaged M_A

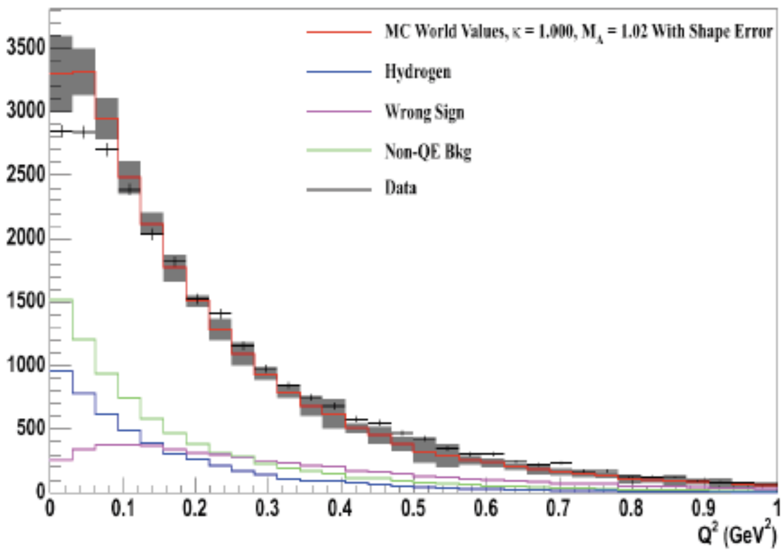

anti-nCCQE Q^2 plot with new M_A extracted from νCCQE

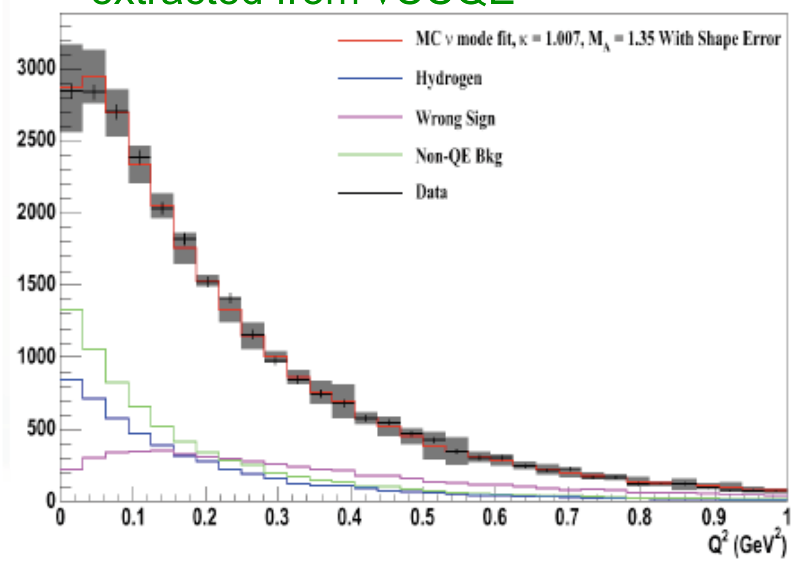

by many people

0-9. NuInt09 conclusions

All talks proceedings are available on online (open access),
http://proceedings.aip.org/proceedings/confproceed/1189.jsp

Some realizations from NuInt09
NuInt is the far most advanced place to discuss neutrino cross sections.

1. Importance to use the better models for neutrino interaction generators

2. Importance to provide data with the form available for theorists, this includes,
   i) detector efficiency is corrected
   ii) free from reconstruction biases (data as a function of measured quantities)
   iii) free from model dependent background subtraction, rather provide inclusive data

e.g.) MC comparison of double differential cross section of NCπ^o production with En=0.5GeV, angle=60^o

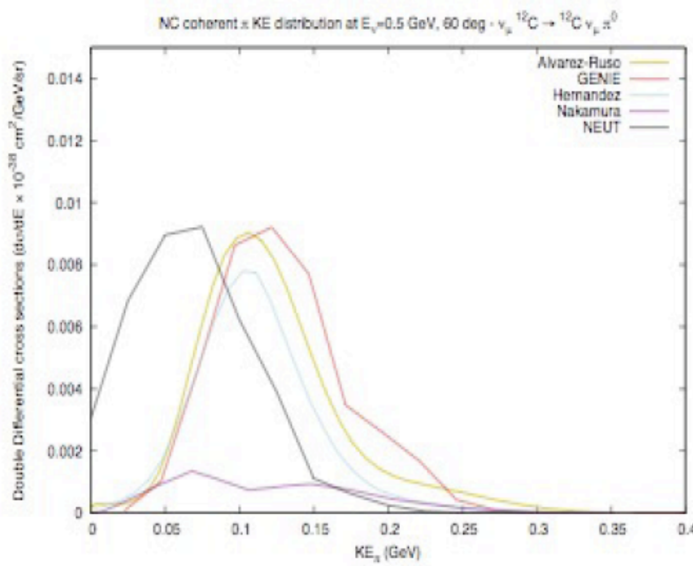

1. **Booster neutrino beamline**

2. **MiniBooNE detector**

3. **CCQE events in MiniBooNE**

4. **CC1π background constraint**

5. **CCQE M_A^{eff}-κ shape-only fit**

6. **CCQE absolute cross section**

7 **Conclusion**

MiniBooNE collaboration,
PRD79(2009)072002

1. Booster Neutrino Beamline

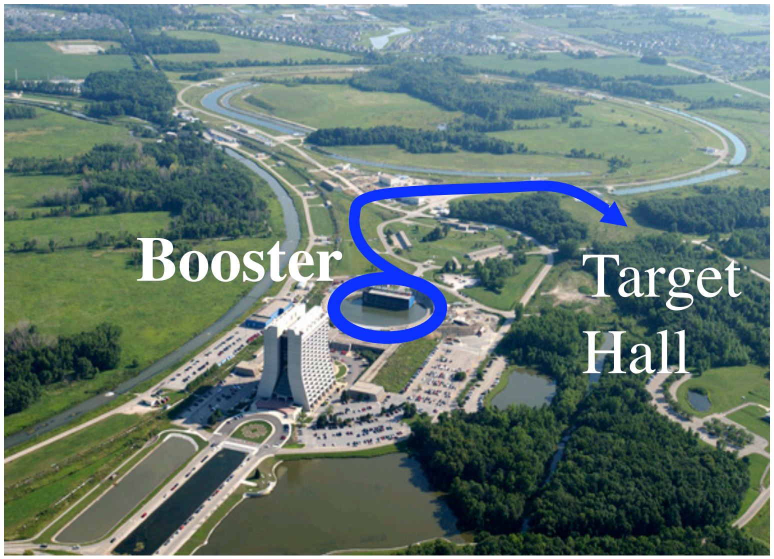

MiniBooNE extracts 8.9 GeV/c momentum proton beam from the Booster

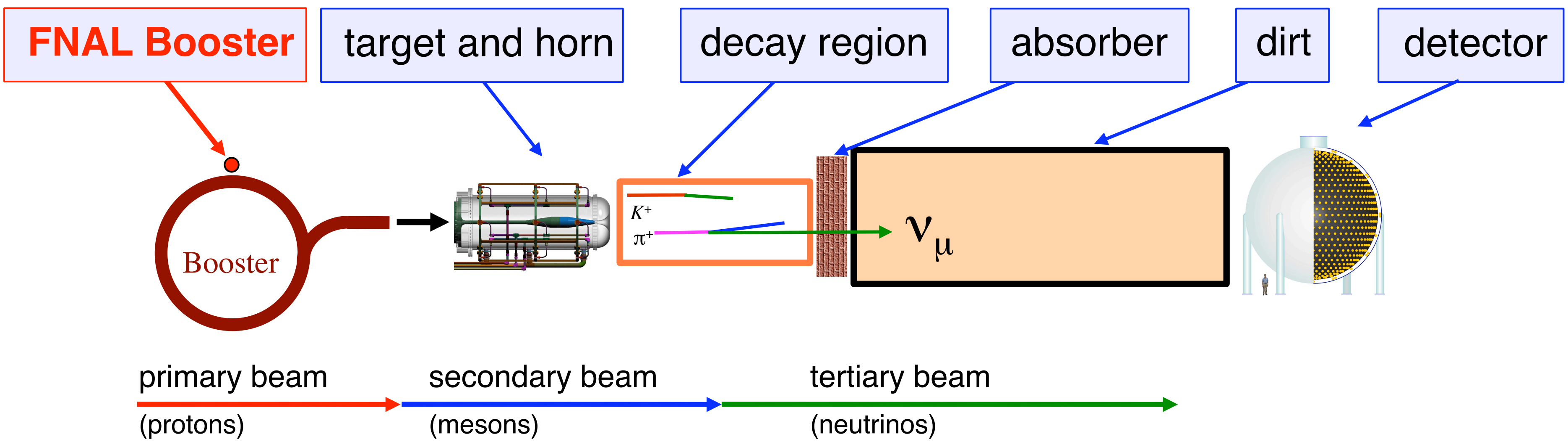

MiniBooNE collaboration,
PRD79(2009)072002

1. Booster Neutrino Beamline

Magnetic focusing horn

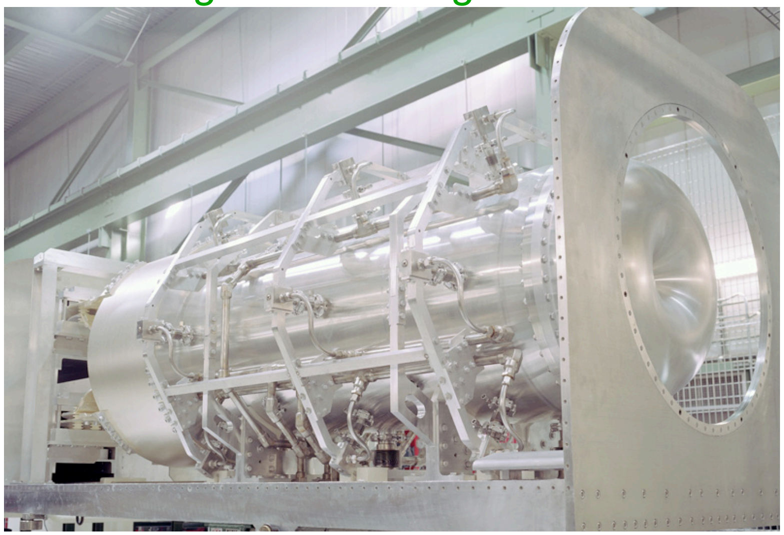

Protons are delivered to a beryllium target in a magnetic horn
(flux increase ~6 times)

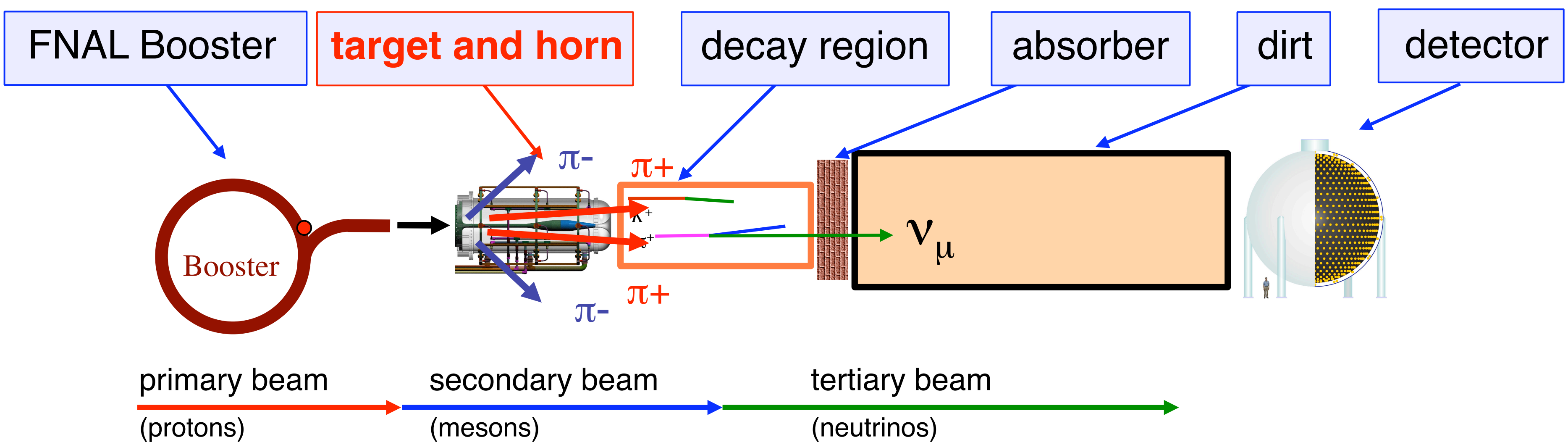

MiniBooNE collaboration,
PRD79(2009)072002

1. Booster Neutrino Beamline

HARP experiment (CERN)

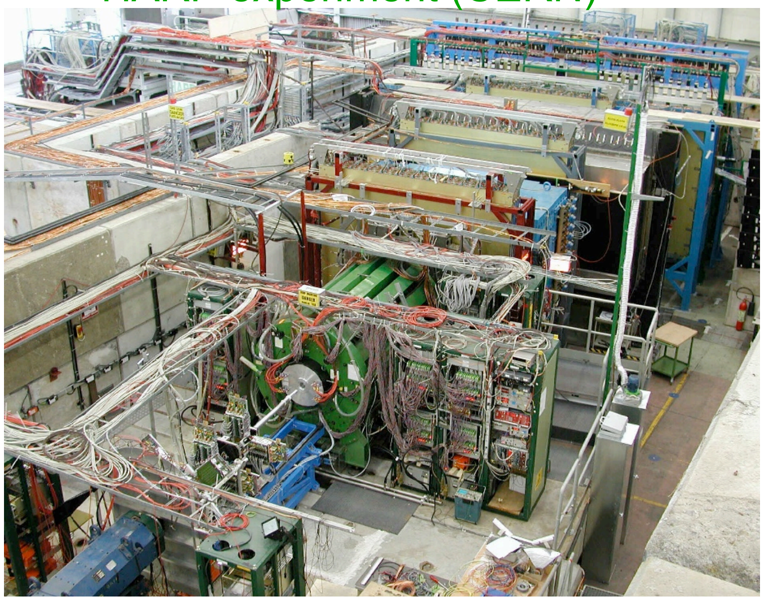

Majority of pions create neutrinos in MiniBooNE are directly measured by HARP (>80%)

Modeling of meson production is based on the measurement done by HARP collaboration

- Identical, but 5% λ Beryllium target
- 8.9 GeV/c proton beam momentum

HARP collaboration,
Eur.Phys.J.C52(2007)29

Booster neutrino beamline pion kinematic space

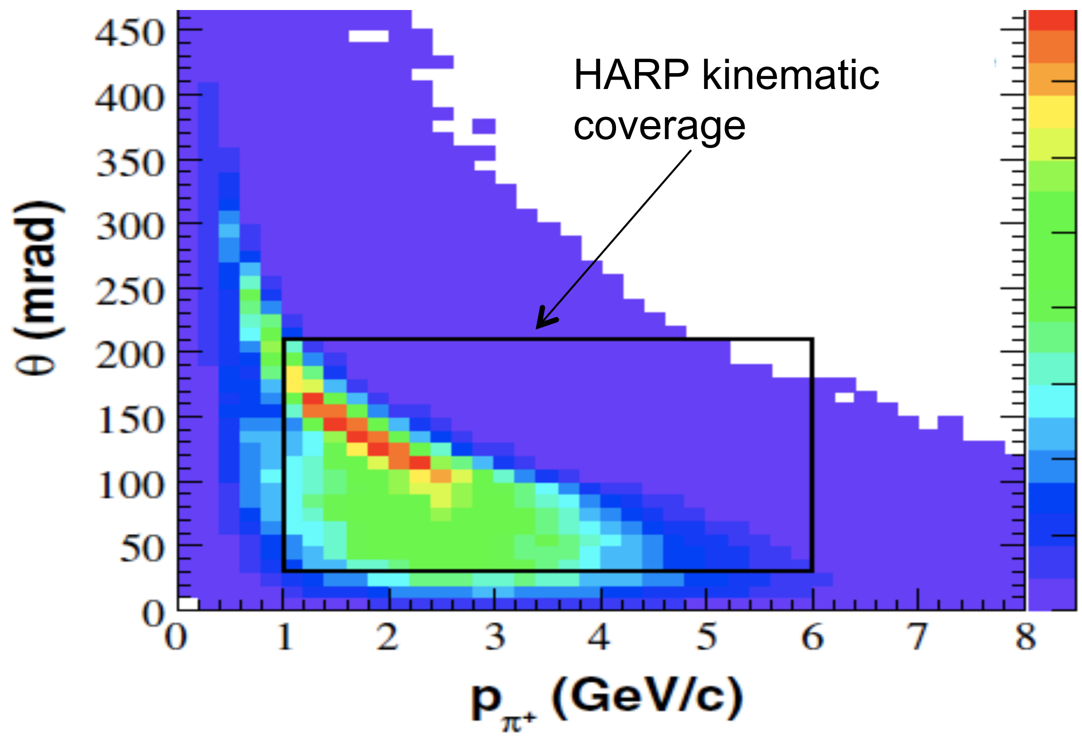

MiniBooNE collaboration,
PRD79(2009)072002

1. Booster Neutrino Beamline

HARP experiment (CERN)

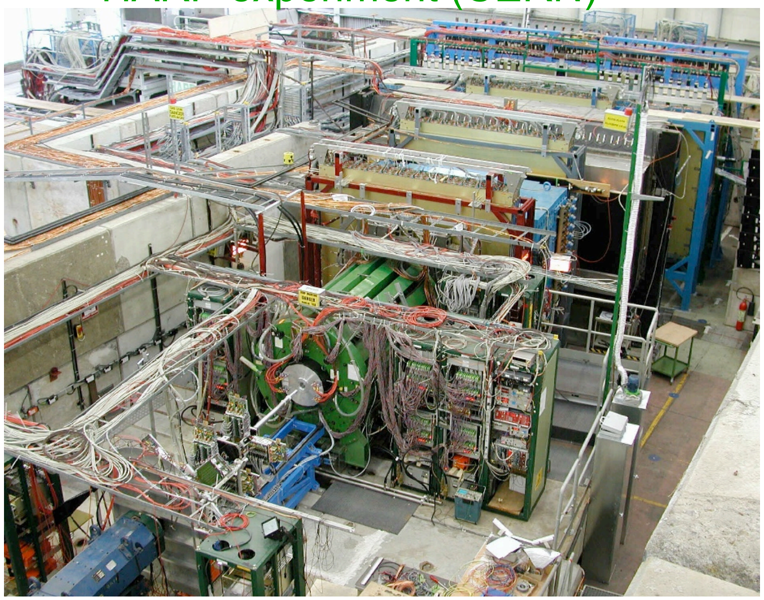

Modeling of meson production is based on the measurement done by HARP collaboration

- Identical, but 5% λ Beryllium target
- 8.9 GeV/c proton beam momentum

HARP collaboration,
Eur.Phys.J.C52(2007)29

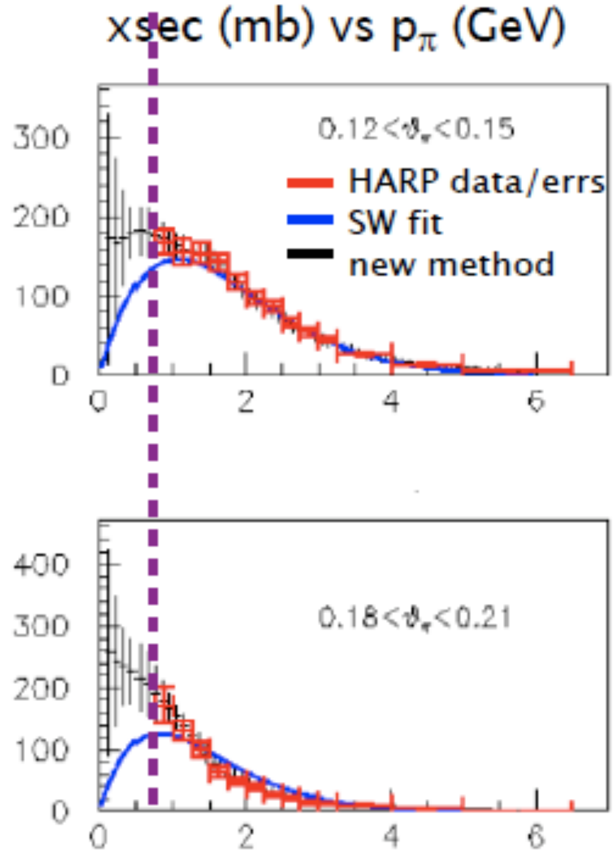

HARP data with 8.9 GeV/c proton beam momentum

The error on the HARP data (~7%) directly propagates.
The neutrino flux error is the dominant source of normalization error for an absolute cross section in MiniBooNE.

MiniBooNE collaboration,
PRD79(2009)072002

1. Booster Neutrino Beamline

Predicted ν_μ-flux in MiniBooNE

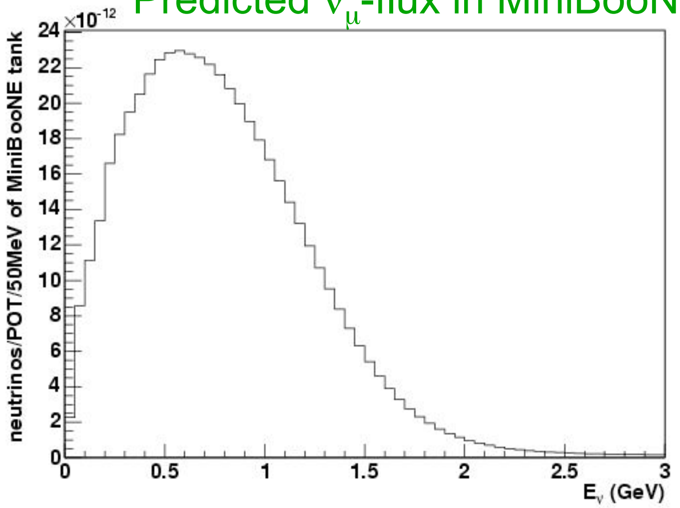

The decay of mesons make the neutrino beam. The neutrino beam is dominated by ν_μ (93.6%), of this, 96.7% is made by π^+-decay

$$\pi^+ \rightarrow \mu^+ + \nu_\mu$$

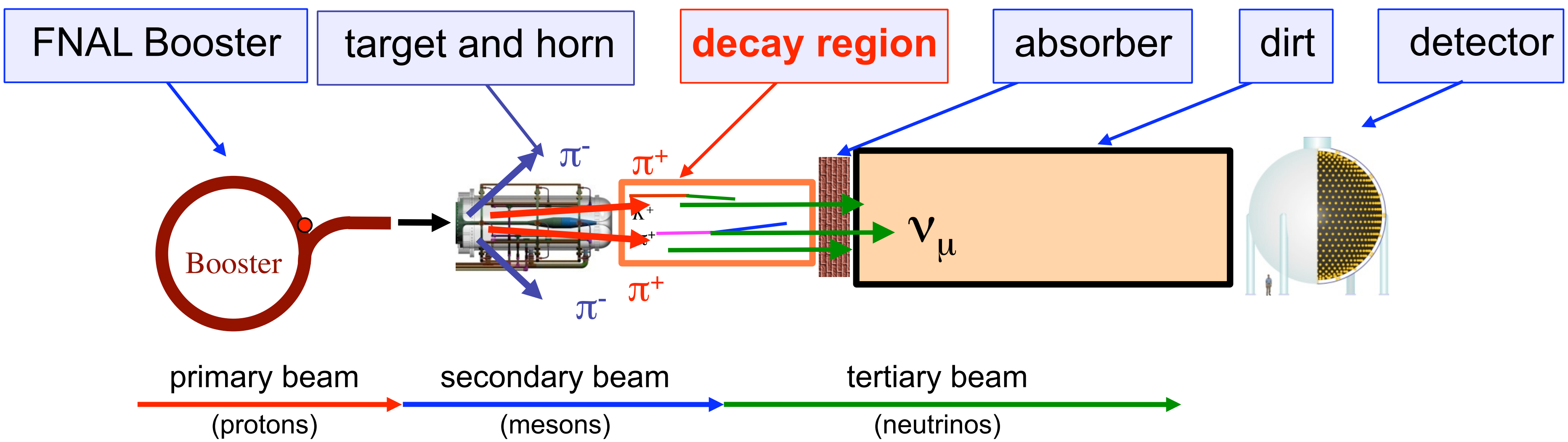

1. Booster neutrino beamline

2. MiniBooNE detector

3. CCQE events in MiniBooNE

4. CC1π background constraint

5. CCQE M_A^{eff}-κ shape-only fit

6. CCQE absolute cross section

7 Conclusion

MiniBooNE collaboration,
NIM.A599(2009)28

2. MiniBooNE detector

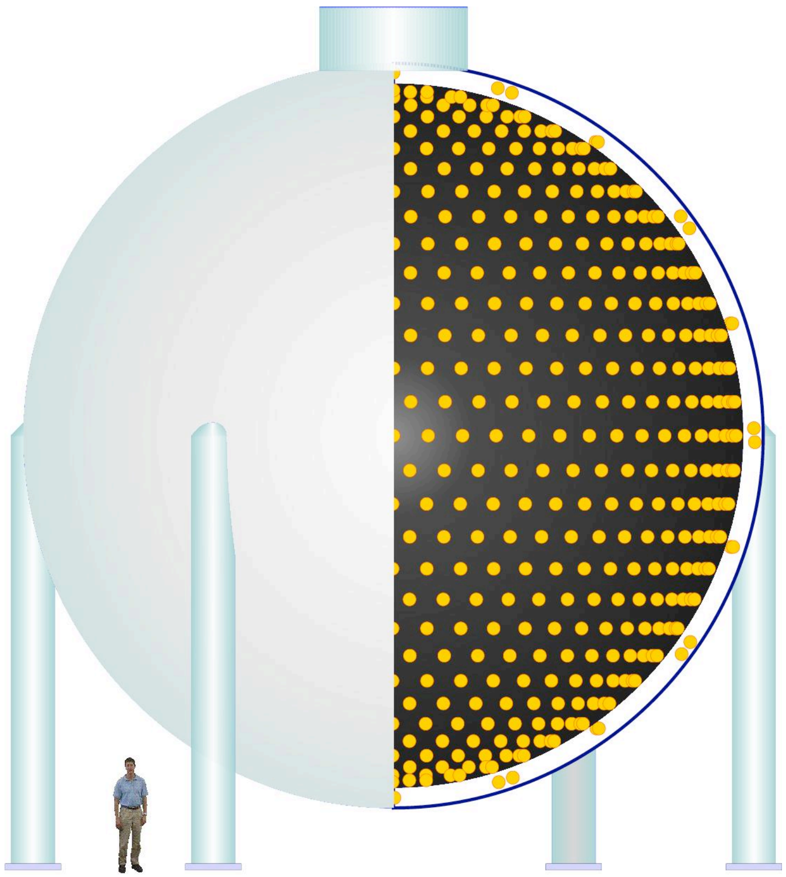

The MiniBooNE Detector

- 541 meters downstream of target
- 3 meter overburden
- 12 meter diameter sphere

  (10 meter “fiducial” volume)
- Filled with 800 t of pure mineral oil (CH_2)

  (Fiducial volume: 450 t)
- 1280 inner phototubes,
- 240 veto phototubes

  Simulated with a GEANT3 Monte Carlo

MiniBooNE collaboration,
NIM.A599(2009)28

2. MiniBooNE detector

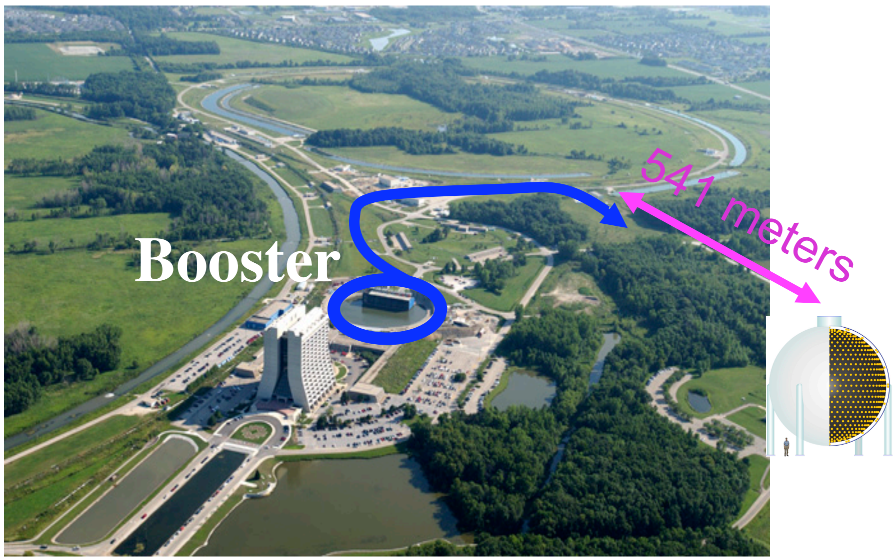

The MiniBooNE Detector

- 541 meters downstream of target
- 3 meter overburden
- 12 meter diameter sphere
  (10 meter “fiducial” volume)
- Filled with 800 t of pure mineral oil (CH_2)
  (Fiducial volume: 450 t)
- 1280 inner phototubes,
- 240 veto phototubes

Simulated with a GEANT3 Monte Carlo

MiniBooNE collaboration,
NIM.A599(2009)28

2. MiniBooNE detector

The MiniBooNE Detector

- 541 meters downstream of target
- 3 meter overburden
- 12 meter diameter sphere

  (10 meter “fiducial” volume)
- Filled with 800 t of pure mineral oil (CH_2)

  (Fiducial volume: 450 t)
- 1280 inner phototubes,
- 240 veto phototubes

  Simulated with a GEANT3 Monte Carlo

MiniBooNE collaboration,
NIM.A599(2009)28

2. MiniBooNE detector

The MiniBooNE Detector

- 541 meters downstream of target
- 3 meter overburden
- 12 meter diameter sphere

  (10 meter “fiducial” volume)
- Filled with 800 t of pure mineral oil (CH_2)

  (Fiducial volume: 450 t)
- 1280 inner phototubes,
- 240 veto phototubes

  Simulated with a GEANT3 Monte Carlo

MiniBooNE collaboration,
NIM.A599(2009)28

2. MiniBooNE detector

Extinction rate of MiniBooNE oil

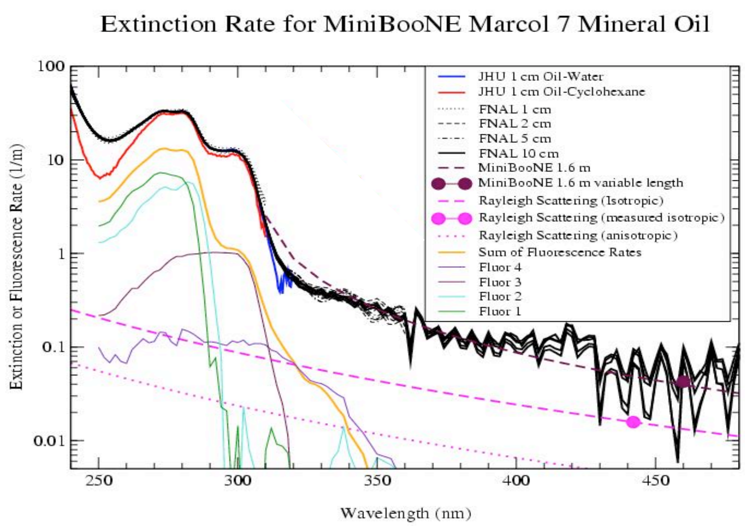

The MiniBooNE Detector

- 541 meters downstream of target
- 3 meter overburden
- 12 meter diameter sphere

  (10 meter “fiducial” volume)
- Filled with 800 t of pure mineral oil (CH_2)

  (Fiducial volume: 450 t)
- 1280 inner phototubes,
- 240 veto phototubes

  Simulated with a GEANT3 Monte Carlo

MiniBooNE collaboration,
NIM.A599(2009)28

2. MiniBooNE detector

The MiniBooNE Detector

- 541 meters downstream of target
- 3 meter overburden
- 12 meter diameter sphere

  (10 meter “fiducial” volume)
- Filled with 800 t of pure mineral oil (CH_2)

  (Fiducial volume: 450 t)
- 1280 inner phototubes,
- 240 veto phototubes

  Simulated with a GEANT3 Monte Carlo

MiniBooNE collaboration, NIM.A599(2009)28

2. MiniBooNE detector

Times of hit-clusters (subevents)

Beam spill (1.6μs) is clearly evident

simple cuts eliminate cosmic backgrounds

Neutrino Candidate Cuts

<6 veto PMT hits

Gets rid of muons

>200 tank PMT hits

Gets rid of Michels

Only neutrinos are left!

Beam and Cosmic BG

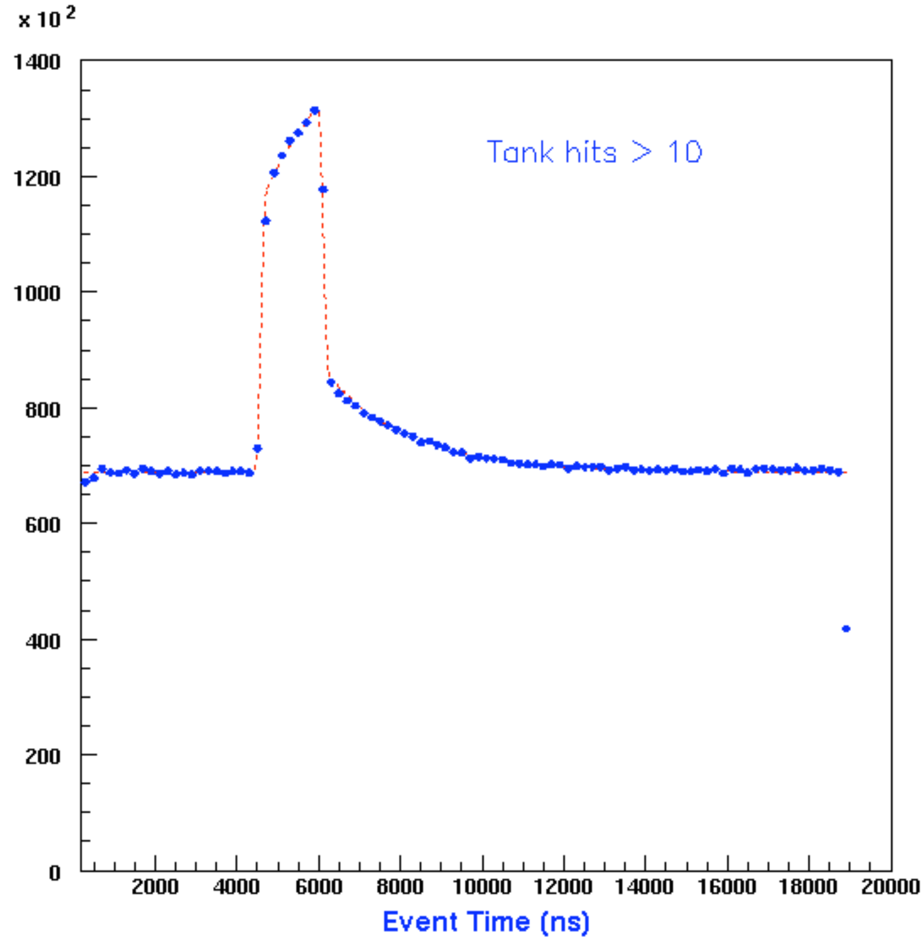

MiniBooNE collaboration,
NIM.A599(2009)28

2. MiniBooNE detector

Times of hit-clusters (subevents)

Beam spill (1.6μs) is clearly evident

- simple cuts eliminate cosmic backgrounds

Neutrino Candidate Cuts

- <6 veto PMT hits
  - Gets rid of muons
- >200 tank PMT hits
  - Gets rid of Michels

Only neutrinos are left!

Beam and Michels

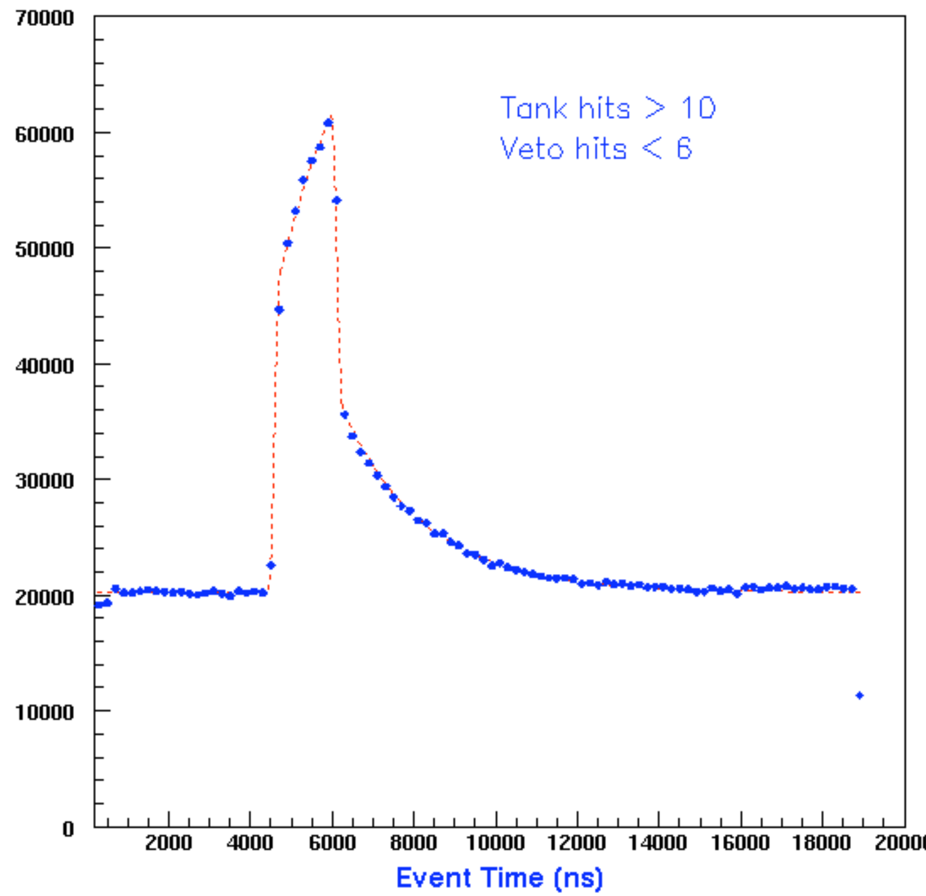

MiniBooNE collaboration,
NIM.A599(2009)28

2. MiniBooNE detector

Times of hit-clusters (subevents)

Beam spill (1.6μs) is clearly evident

- simple cuts eliminate cosmic backgrounds

Neutrino Candidate Cuts

- <6 veto PMT hits
  - Gets rid of muons
- >200 tank PMT hits
  - Gets rid of Michels

Only neutrinos are left!

Beam Only

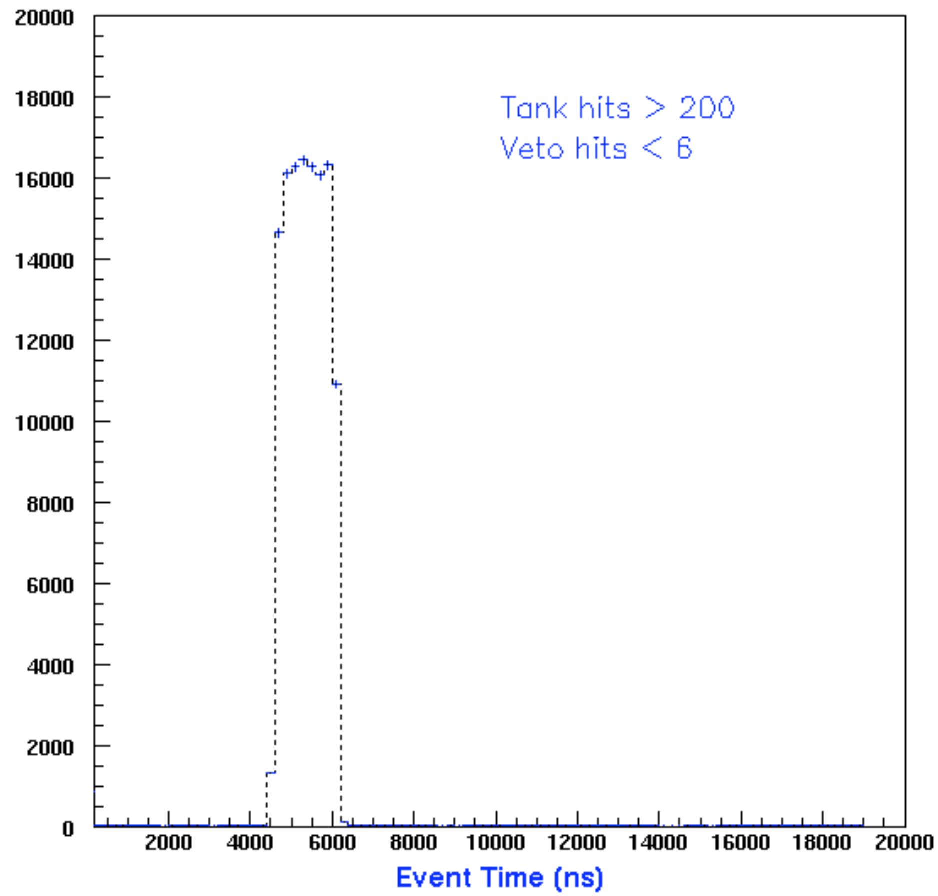

2. Events in the detector

MiniBooNE collaboration, NIM.A599(2009)28

- ***Muons***
  - ***Sharp, clear rings***
    - ***Long, straight tracks***
- Electrons
  - Scattered rings
    - Multiple scattering
    - Radiative processes
- Neutral Pions
  - Double rings
    - Decays to two photons

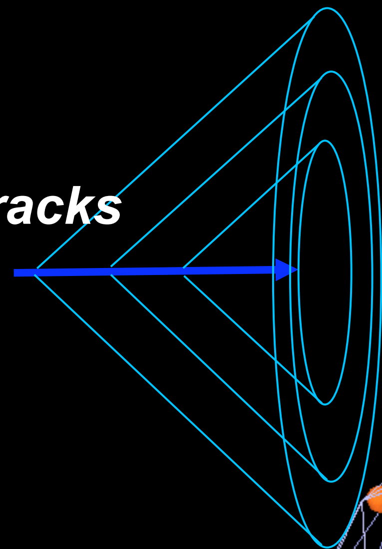

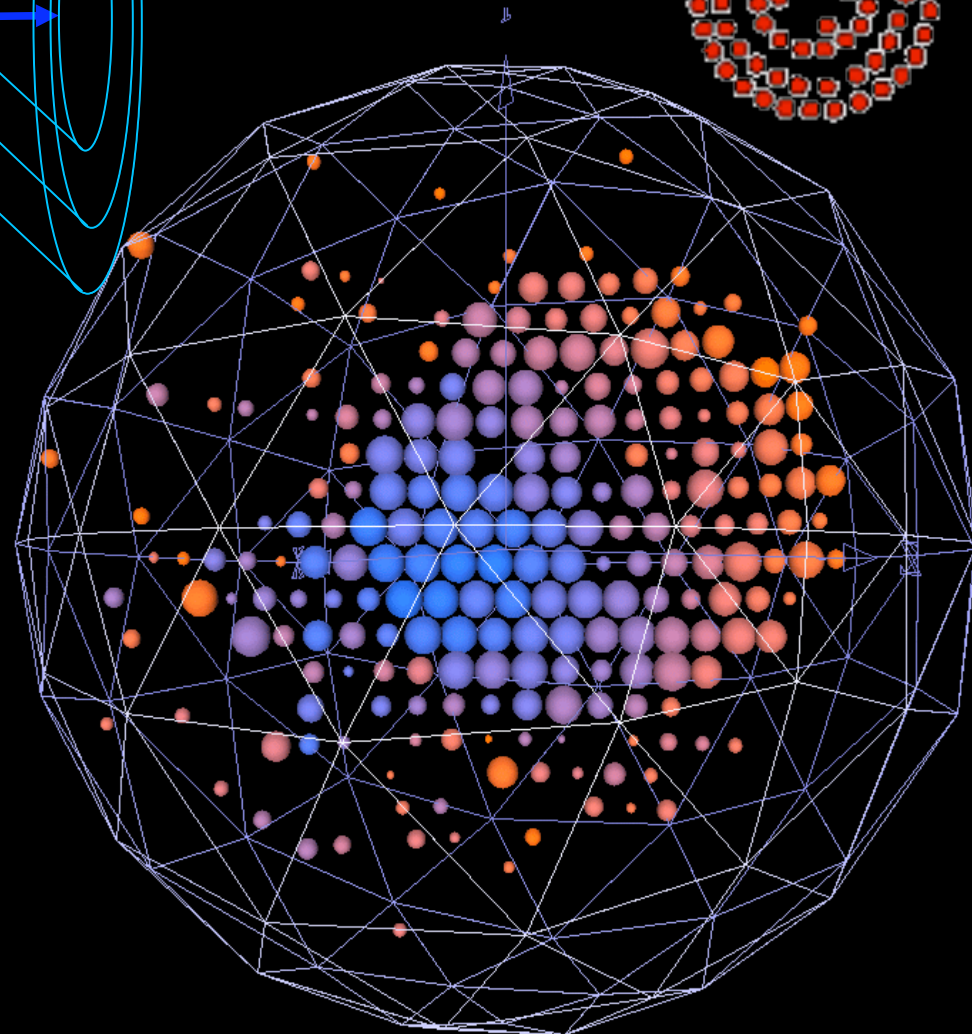

2. Events in the detector

MiniBooNE collaboration, NIM.A599(2009)28

- Muons
  - Sharp, clear rings
    - Long, straight tracks
- ***Electrons***
  - ***Scattered rings***
    - ***Multiple scattering***
    - ***Radiative processes***
- Neutral Pions
  - Double rings
    - Decays to two photons

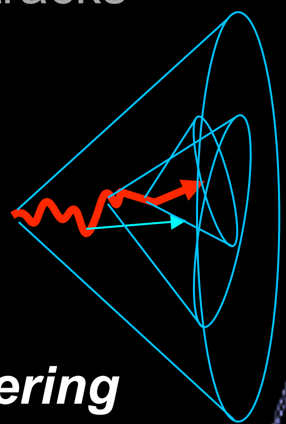

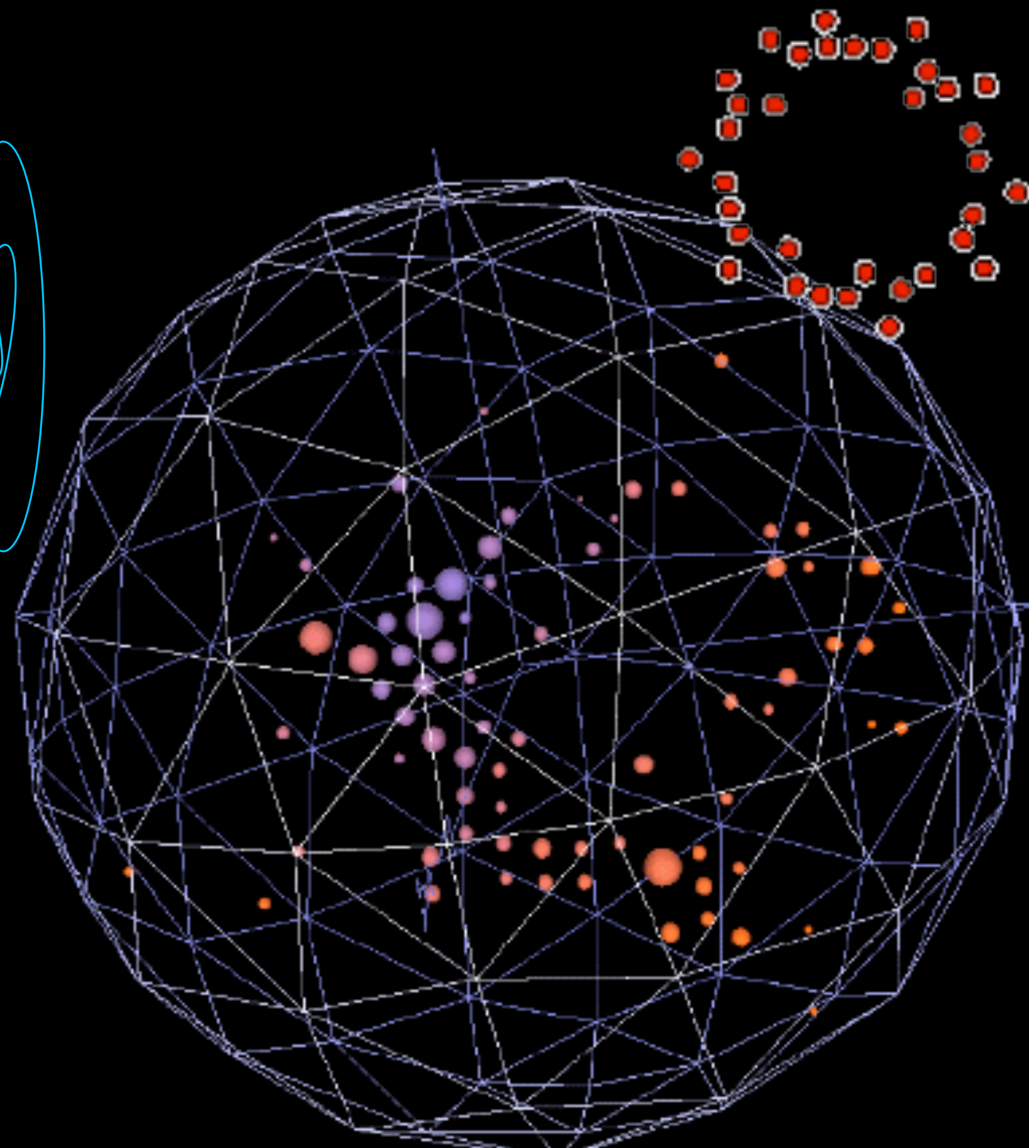

2. Events in the detector

MiniBooNE collaboration, NIM.A599(2009)28

- Muons
  - Sharp, clear rings
    - Long, straight tracks
- Electrons
  - Scattered rings
    - Multiple scattering
    - Radiative processes
- ***Neutral Pions***
  - ***Double rings***
    - ***Decays to two photons***

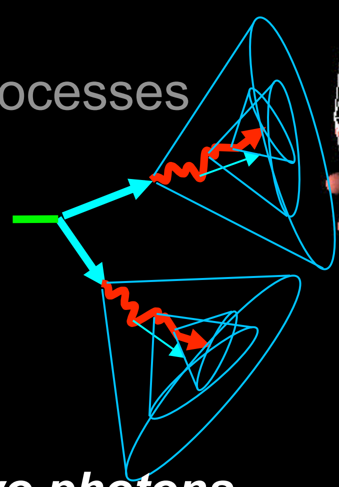

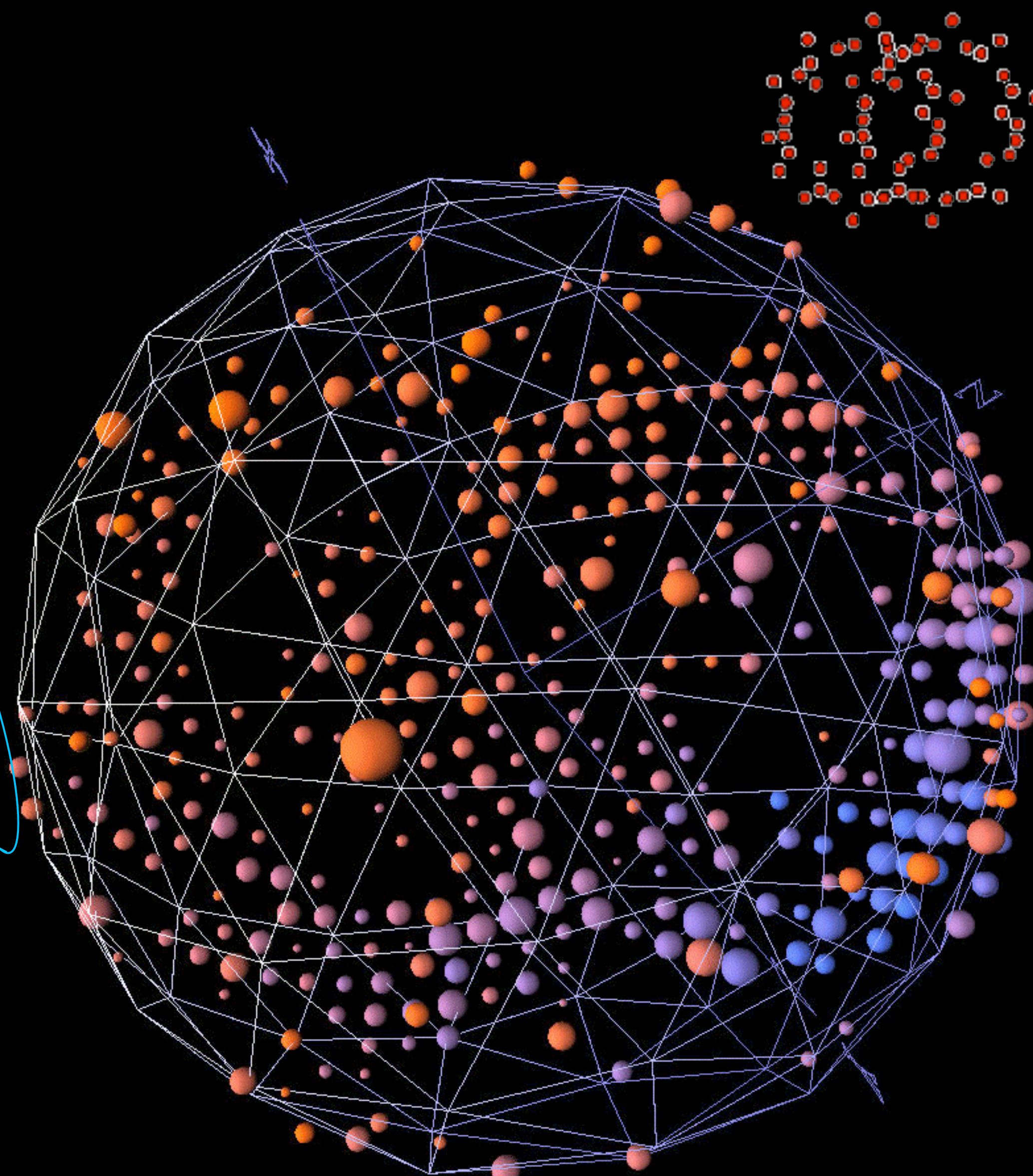

1. Booster neutrino beamline

2. MiniBooNE detector

3. CCQE events in MiniBooNE

4. CC1π background constraint

5. CCQE M_A^{eff}-κ shape-only fit

6. CCQE absolute cross section

7 Conclusion

3. CCQE event measurement in MiniBooNE

ν_μ charged current quasi-elastic (ν_μ CCQE) interaction is an important channel for the neutrino oscillation physics and the most abundant (~40%) interaction type in MiniBooNE detector

$$\nu_\mu + n \rightarrow p + \mu^-$$

$$(\nu_\mu + {}^{12}C \rightarrow X + \mu^-)$$

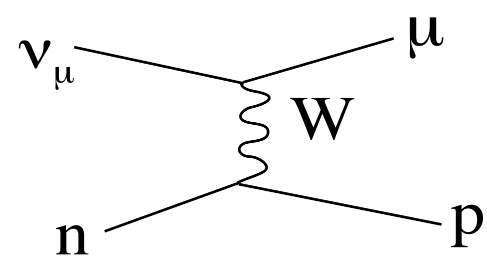

MiniBooNE detector

(spherical Cherenkov detector)

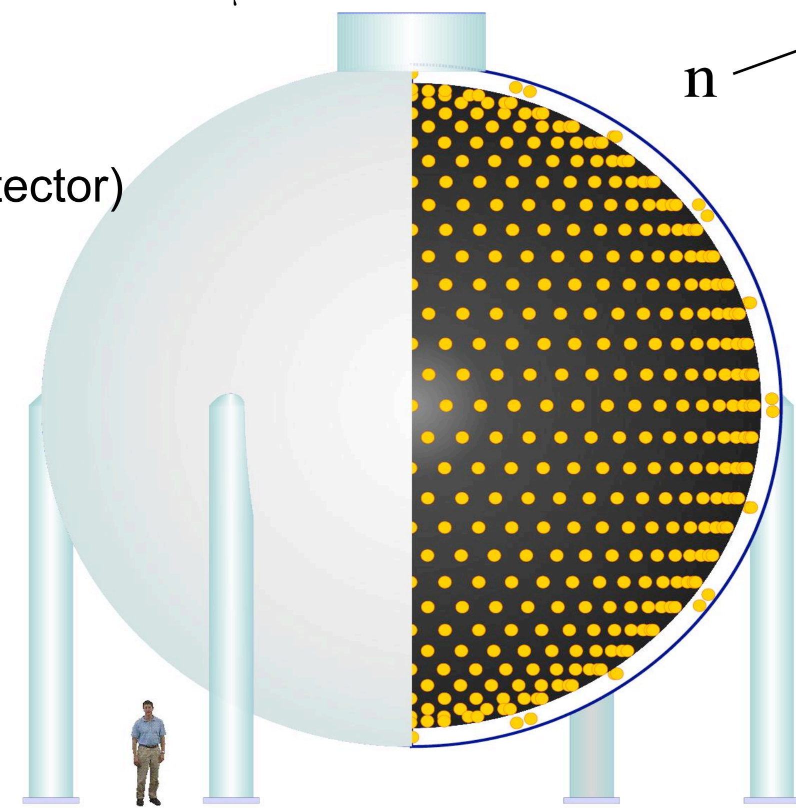

3. CCQE event measurement in MiniBooNE

ν_μ charged current quasi-elastic (ν_μ CCQE) interaction is an important channel for the neutrino oscillation physics and the most abundant (~40%) interaction type in MiniBooNE detector

$$\nu_\mu + n \rightarrow p + \mu^-$$

$$(\nu_\mu + {}^{12}C \rightarrow X + \mu^-)$$

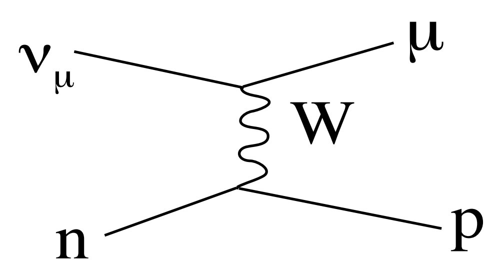

MiniBooNE detector
(spherical Cherenkov detector)

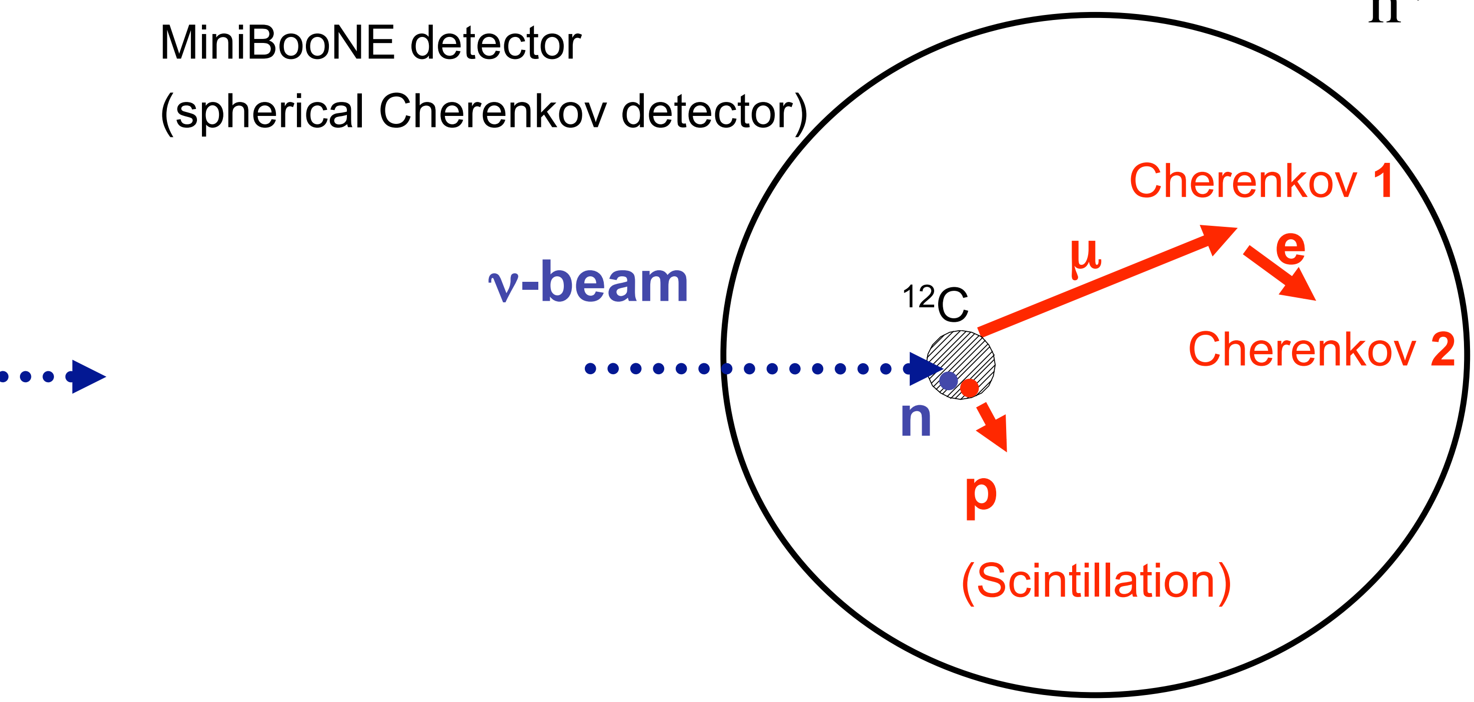

muon like Cherenkov light and subsequent decayed electron (Michel electron) like Cherenkov light are the signal of CCQE event

3. CCQE event measurement in MiniBooNE

ν_μ CCQE interactions (ν+n → μ+p) has characteristic two "subevent" structure from muon decay

$$\nu_\mu + n \rightarrow \overset{1}{\boxed{\mu^-}} + p \rightarrow \nu_\mu + \overline{\nu_e} + \overset{2}{\boxed{e^-}} + p$$

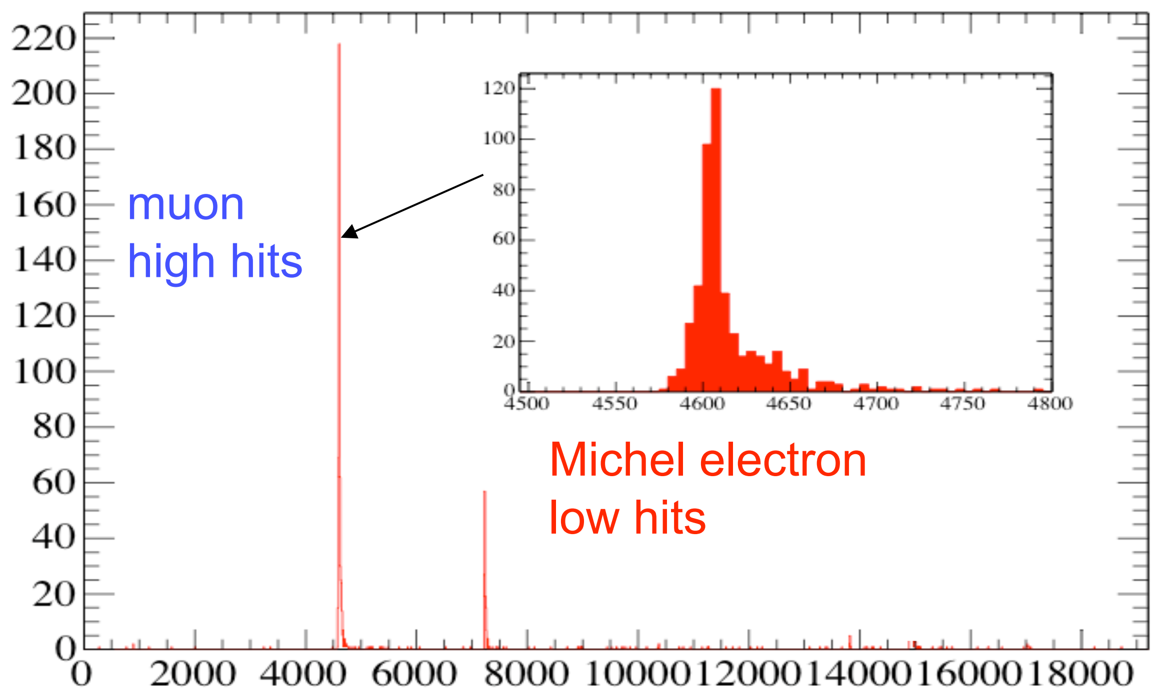

27% efficiency
77% purity
146,070 events
with 5.58E20POT

3. CCQE event measurement in MiniBooNE

All kinematics are specified from 2 observables, muon energy E_μ and muon scattering angle θ_μ

Energy of the neutrino E_ν^{QE} and 4-momentum transfer Q^2_{QE} can be reconstructed by these 2 observables, under the assumption of CCQE interaction with bound neutron at rest ("QE assumption")

$$E_\nu^{QE} = \frac{2(M - E_B)E_\mu - (E_B^2 - 2ME_B + m_\mu^2 + \Delta M^2)}{2[(M - E_B) - E_\mu + p_\mu \cos\theta_\mu]}$$

$$Q^2_{QE} = -m_\mu^2 + 2E_\nu^{QE}(E_\mu - p_\mu \cos\theta_\mu)$$

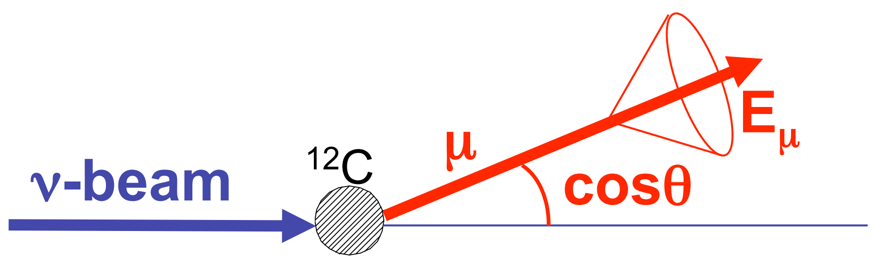

1. Booster neutrino beamline

2. MiniBooNE detector

3. CCQE events in MiniBooNE

4. CC1π background constraint

5. CCQE M_A^{eff}-κ shape-only fit

6. CCQE absolute cross section

7 Conclusion

4. CC1π background constraint, introduction

data-MC comparison, in 2 subevent sample (absolute scale)

Problem 1

CCQE sample shows good agreement in shape, because we tuned relativistic Fermi gas (RFG) parameters.

MiniBooNE collaboration, PRL100(2008)032301

However absolute normalization does not agree.

The background is dominated with CC1π without pion (CCQE-like). We need a background prediction with an absolute scale.

CCQE

$$\nu_\mu + n \rightarrow \overset{1}{\boxed{\mu^-}} + p \rightarrow \nu_\mu + \overline{\nu}_e + \overset{2}{\boxed{e^-}} + p$$

CC1π

$$\nu_\mu + N \rightarrow \overset{1}{\boxed{\mu^-}} + \cancel{\pi^+} + N \rightarrow \nu_\mu + \overline{\nu}_e + \overset{2}{\boxed{e^-}} + N$$

(π-absorption)

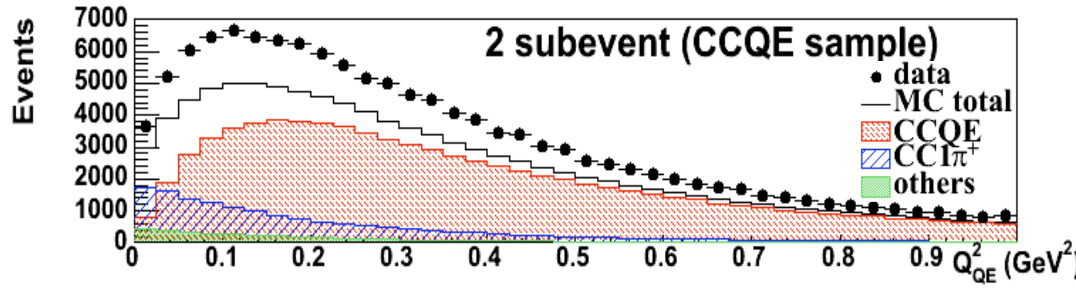

4. CC1π background constraint, introduction

data-MC comparison, in 3 subevent sample (absolute scale)

Problem 2

CC1π sample is worse situation, data and MC do not agree in shape nor normalization.

Under this situation, we cannot use CC1π prediction for background subtraction for CCQE absolute cross section measurement.

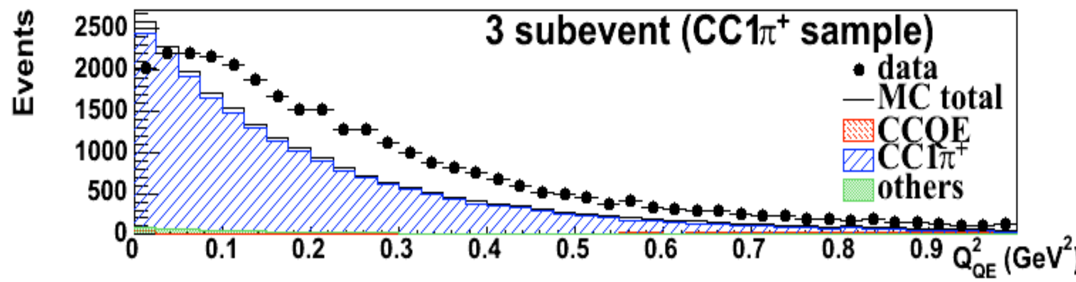

CC1π

$$\nu_\mu + N \to \overset{1}{\boxed{\mu^-}} + \pi^+ + N \to \nu_\mu + \overline{\nu}_e + \overset{2}{\boxed{e^-}} + N$$

$$\pi^+ \to \nu_\mu + \mu^+ \to \nu_\mu + \overline{\nu}_e + \overset{3}{\boxed{e^+}} + N$$

4. CC1π background constraint

data-MC comparison, before CC1π constraint (absolute scale)

Solution

Use data-MC Q^2 ratio in CC1π sample to correct all CC1π events in MC.

Then, this "new" MC is used to predicts CC1π background in CCQE sample

This correction gives both CC1π background normalization and shape in CCQE sample

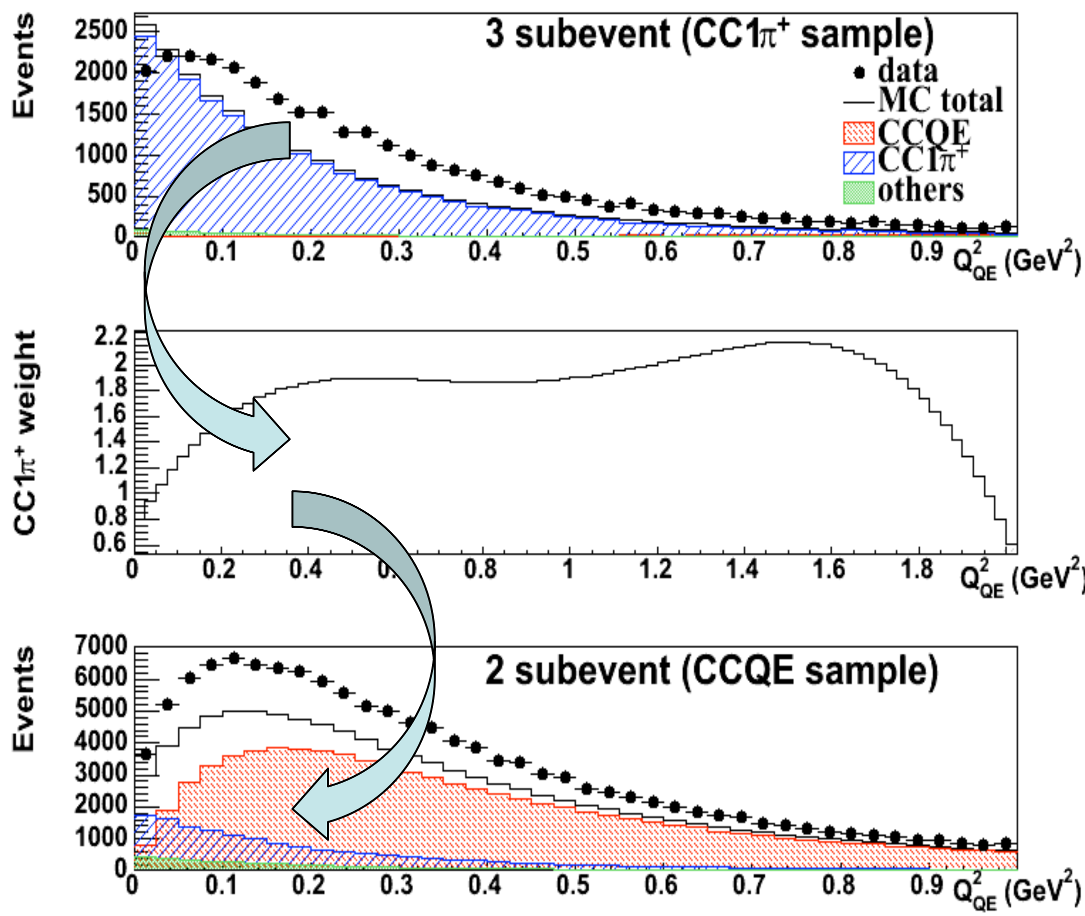

4. CC1π background constraint

data-MC comparison, after CC1π constraint (absolute scale)

Now we have an absolute prediction of CC1π background in CCQE sample.

We are ready to measure the absolute CCQE cross section!

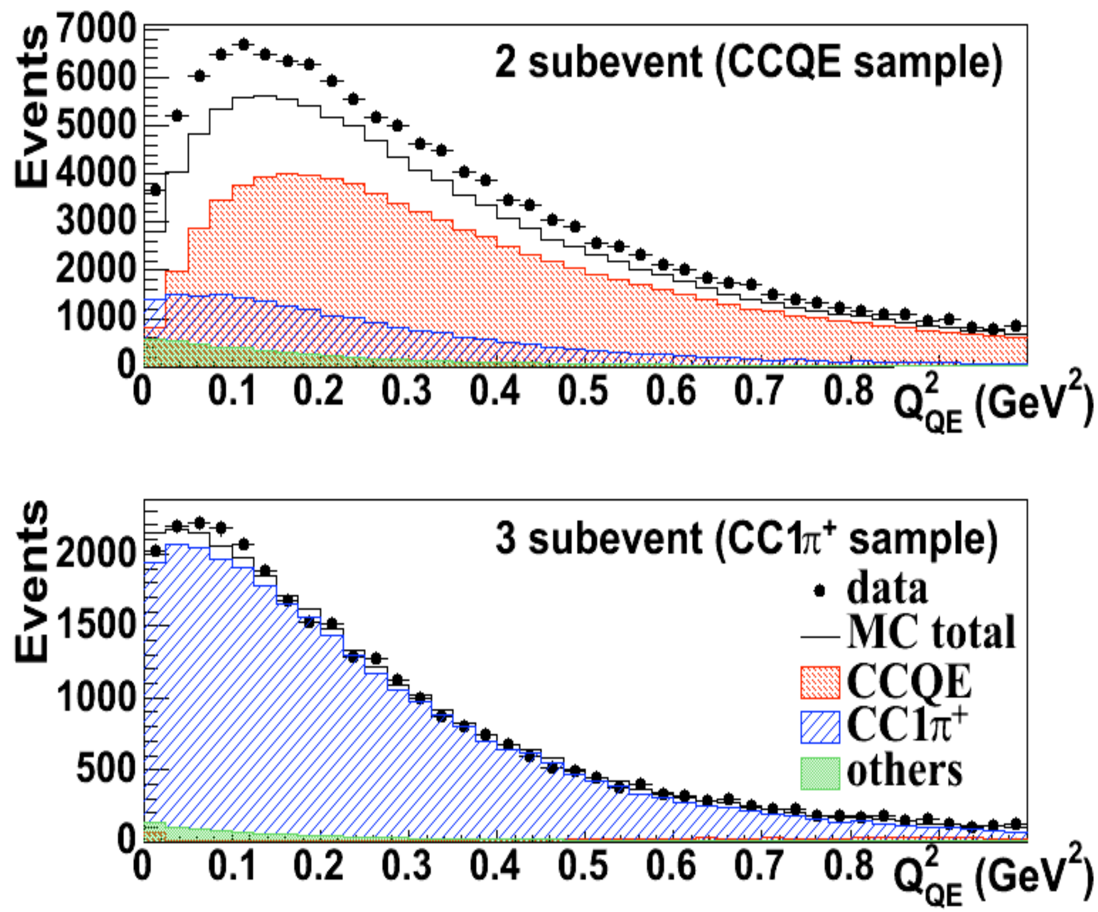

4. CC1π background constraint

This data driven MC tuning is based on 2 assumptions.

1. Kinematics measurement consistency between 2 and 3 subevent sample

Since 3 subevent has an additional particle (=pion), light profile is different. ~9% of events are misreconstructed to high Q^2 in 3 subevent, but majority of them are Q^2>0.5GeV^2, so they don't join the background subtraction.

2. Pion absorption

The background subtraction is based on the assumption that our pion absorption model in the MC is right. We assume 25% error for nuclear pion absorption, 30% for nuclear pion charge exchange, 35% for detector pion absorption, and 50% for detector pion charge exchange.
On top of that, we also include the shape error of pion absorption by change the fraction of resonance and coherent component.

1. Booster neutrino beamline

2. MiniBooNE detector

3. CCQE events in MiniBooNE

4. CC1π background constraint

5. CCQE M_A^{eff}-κ shape-only fit

6. CCQE absolute cross section

7 Conclusion

Smith and Moniz, Nucl.,Phys.,B43(1972)605

5. Relativistic Fermi Gas (RFG) model

Relativistic Fermi Gas (RFG) Model

Carbon is described by the collection of incoherent Fermi gas particles.
All details come from hadronic tensor.

$$(W_{\mu\nu})_{ab} = \int_{Elo}^{Ehi} f(\vec{k},\vec{q},w)T_{\mu\nu}dE : \text{hadronic tensor}$$

$$f(\vec{k},\vec{q},w) \;:\; \text{nucleon phase space density function}$$

$$T_{\mu\nu} = T_{\mu\nu}(F_1,F_2,F_A,F_P) \;:\; \text{nucleon tensor}$$

$$F_A(Q^2) = g_A/(1+Q^2/\boxed{M_A^2})^2 \;: \text{Axial form factor}$$

$$Ehi \;:\; \text{the highest energy state of nucleon} = \sqrt{(p_F^2 + M^2)}$$

$$Elo \;:\; \text{the lowest energy state of nucleon} = \boxed{\kappa}\left(\sqrt{(p_F^2 + M^2)} - \omega + E_B\right)$$

We tuned following 2 parameters using Q^2 distribution by least χ^2 fit;

M_A = effective axial mass

κ = Pauli blocking parameter

MiniBooNE collaboration,
PRL100(2008)032301

5. Pauli blocking parameter “kappa”, κ

We performed shape-only fit for Q^2 distribution to fix CCQE shape within RFG model, by tuning M_A^{eff} (effective axial mass) and κ

Pauli blocking parameter "kappa”, κ

To enhance the Pauli blocking at low Q^2, we introduced a new parameter κ, which is the energy scale factor of lower bound of nucleon sea in RFG model in Smith-Moniz formalism, and controls the size of nucleon phase space

$$\mathrm{Elo} = \boxed{\kappa}\left(\sqrt{(p_F^2 + M^2)} - w + E_B\right)$$

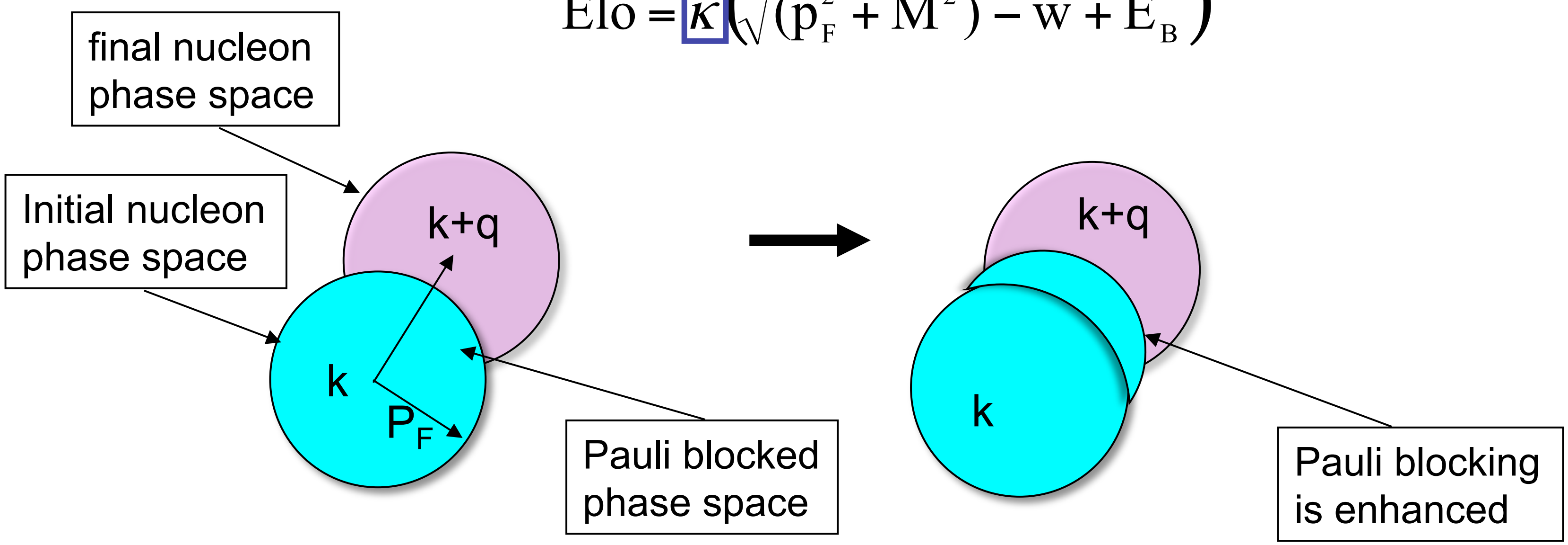

5. Kappa and (e,e’) experiments

Butkevich and Mikheyev,
Phys.Rev.C72:025501,2005

In low |q|, The RFG model systematically over predicts cross section for electron scattering experiments at low |q| (~low Q^2)

Data and predicted xs difference for ^{12}C

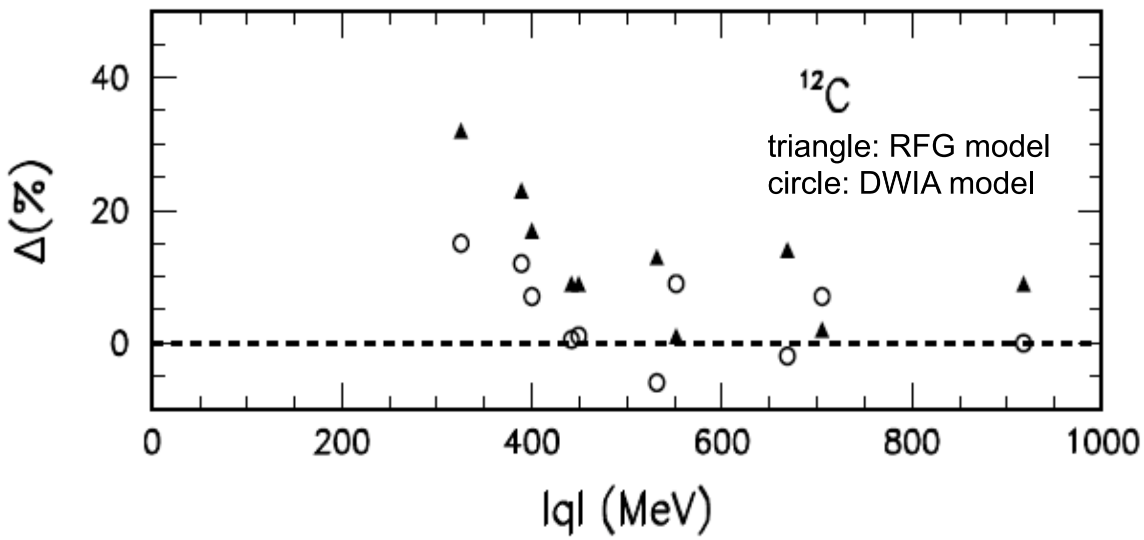

5. Kappa and (e,e') experiments

In low |q|, The RFG model systematically over predicts cross section for electron scattering experiments at low |q| (~low Q^2)

We had investigated the effect of Pauli blocking parameter "κ" in (e,e') data. κ cannot fix the shape mismatching of (e,e') data for each angle and energy, but it can fix integral of each cross section data, which is the observables for neutrino experiments. We conclude κ is consistent with (e,e') data.

black: (e,e') energy transfer data
red: RFG model with kappa (=1.019)
blue: RFG model without kappa

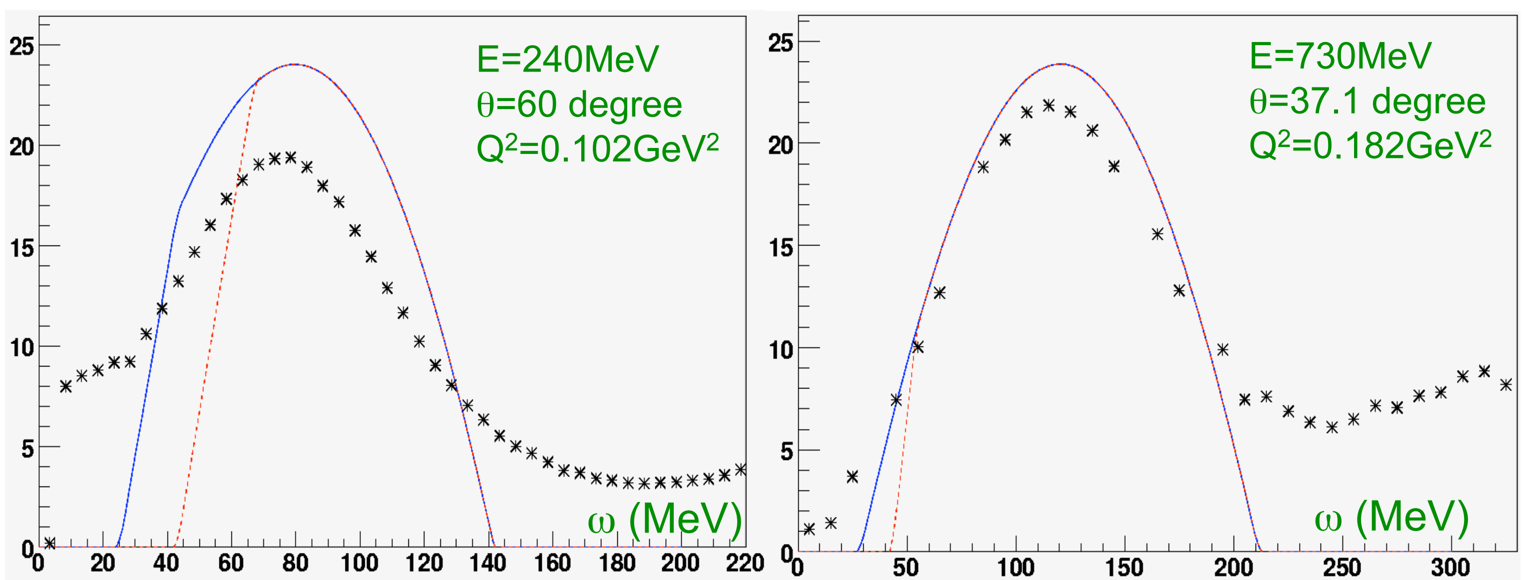

5. Kappa and (e,e') experiments

In low |q|, The RFG model systematically over predicts cross section for electron scattering experiments at low |q| (~low Q^2)

We had investigated the effect of Pauli blocking parameter "κ" in (e,e') data. κ cannot fix the shape mismatching of (e,e') data for each angle and energy, but it can fix integral of each cross section data, which is the observables for neutrino experiments. We conclude κ is consistent with (e,e') data.

RFG prediction-(e,e') data ratio in Q^2 (GeV^2)

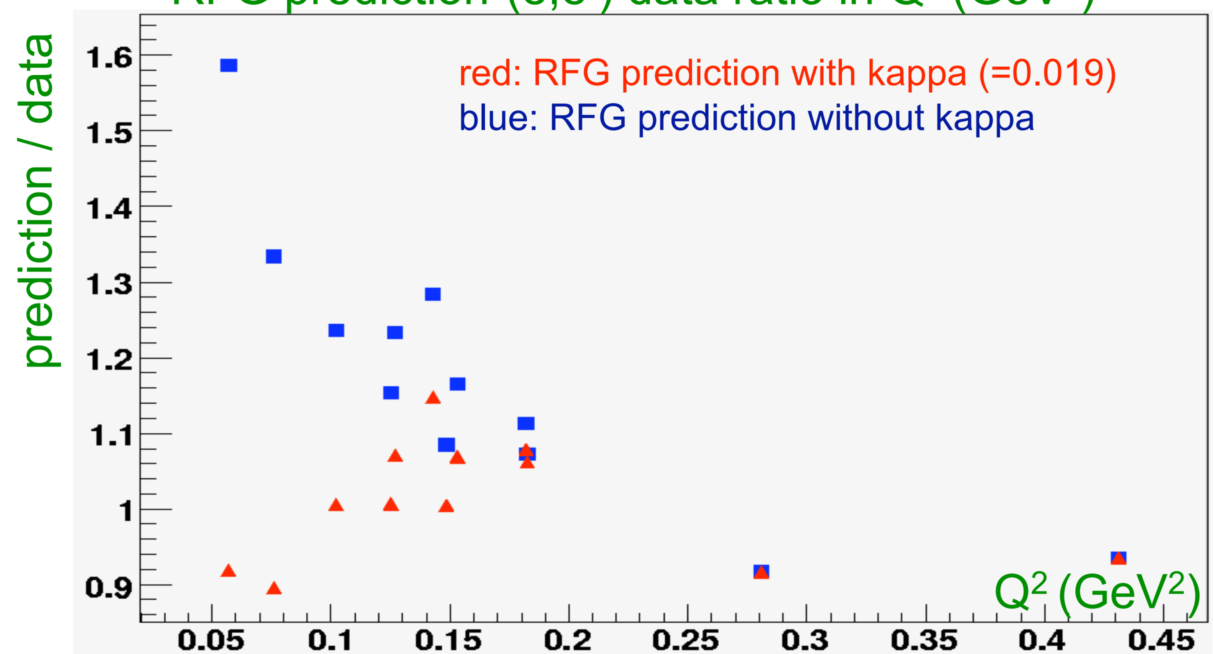

5. M_A^{eff}-κ shape-only fit

M_A^{eff} - κ shape-only fit result

M_A^{eff} = 1.35 ± 0.17 GeV (stat+sys)
κ = 1.007 $^{+0.007}_{-\infty}$ (stat+sys)
χ^2/ndf = 47.0/38

Q2 fits to MB ν_μ CCQE data using the nuclear parameters:

$M_A$eff - effective axial mass
κ - Pauli Blocking parameter

Relativistic Fermi Gas Model with tuned parameters describes ν_μ CCQE data well

Q2 distribution before and after fitting

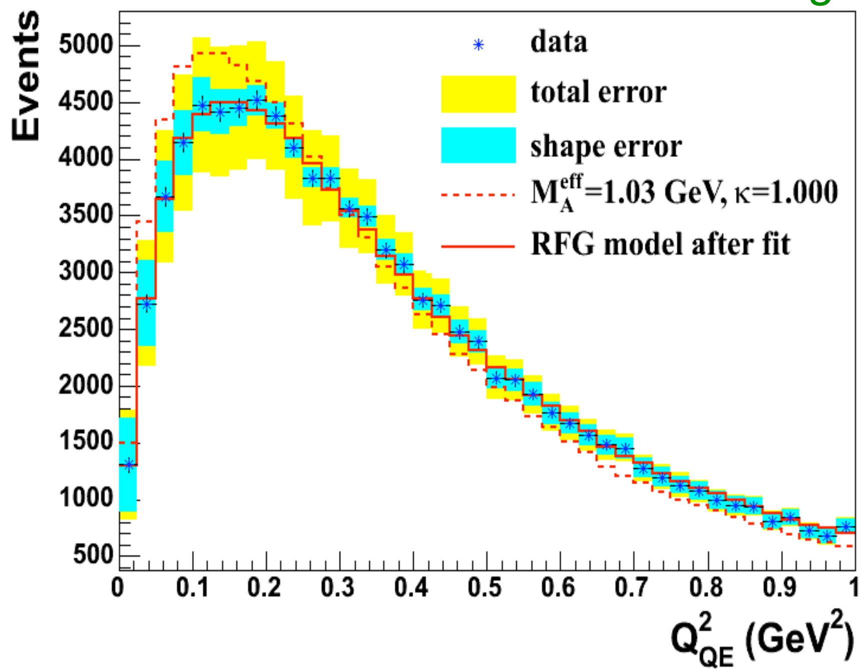

5. M_A^{eff}-κ shape-only fit

M_A^{eff} - κ shape-only fit result

M_A^{eff} = 1.35 ± 0.17 GeV (stat+sys)
$\kappa = 1.007^{+0.007}_{-\infty}$ (stat+sys)
χ^2/ndf = 47.0/38

M_A^{eff} only fit
M_A^{eff} = 1.37 ± 0.12 GeV
χ^2/ndf = 48.6/39

M_A^{eff} goes even up, this is related to our new background subtraction.

κ goes down due to the shape change of the background. Now κ is consistent with 1.
κ doesn't affects cross section below ~0.995.

Fit parameter space

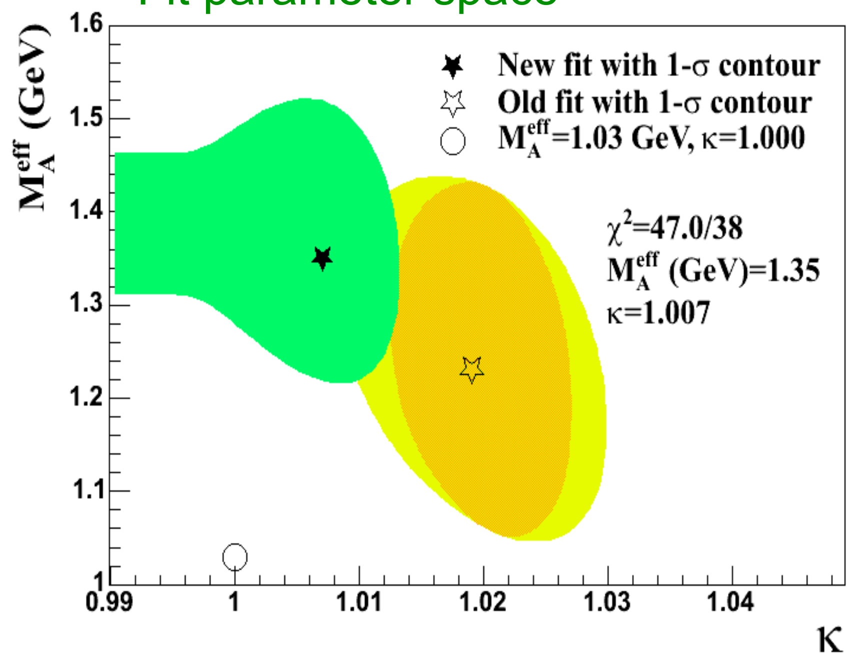

5. M_A^{eff}-κ shape-only fit

M_A^{eff} - κ shape-only fit result

M_A^{eff} = 1.35 ± 0.17 GeV (stat+sys)
κ = 1.007 $^{+0.007}_{-\infty}$ (stat+sys)

Data-MC agreement in T_μ-$\cos\theta$ kinematic plane is good.

World averaged RFG model
M_A^{eff} = 1.03, κ = 1.000

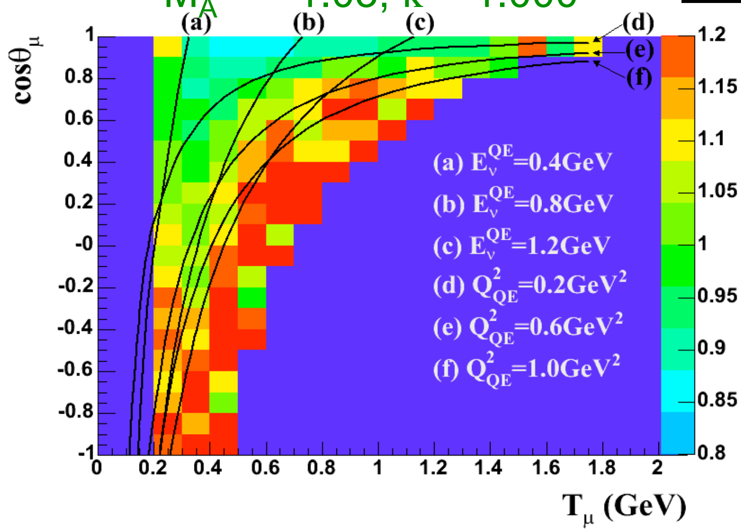

This new CCQE model doesn't affect our cross section result.

data-MC ratio in T_μ-$\cos\theta$ kinematic plane after fit

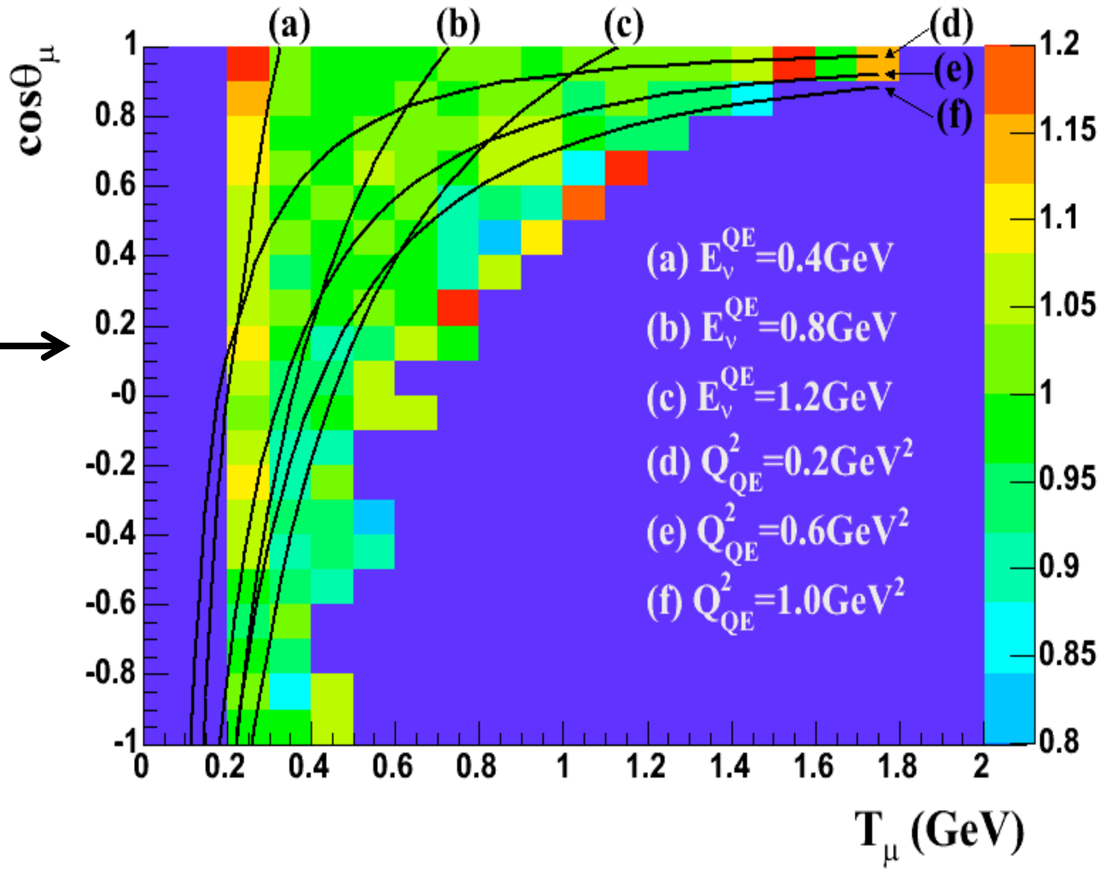

MiniBooNE collaboration,
PRL100(2008)032301

5. T_μ-$\cos\theta_\mu$ plane

Without knowing flux perfectly, we cannot modify cross section model

$$R(\mathrm{interaction}) \propto \int (\mathrm{flux}) \times (\mathrm{xs})$$

Data-MC ratio for T_μ-$\cos\theta_\mu$ plane, before tuning

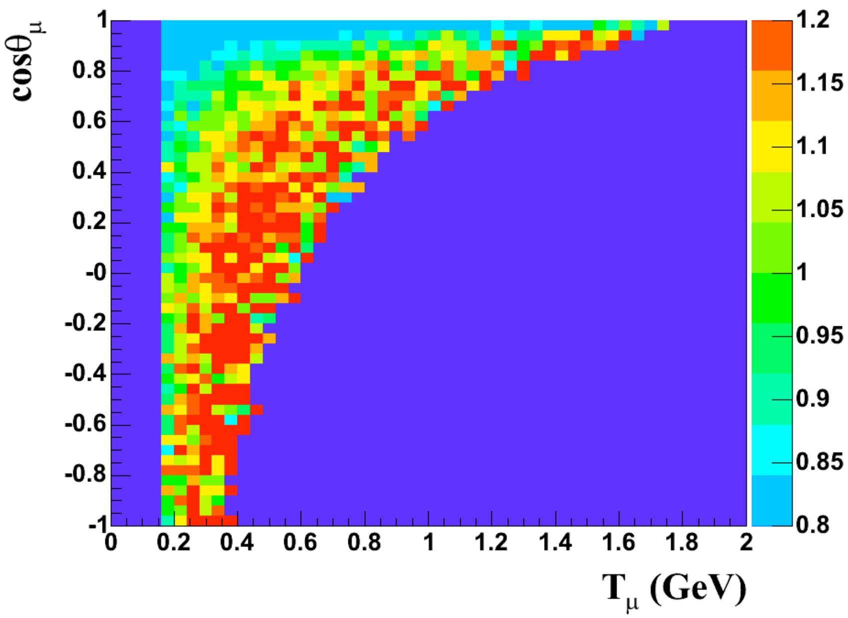

MiniBooNE collaboration,
PRL100(2008)032301

5. T_μ-$\cos\theta_\mu$ plane

Without knowing flux perfectly, we cannot modify cross section model

$$R(\mathrm{interaction}[E_\nu, Q^2]) \propto \int (\mathrm{flux}[E_\nu]) \times (\mathrm{xs}[Q^2])$$

Data-MC mismatching follows Q2 lines, not E_ν lines, therefore we can see the problem is not the flux prediction, but the cross section model

Data-MC ratio for T_μ-$\cos\theta_\mu$ plane, before tuning

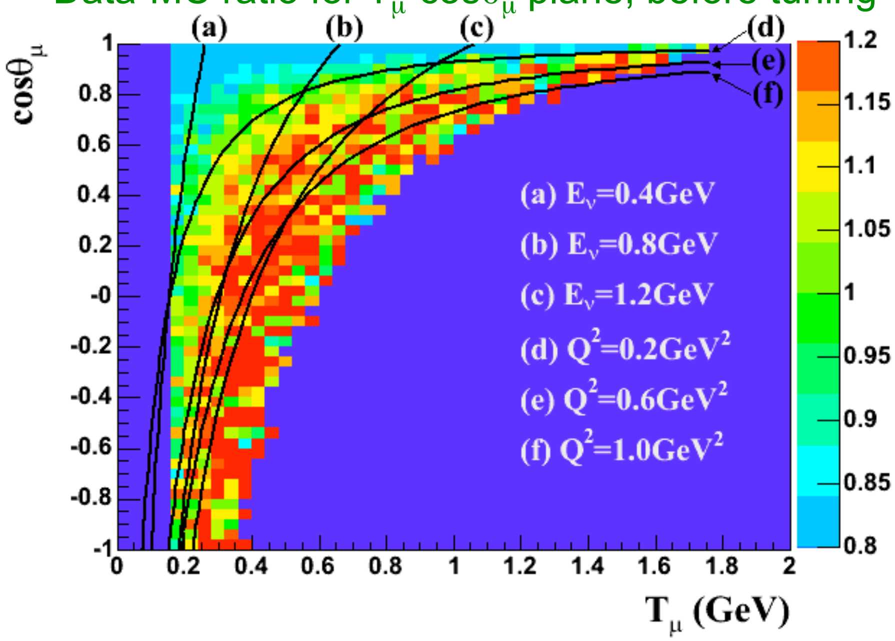

MiniBooNE collaboration,
PRL100(2008)032301

5. T_μ-$\cos\theta_\mu$ plane

Without knowing flux perfectly, we cannot modify cross section model

$$R(\mathrm{interaction}[E_\nu, Q^2]) \propto \int (\mathrm{flux}[E_\nu]) \times (\mathrm{xs}[Q^2])$$

Data-MC mismatching follows Q2 lines, not E_ν lines, therefore we can see the problem is not the flux prediction, but the cross section model

Data-MC ratio for T_μ-$\cos\theta_\mu$ plane, before tuning

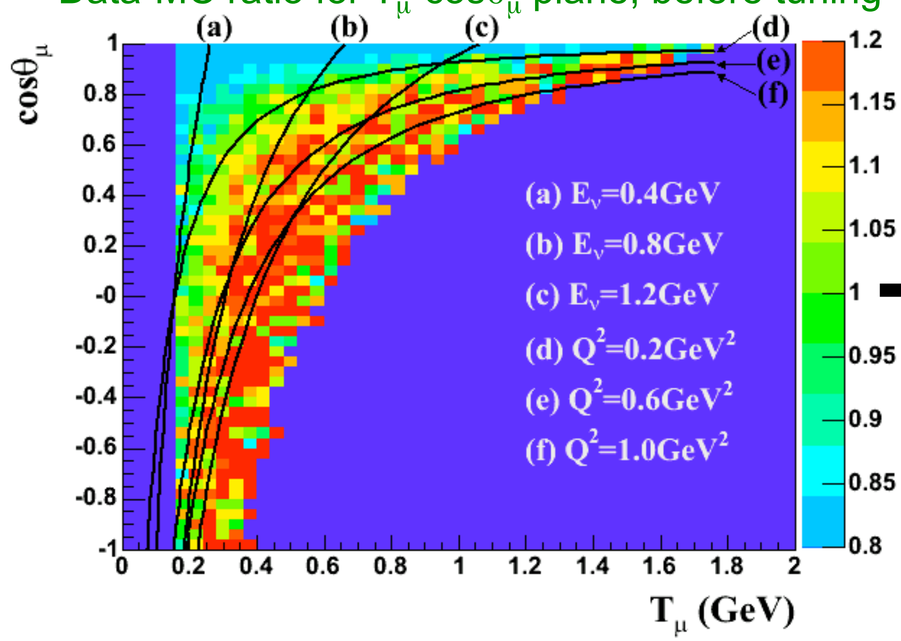

Data-MC ratio for T_μ-$\cos\theta_\mu$ plane,after tuning

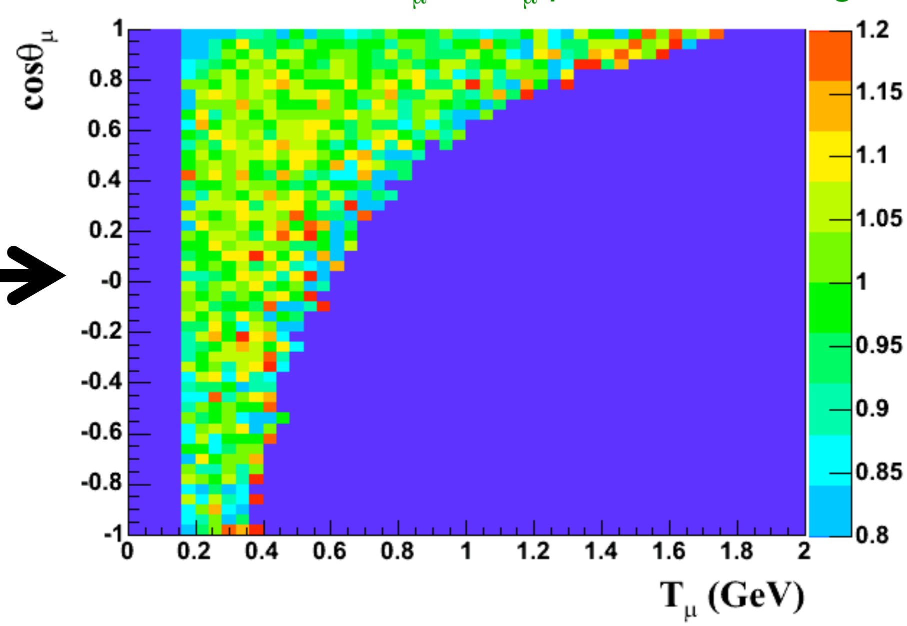

1. Booster neutrino beamline

2. MiniBooNE detector

3. CCQE events in MiniBooNE

4. CC1π background constraint

5. CCQE M_A^{eff}-κ shape-only fit

6. CCQE absolute cross section

7 Conclusion

6. CCQE absolute cross section

Absolute flux-averaged differential cross section formula

i :true index
j : reconstructed index

The cross section is function of true value, for example, $d\sigma^2/T_\mu/\cos\theta_\mu$, $d\sigma/dQ^2_{QE}$, etc

Integrated flux is removed, so it is called flux-averaged cross section
If flux is corrected bin-by bin, it is called flux-unfolded cross section

U_{ij} :unsmearing matrix

d_j :data vector

b_j :predicted background

$$\sigma_i = \frac{\sum_j U_{ij}(d_j - b_j)}{\varepsilon_i (\Phi T)}$$

T :integrated target number

ε_i :efficiency

Φ :integrated ν-flux

6. CCQE absolute cross section

$$\sigma_i = \frac{\sum_j U_{ij} \boxed{(d_j - b_j)}}{\varepsilon_i (\Phi T)}$$

Absolute flux-averaged differential cross section formula

i :true index
j : reconstructed index

The predicted background (MC based on data driven tuning) is subtracted from data bin by bin (reconstructed bin)

MC also provide the distribution of irreducible background (have to be defined carefully).

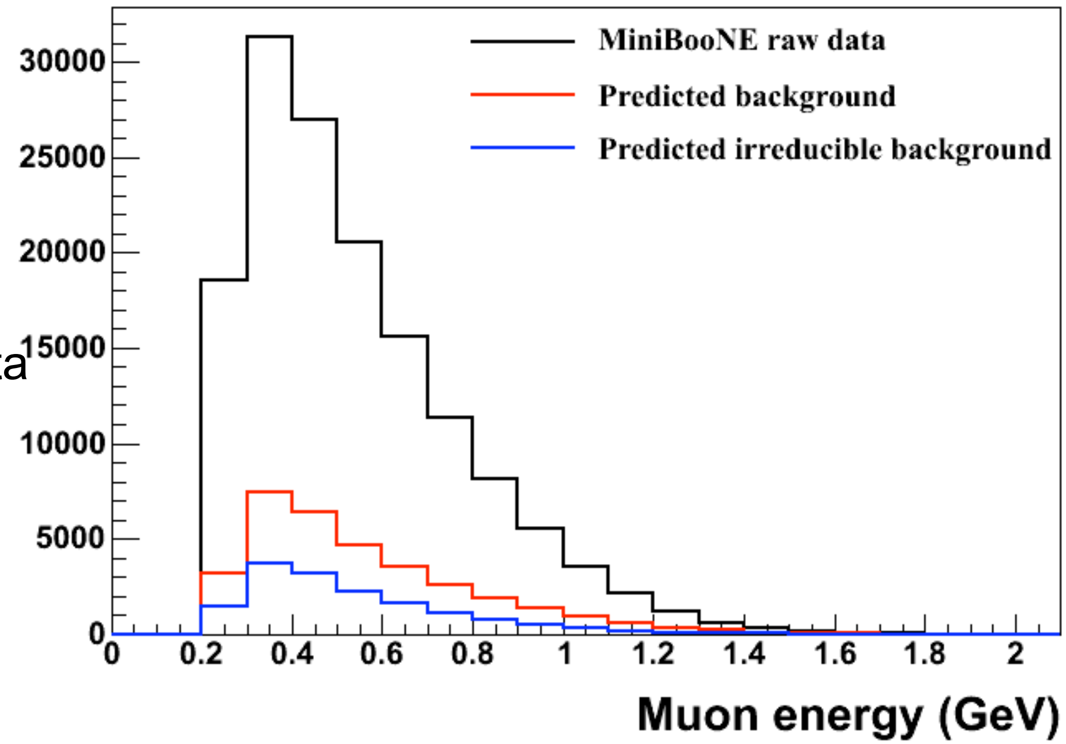

6. CCQE absolute cross section

D'Agostini, NIM.A362(1995)487

$$\sigma_i = \frac{\sum_j \boxed{U_{ij}} (d_j - b_j)}{\varepsilon_i (\Phi T)}$$

Absolute flux-averaged differential cross section formula

i :true index
j : reconstructed index

True distribution is obtained from unsmearing matrix made by MC. This technique is called "iterative Bayesian method" and known to be biased (discuss later).

Notice, this unsmearing corrects detector effect of muon detection, and no nuclear model dependence.

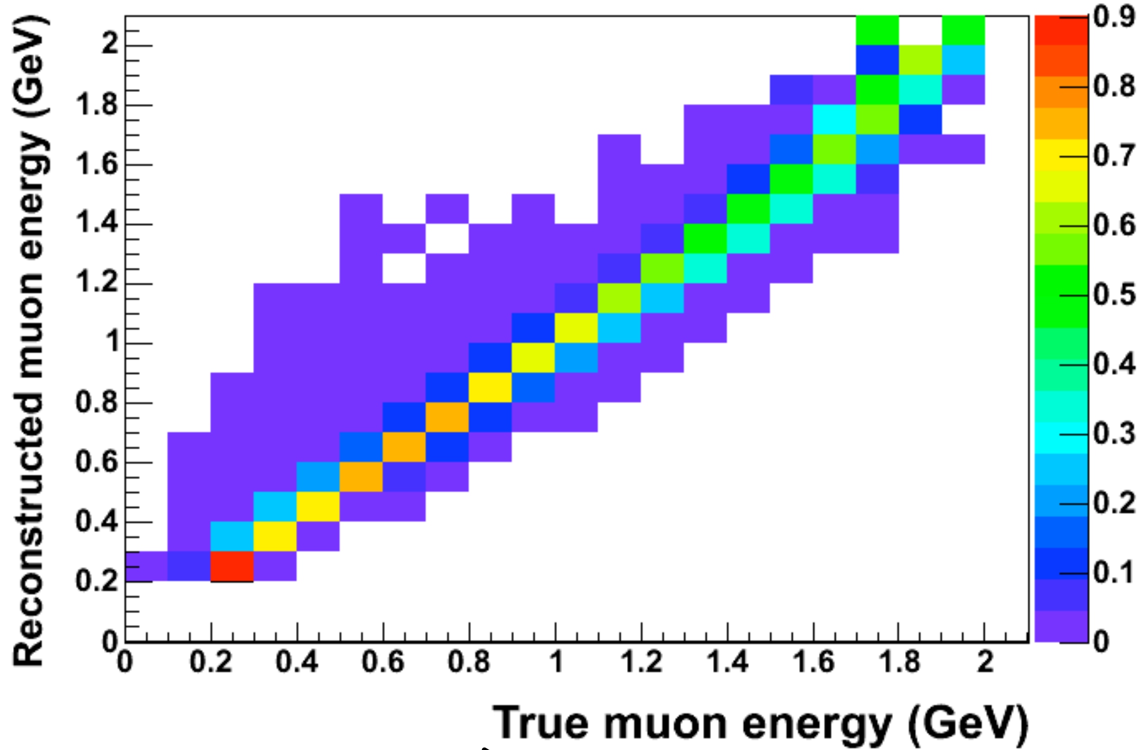

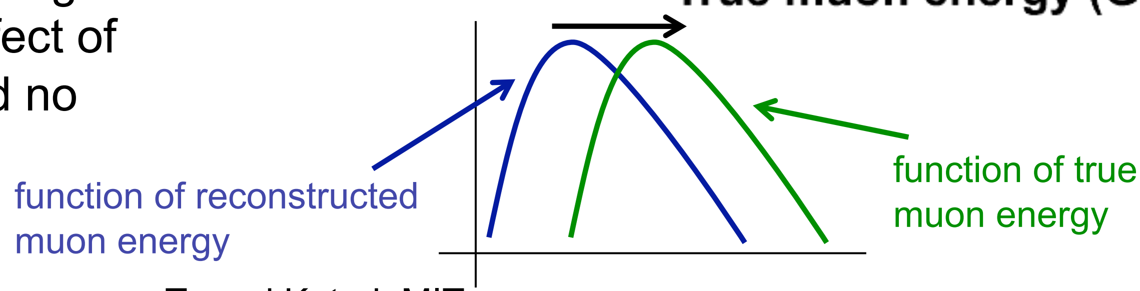

6. CCQE absolute cross section

D'Agostini, NIM.A362(1995)487

$$\sigma_i = \frac{\sum_j U_{ij}(d_j - b_j)}{\boxed{\varepsilon_i}\,(\Phi T)}$$

Absolute flux-averaged differential cross section formula

i :true index
j : reconstructed index

Then, efficiency is corrected bin by bin (true bin).

Again, efficiency correction correct detection efficiency of muon, and no nuclear model dependence.

Other word, if target distribution is reconstructed variable (Q^2, $E\nu$, etc), you have to be careful how these processes have been done.

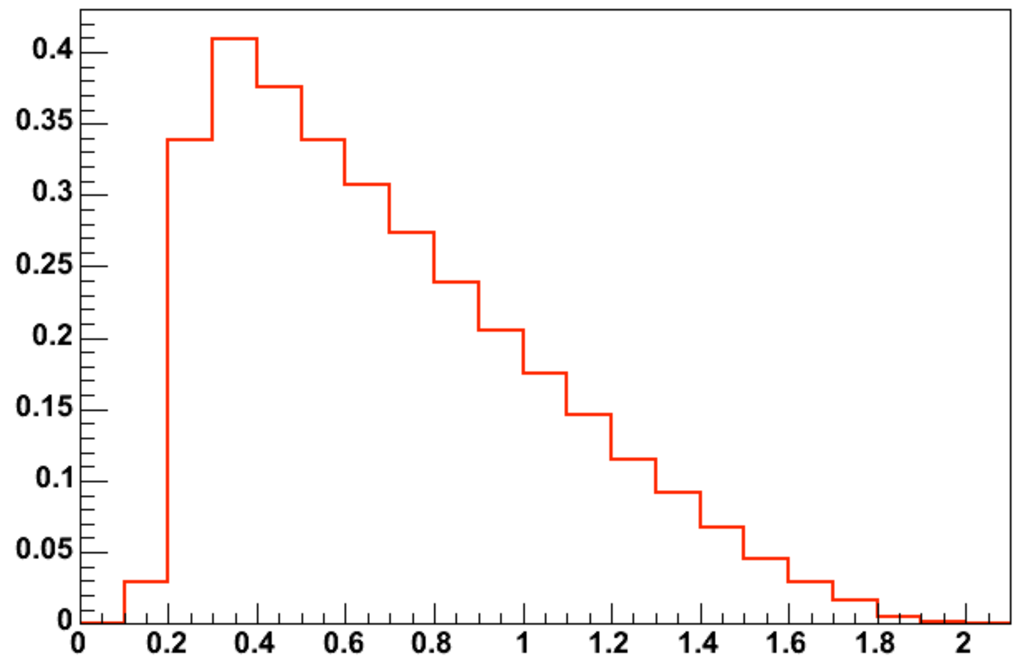

Efficiency of muon detection (GeV)

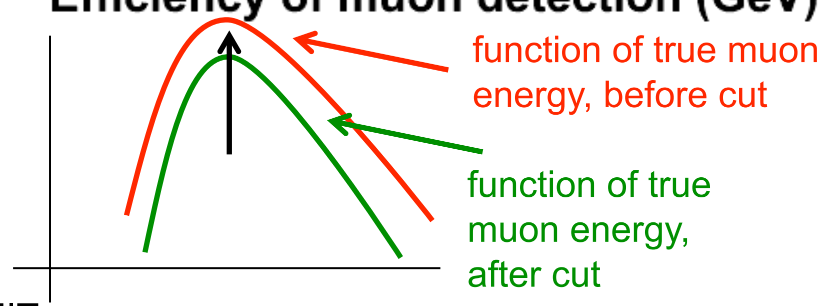

6. CCQE absolute cross section

D'Agostini, NIM.A362(1995)487

$$\sigma_i = \frac{\sum_j \boxed{U_{ij}} (d_j - b_j)}{\boxed{\varepsilon_i} (\Phi T)}$$

Absolute flux-averaged differential cross section formula

i :true index
j : reconstructed index

Then, efficiency corrected data is used to generate next unsmearing matrix (1st iteration). Any higher iteration gives ~same result.

Irreducible background is unfolded same way, by assuming efficiency is same.

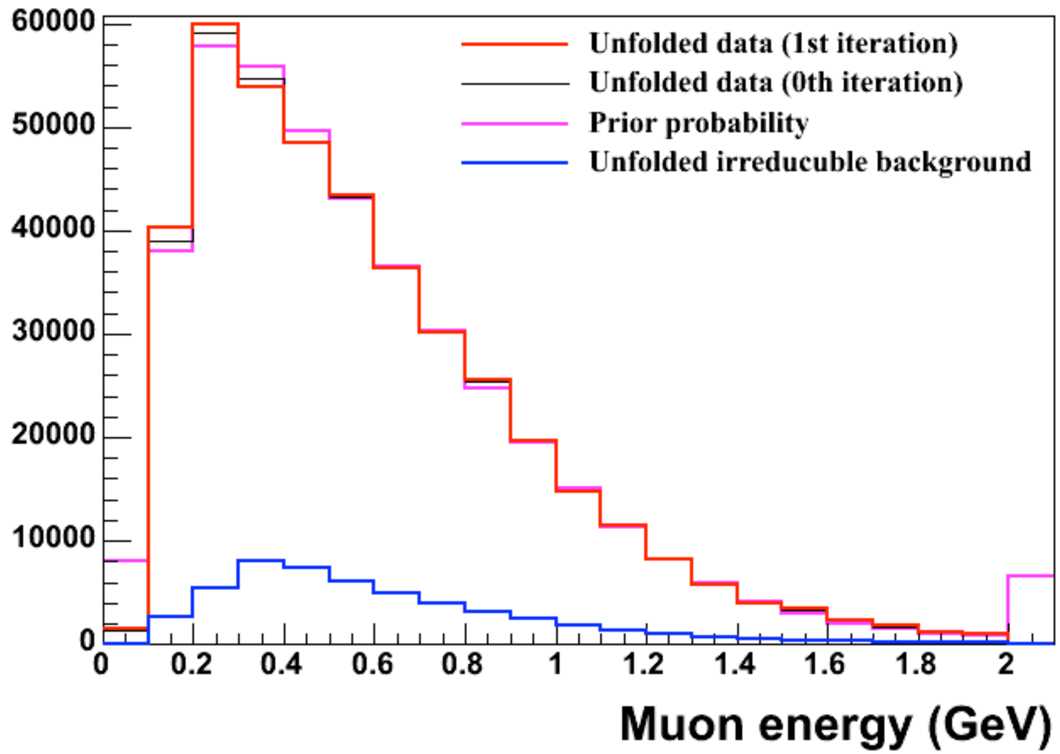

6. CCQE absolute cross section

$$\sigma_i = \frac{\sum_j U_{ij}(d_j - b_j)}{\varepsilon_i \boxed{(\Phi T)}}$$

Absolute flux-averaged differential cross section formula

i :true index
j : reconstructed index

Finally, total flux and target number are corrected.

MiniBooNE flux prediction 100% rely on external beam measurement (HARP) and beamline simulation, and it doesn't depend on neutrino measurements by MiniBooNE.

Predicted ν_μ-flux in MiniBooNE

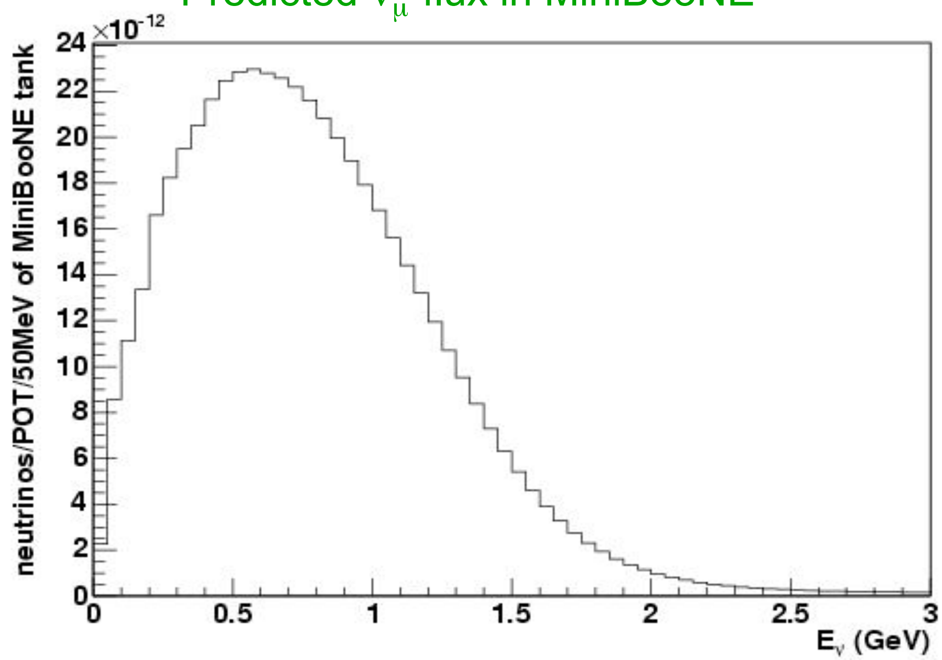

Flux Φ = integral of predicted ν_μ-flux
T = volume X oil density X neutron fraction

6. CCQE absolute cross section

Flux-averaged single differential cross section (Q^2_{QE})

The data is compared with various RFG model with neutrino flux averaged.

Compared to the world averaged CCQE model (red), our CCQE data is 30% high

Our model extracted from shape-only fit has better agreement (within our total normalization error).

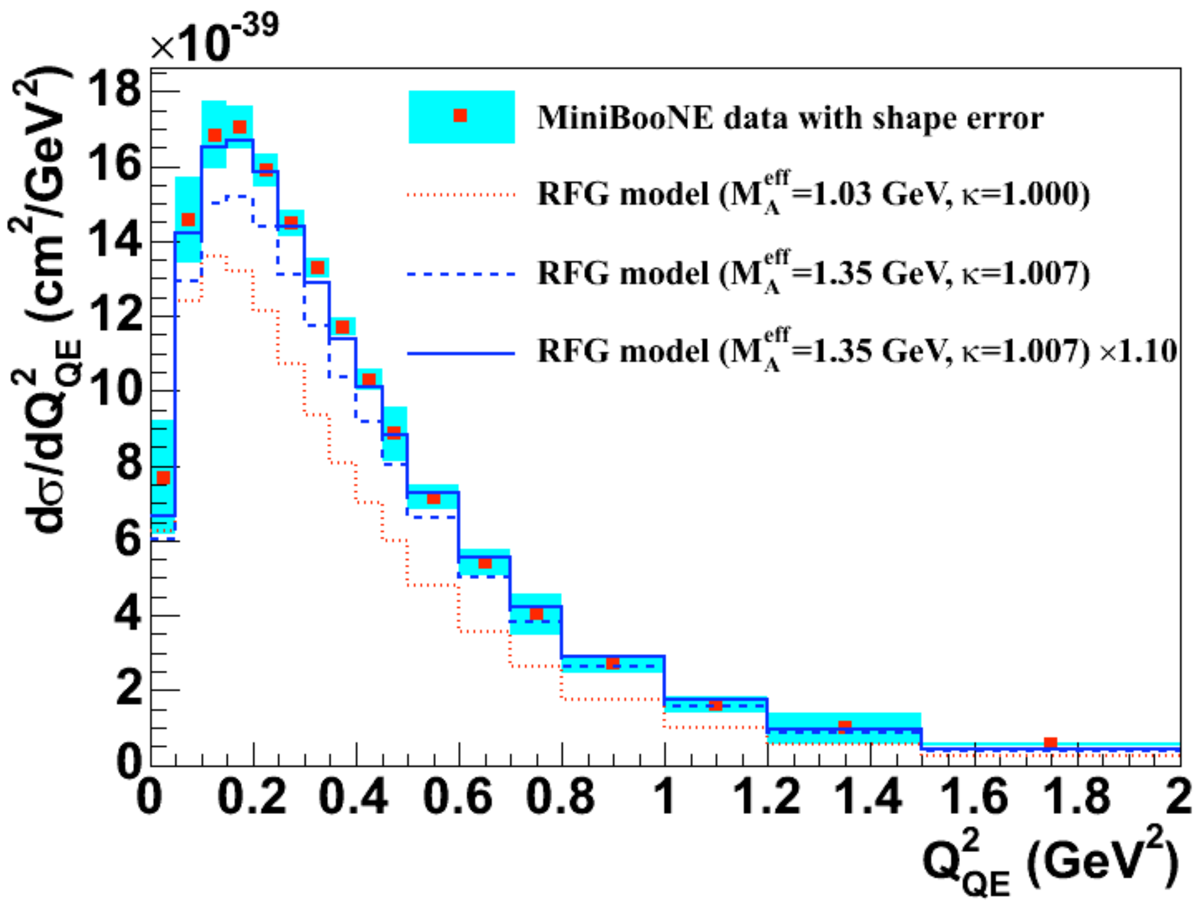

6. CCQE absolute cross section

Flux-averaged single differential cross section (Q^2_{QE})

Irreducible background distribution is overlaid.

Sum of CCQE cross section and irreducible background makes cross section of CCQE-like sample.

Remember, to do that, we need to assume irreducible background has same efficiency with CCQE, but that is not completely true.

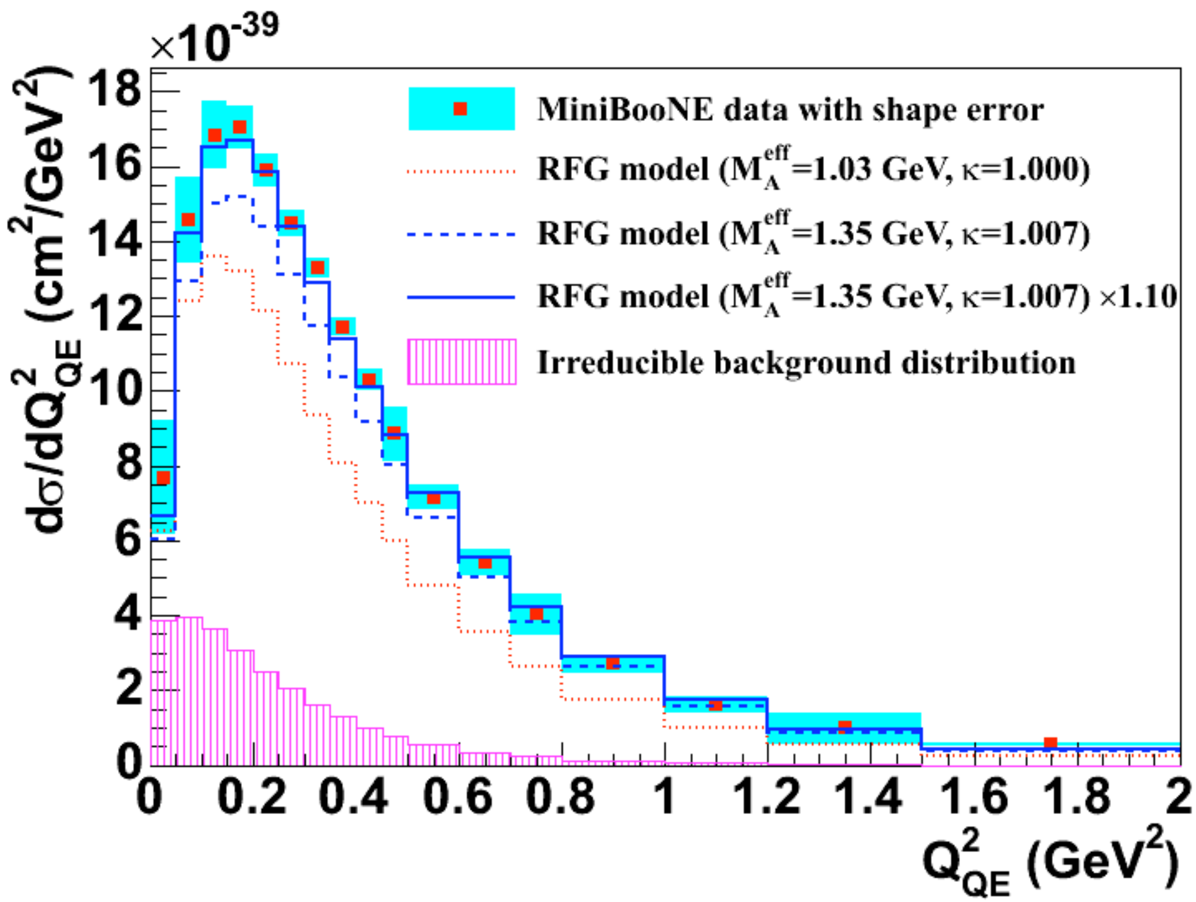

6. CCQE absolute cross section

Flux-unfolded total cross section ($E_\nu^{QE,RFG}$)

New CCQE model is tuned from shape-only fit in Q^2, and it also describes total cross section well.

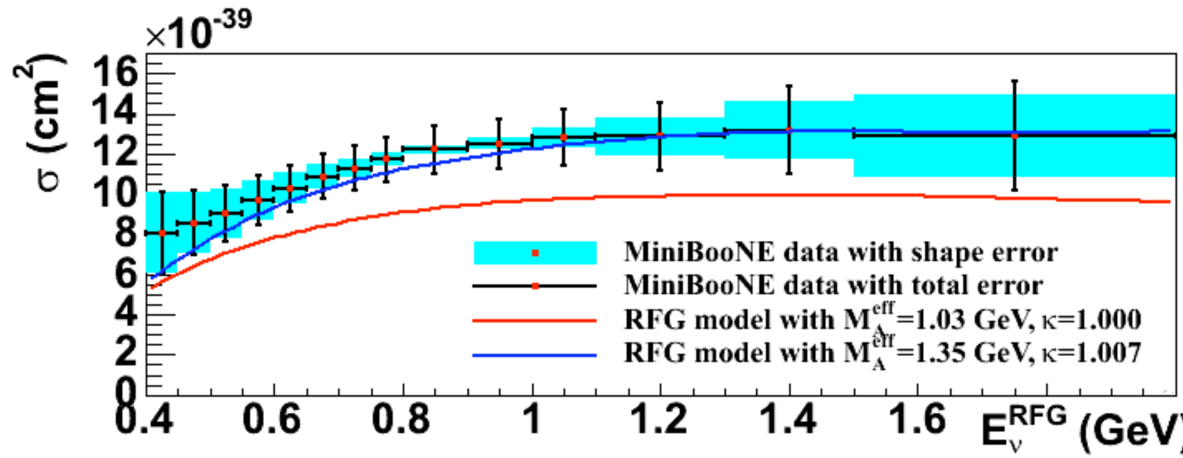

6. CCQE errors

Error summary (systematic error dominant)

Flux error dominates the total normalization error.

Cross section error is small because of high purity and in situ background measurement.

Detector error dominates shape error, because this is related with energy scale.

Unfolding error is the systematic error associated to unfolding (iterative Bayesian method).

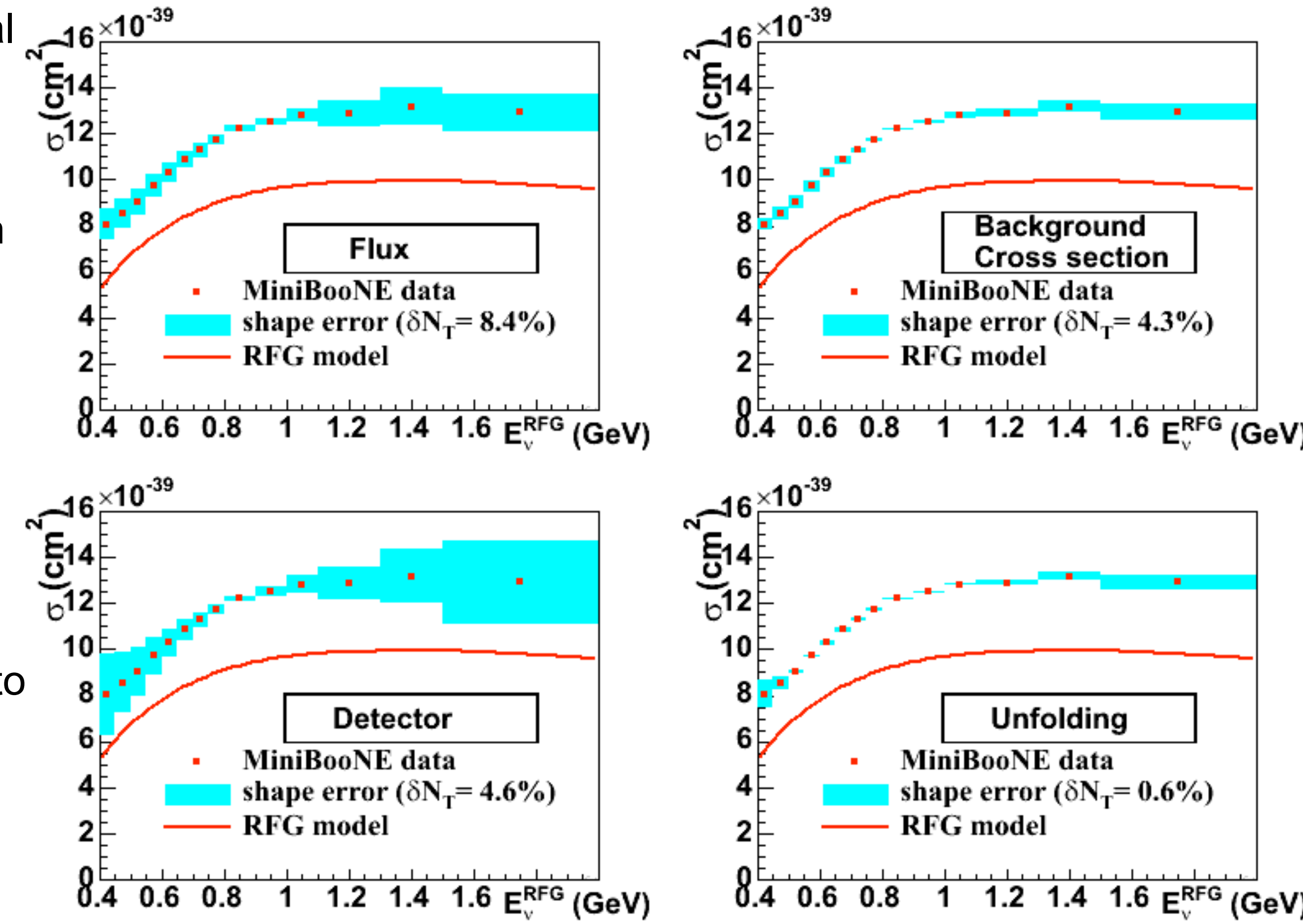

6. QE cross section comparison with NOMAD

Flux-unfolded total cross section ($E_\nu^{QE,RFG}$)

New CCQE model is tuned from shape-only fit in Q^2, and it also describes total cross section well.

Comparing with NOMAD, MiniBooNE cross section is 30% higher, but these 2 experiments leave a gap in energy to allow some interesting physics.

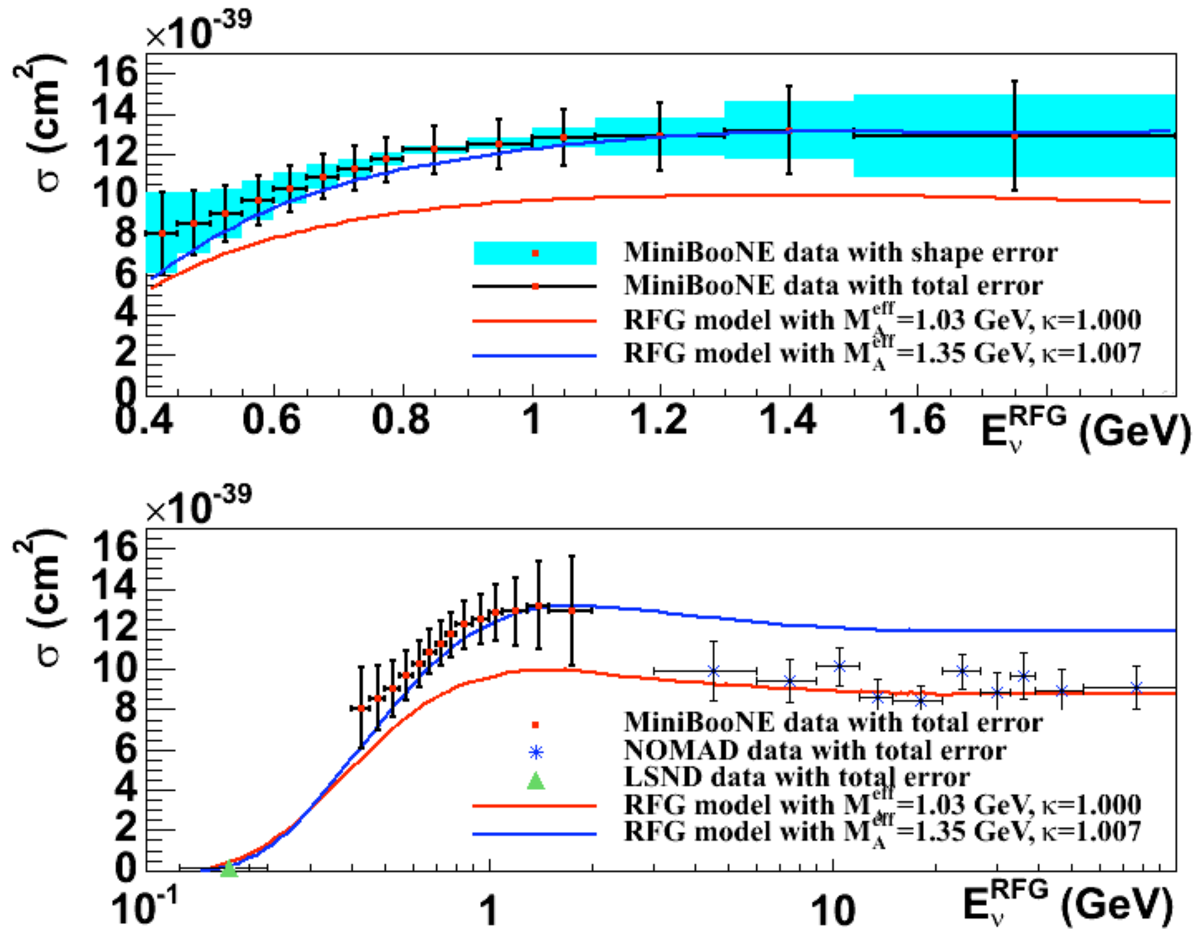

6. CCQE total cross section model dependence

Flux-unfolded total cross section ($E_\nu^{QE,RFG}$)

Unfortunately, flux unfolded cross section is model dependent.

Reconstruction bias due to "QE" assumption is corrected under "RFG" model assumption.

One should be careful when comparing flux-unfolded data from different experiments.

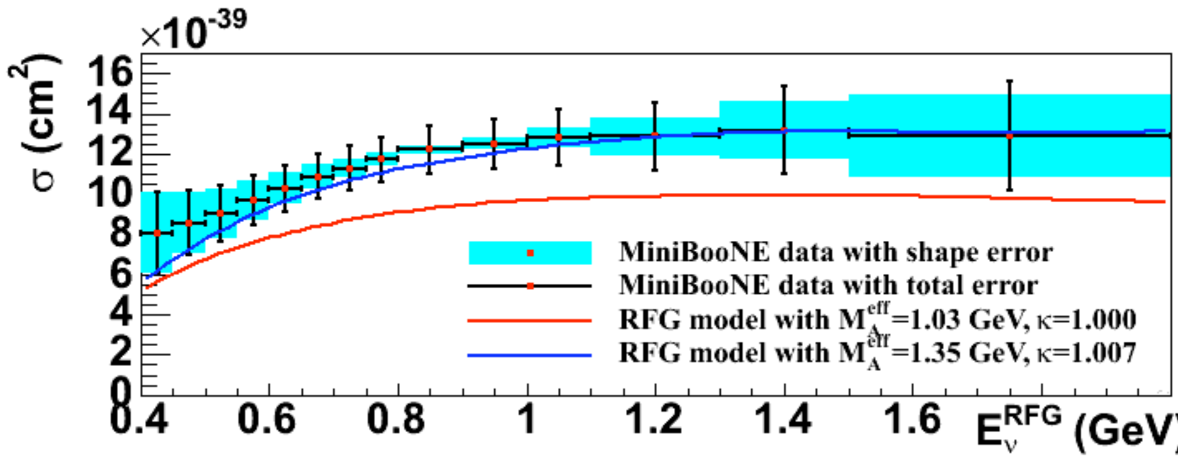

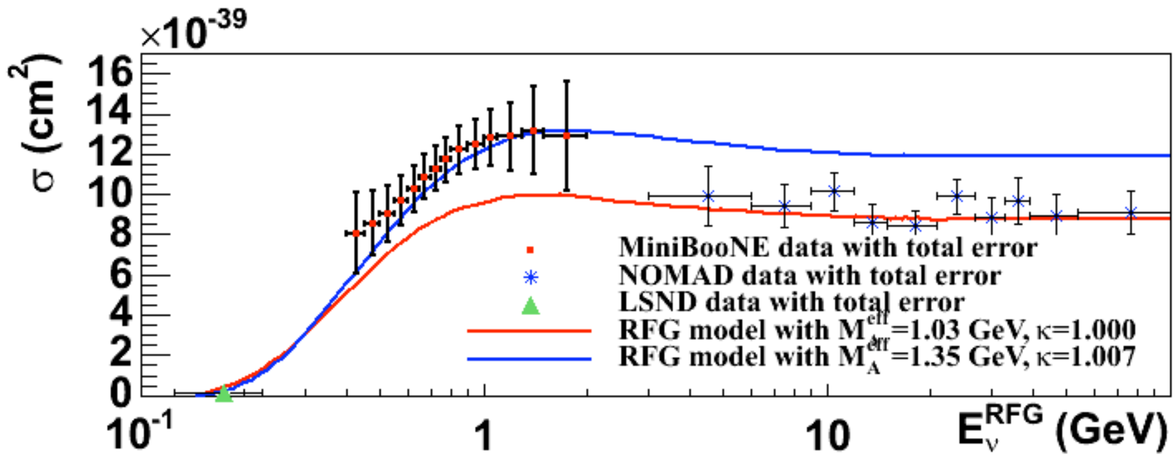

6. CCQE total cross section model dependence

Flux-unfolded total cross section (E_ν^{RFG})

Unfortunately, flux unfolded cross section is model dependent.

Reconstruction bias due to “QE” assumption is corrected under “RFG” model assumption.

One should be careful when comparing flux-unfolded data from different experiments.

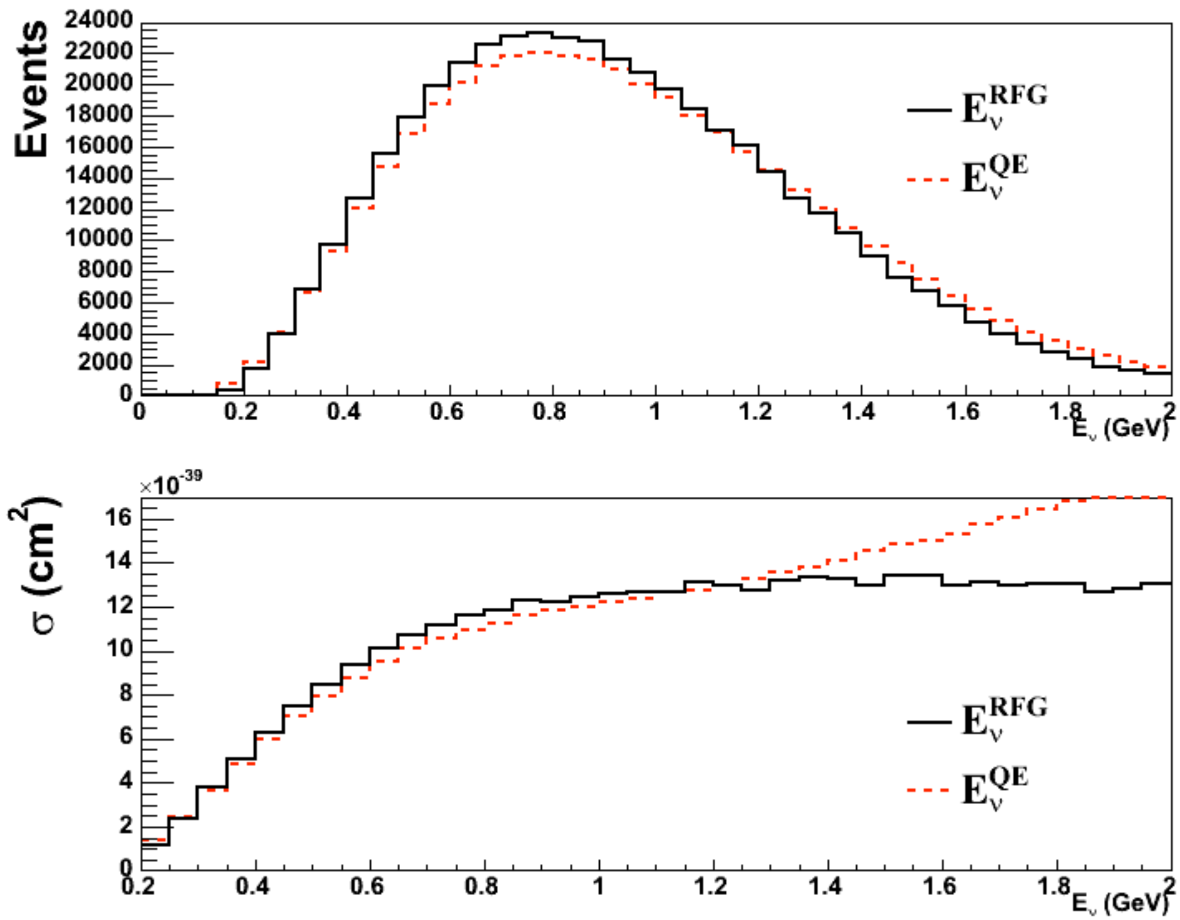

6. CCQE double differential cross section

Flux-averaged double differential cross section (T_μ-$\cos\theta$)

This is the most complete information about neutrino cross section based on muon kinematic measurement.

The error shown here is shape error, a total normalization error (δN_T=10.7%) is separated.

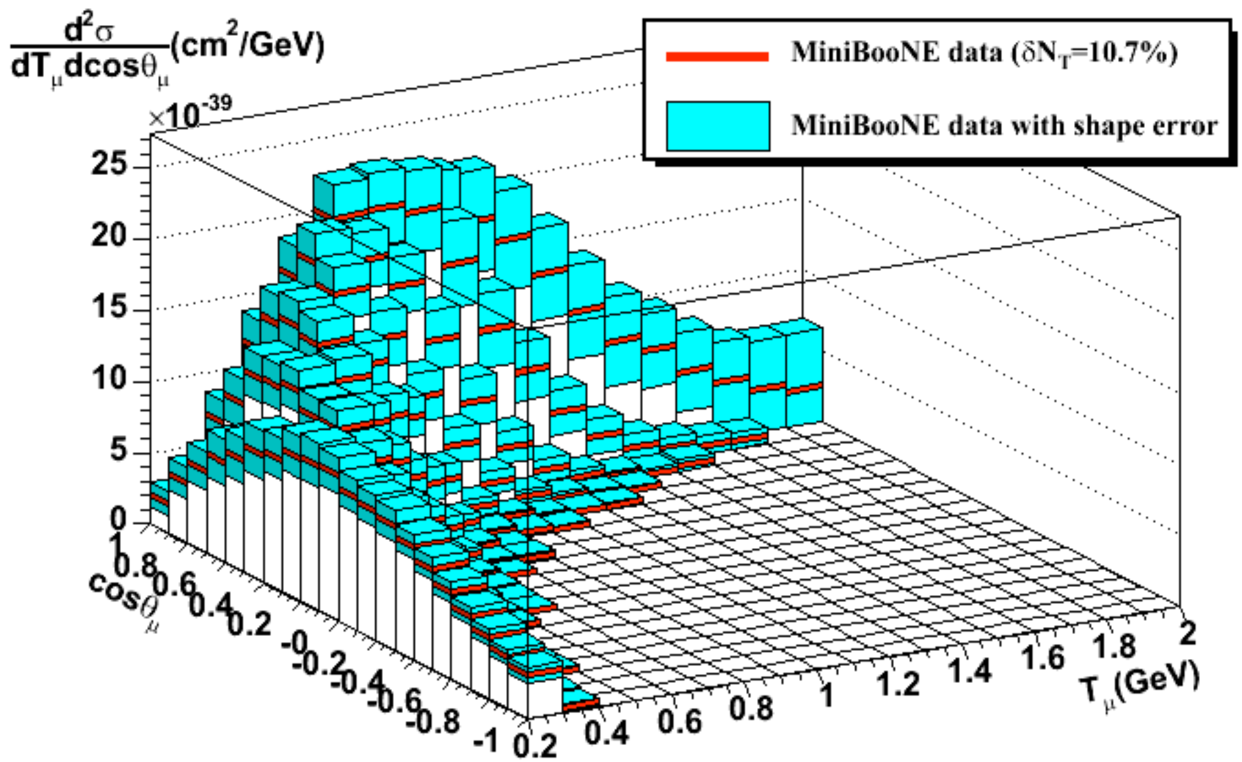

6. CCQE double differential cross section

Flux-averaged double differential cross section (T_{μ}-$\cos\theta$)

This is the most complete information about neutrino cross section based on muon kinematic measurement.

The error shown here is shape error, a total normalization error (δN_T=10.7%) is separated.

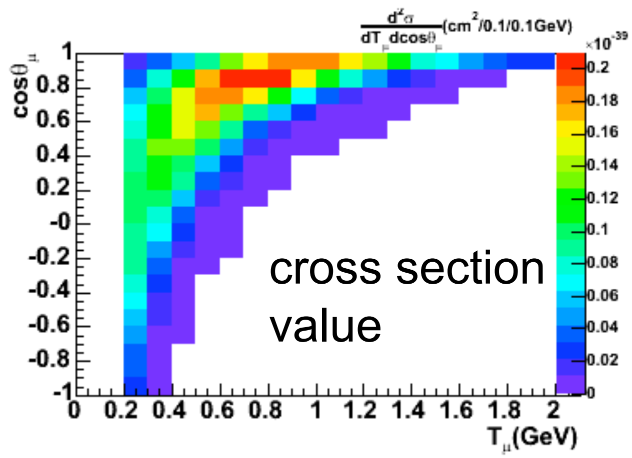

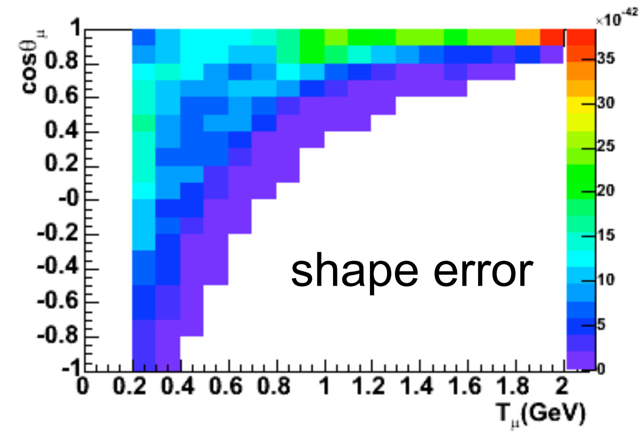

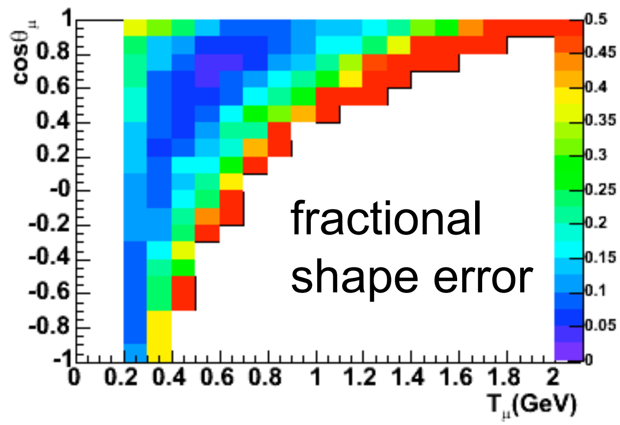

7. Conclusions

Using the high statistics and high purity MiniBooNE ν_μ CCQE data sample (146,070 events, 27% efficiency, and 77% purity), the absolute cross section is measured. We especially emphasize the measurement of flux-averaged double differential cross section, because this is the most complete set of information for muon kinematics based neutrino interaction measurement. The double differential cross section is the model independent result.

We measured 30% higher cross section than RFG model with the world averaged nuclear parameter. Interesting to note, our total cross section is consistent with RFG model with nuclear parameters extracted from shape-only fit in our Q^2 data.

BooNE collaboration

University of Alabama
Bucknell University
University of Cincinnati
University of Colorado
Columbia University
Embry Riddle Aeronautical University
Fermi National Accelerator Laboratory
Indiana University
University of Florida
Los Alamos National Laboratory
Louisiana State University
Massachusetts Institute of Technology
University of Michigan
Princeton University
Saint Mary's University of Minnesota
Virginia Polytechnic Institute
Yale University

Dziękuję bardzo!

Back up

1. CCQE event measurement in MiniBooNE

CC inclusive cut

1. veto hits <6 for all subevents
2. 1st subevent is within beam window, 4400<T(ns)<6400
3. fiducial cut, muon vertex <500cm from tank center
4. visible energy cut, muon kinetic energy >200MeV
5. μ to e log likelihood cut
6. 2 and only 2 subevent
7. μ-e vertex distance cut

This cut is not designed to remove CC1π events, but trying to remove "others". This is an important step for CC1π background fit.

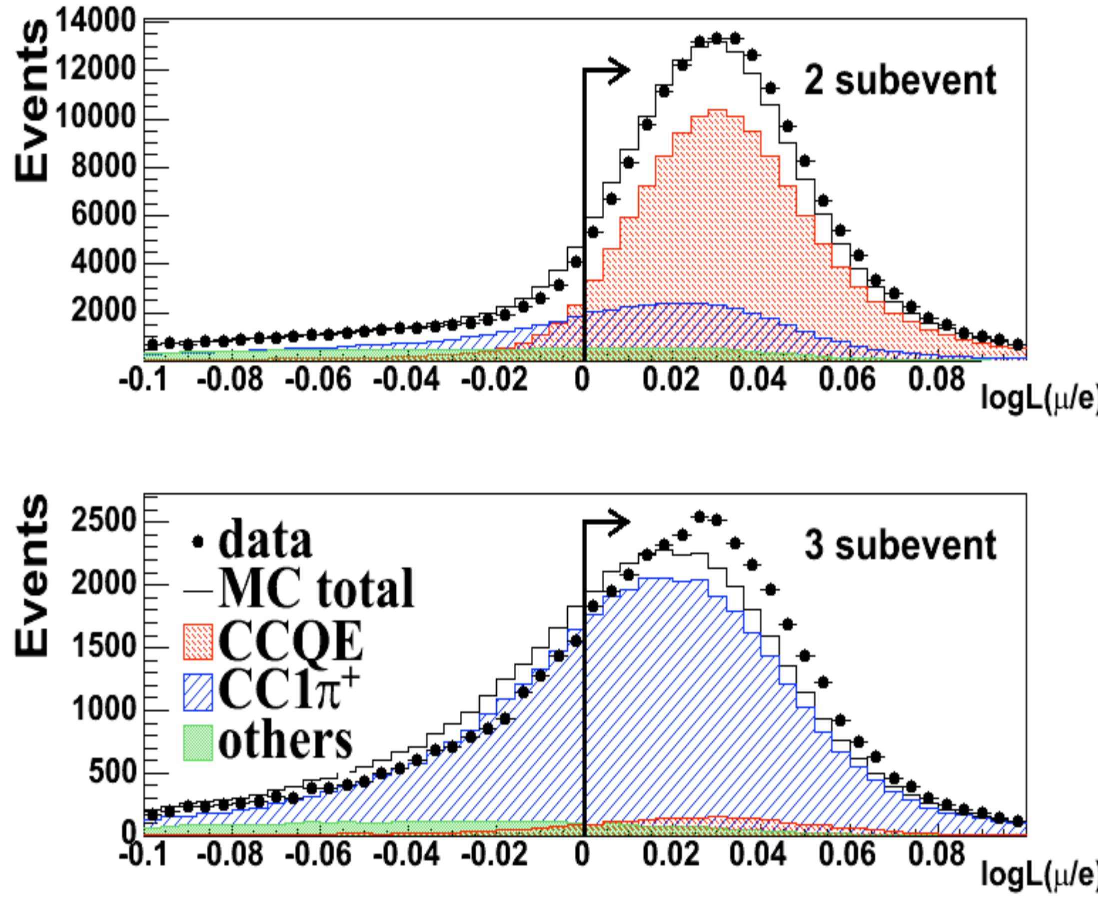

1. CCQE event measurement in MiniBooNE

CC inclusive cut
→ CCQE cut

1. veto hits <6 for all subevents
2. 1st subevent is within beam window, 4400<T(ns)<6400
3. fiducial cut, muon vertex <500cm from tank center
4. visible energy cut, muon kinetic energy >200MeV
5. μ to e log likelihood cut
6. 2 and only 2 subevent
7. μ-e vertex distance cut

ν_μ CCQE interactions (ν+n → μ+p) has characteristic two "subevent" structure from muon decay

$$\nu_\mu + n \rightarrow \boxed{\mu} + p \qquad \mu \rightarrow \nu_\mu + \nu_e + \boxed{e}$$

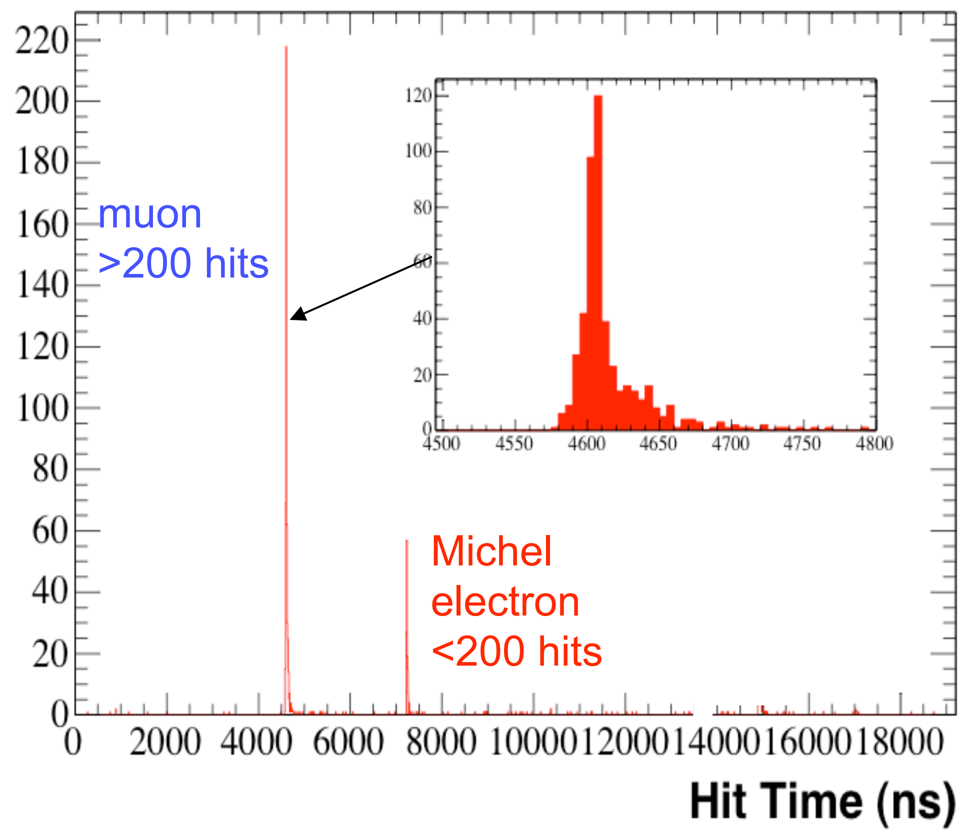

1. CCQE event measurement in MiniBooNE

CC inclusive cut
→ CCQE cut

1. veto hits <6 for all subevents
2. 1^{st} subevent is within beam window, 4400<T(ns)<6400
3. fiducial cut, muon vertex <500cm from tank center
4. visible energy cut, muon kinetic energy >200MeV
5. μ to e log likelihood cut
6. 2 and only 2 subevent
7. μ-e vertex distance cut

This cut is not designed to remove CC1π, but trying to remove "mis-reconstructed CC1π" and "others". This is an important step for CC1π background fit.

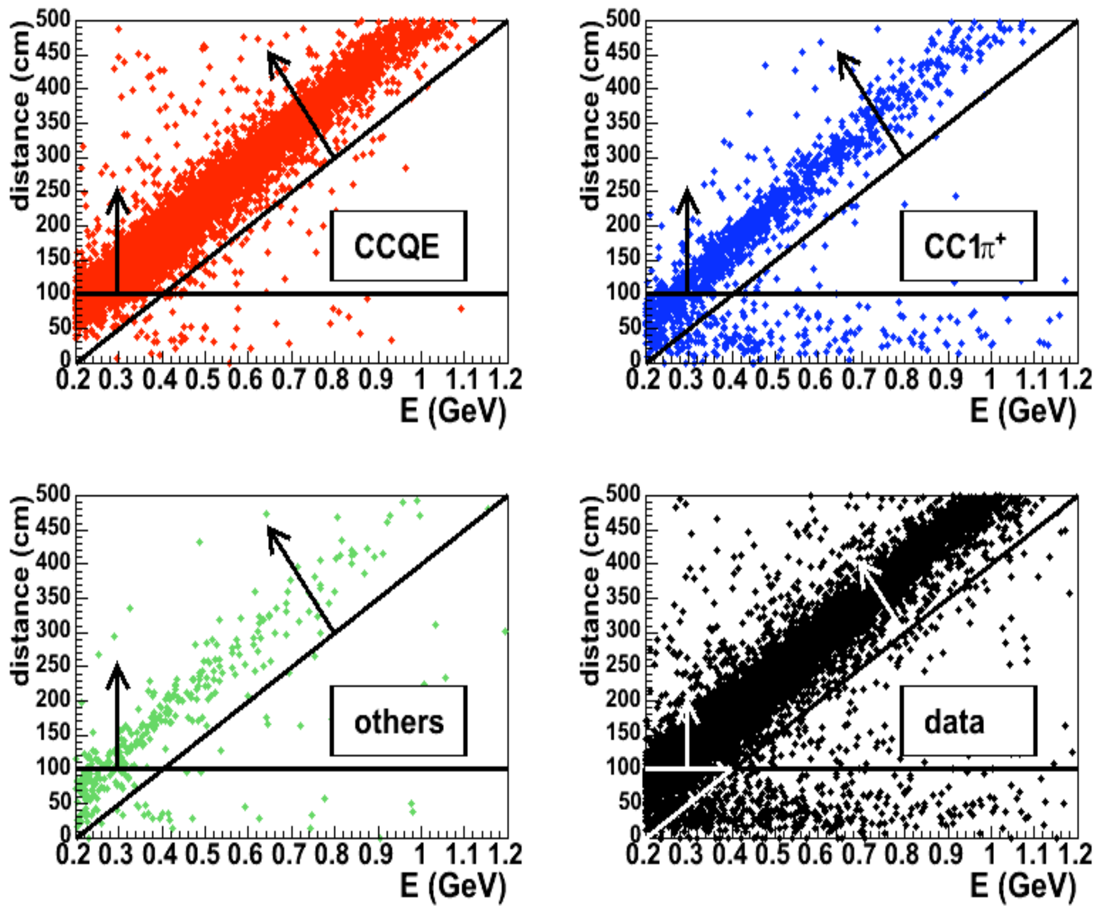

1. CCQE event measurement in MiniBooNE

cut type	efficiency
1. veto hits < 6 for all subevents	45.1
2. 1^{st} subevent time T is in beam window	44.7
3. 1^{st} subevent reconstructed vertex < 500 cm	37.5
4. 1^{st} subevent kinetic energy > 200MeV	32.7
5. μ to e log likelihood cut	31.3
6. 2 subevent total	29.0
7. μ-e vertex distance cut	26.5

26.5% cut efficiency
75.8% purity
146,070 events with
5.58E20POT

2. CC1π background fit

MC T_μ-cosθ plane

CC1π kinematics has different shape from CCQE kinematics.

The background cross section error is maximum at the bins where CC1π has larger number of event comparing with CCQE.

CCQE events with 2 subevent

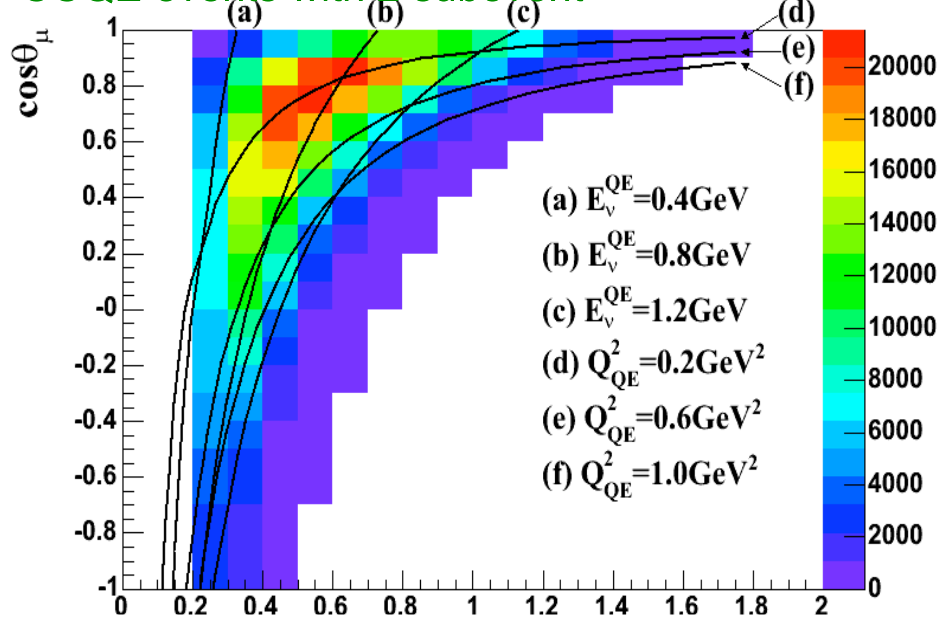

CC1π events with 2 subevent

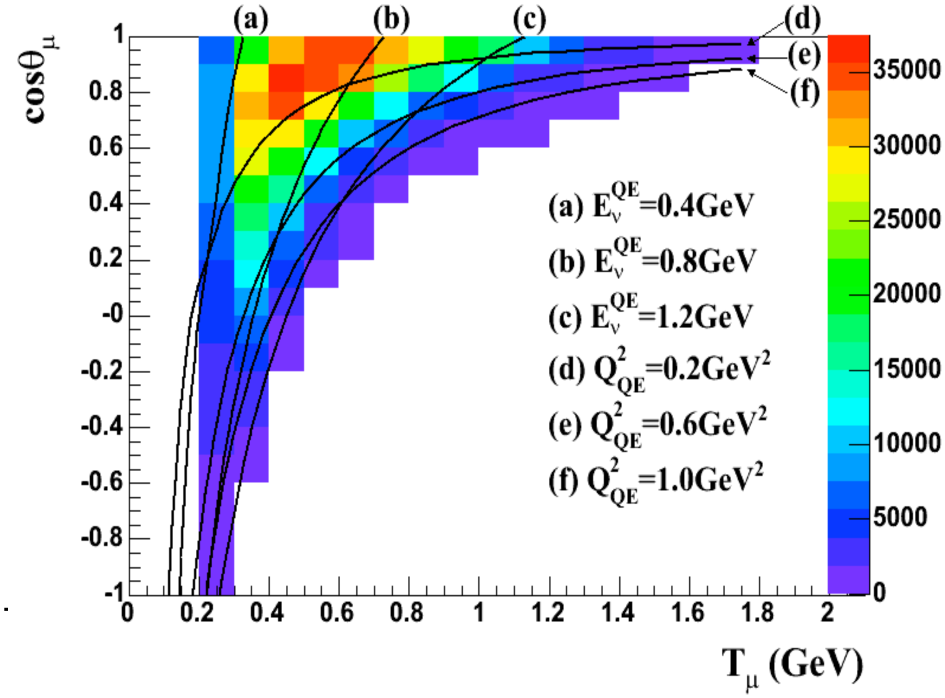

2. Energy scale of MiniBooNE

Mis-calibration of the detector can mimic large M_A value. Roughly, 2% of energy shift correspond to 0.1GeV change of M_A.

To bring M_A=1.0GeV, 7% energy shift is required, but this is highly disfavored from the data.

Question is what is the possible maximum mis-calibration? (without using muon tracker data)

M_A-κ fit for 2% muon energy shifted data

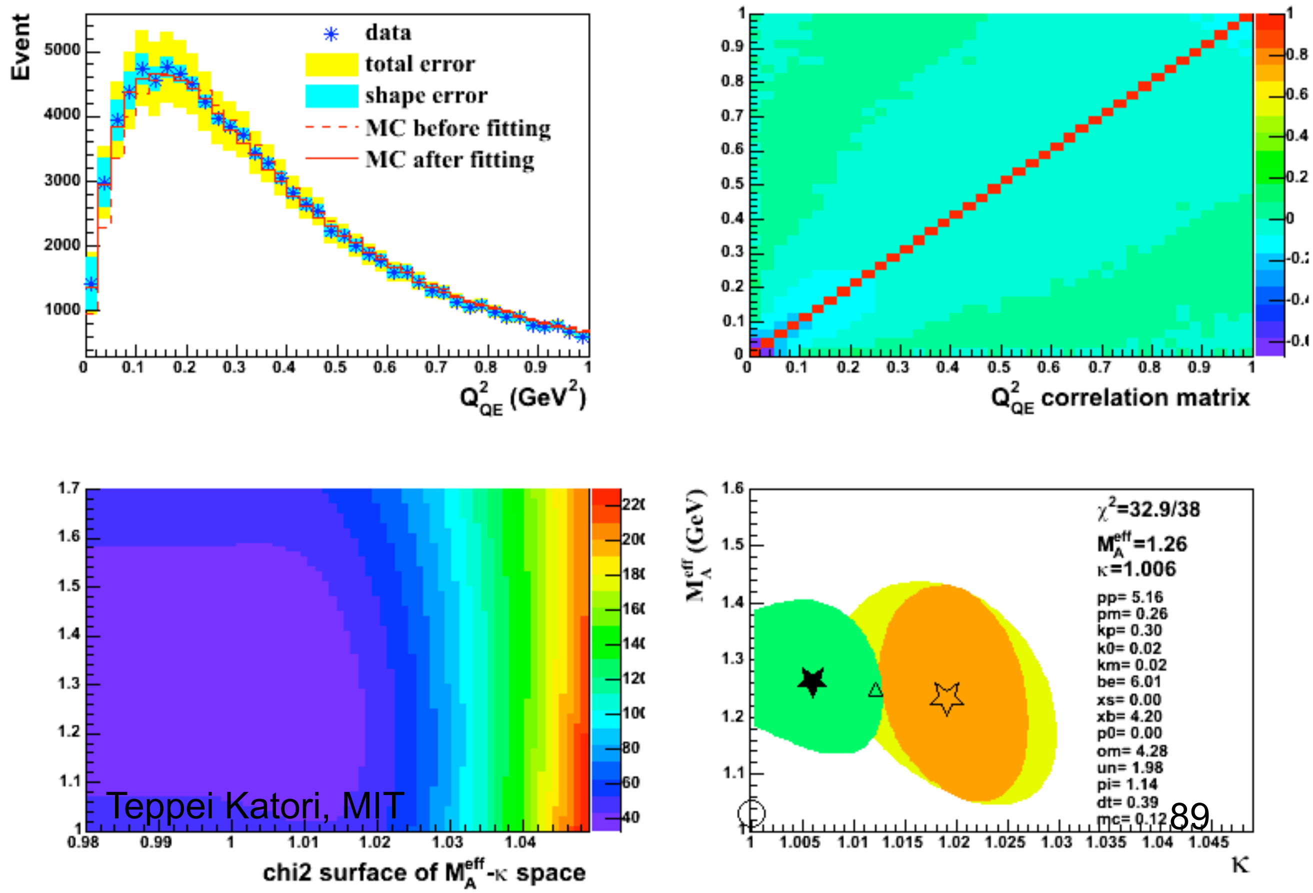

2. Energy scale of MiniBooNE

Energy resolution is very good.
Typical resolution is <10%, and the error is 20-80MeV.

T_μ resolution is various bins of T_μ

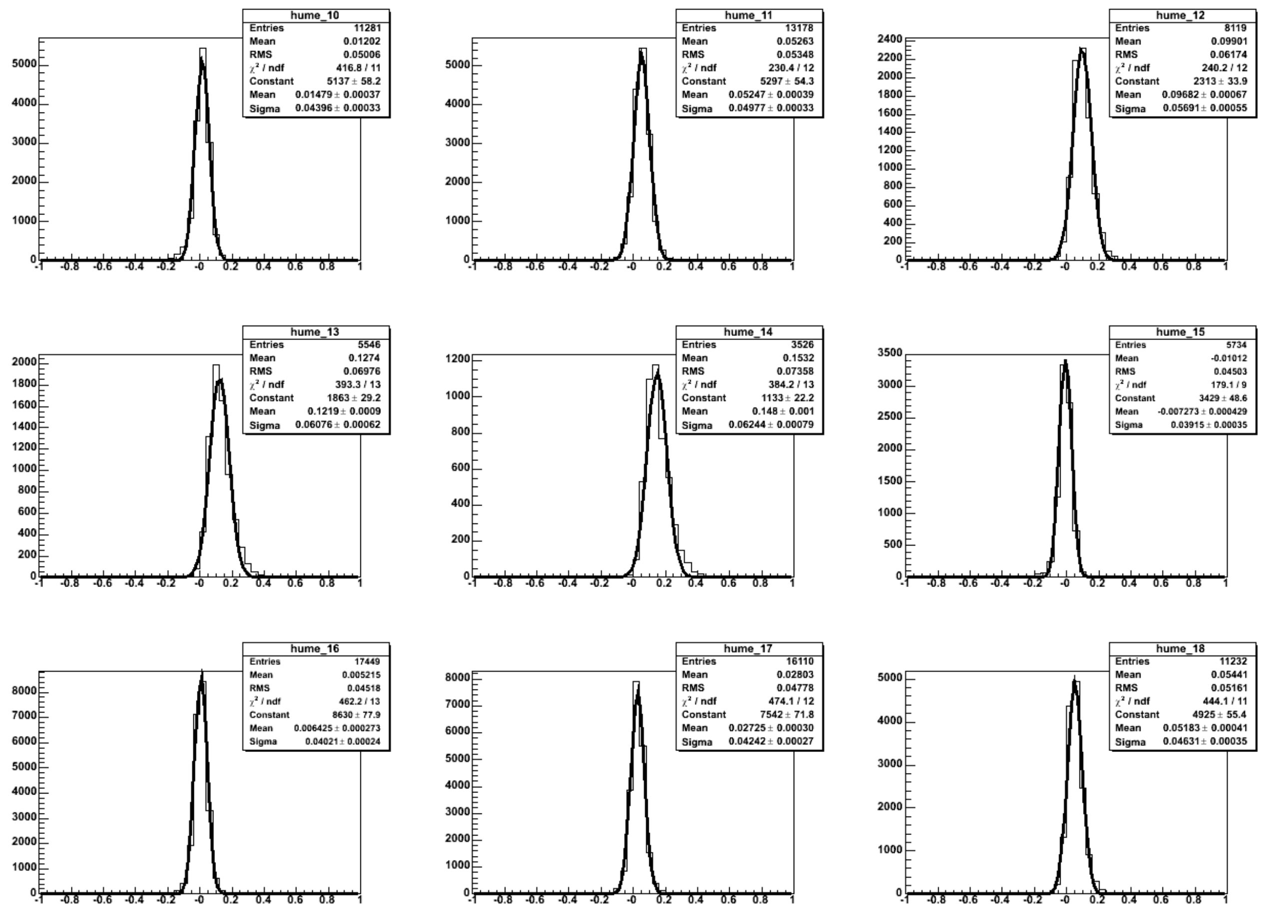

2. Energy scale of MiniBooNE

Range is the independent measure of muon energy. So range-T_μ difference for data and MC can be used to measure the possible mis-calibration.

This variable agrees in all energy regions within 1.5%.

Range - T_μ X 0.5+100

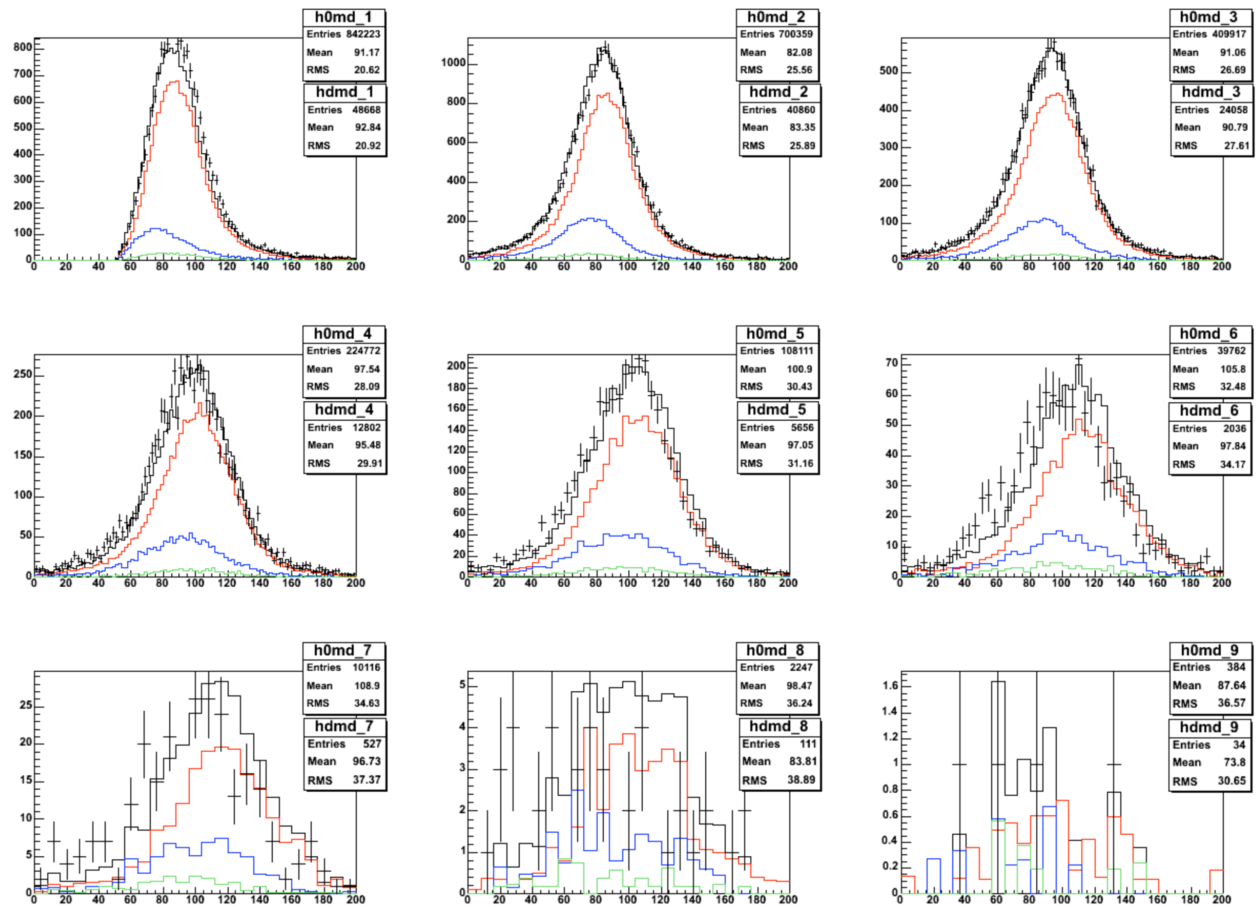

4. CCQE normalization fit

data-MC comparison, after CCQE normalization fit

After the CC1π correction, normalization of CCQE is also found from CCQE sample.

We use limited Q^2 region to find CCQE normalization, so that this fit is insensitive with CCQE shape very much.

Butkevich
arXiv:0904.1472

Now, CCQE normalization and CC1π normalization and CC1π shape looks good, except CCQE shape.

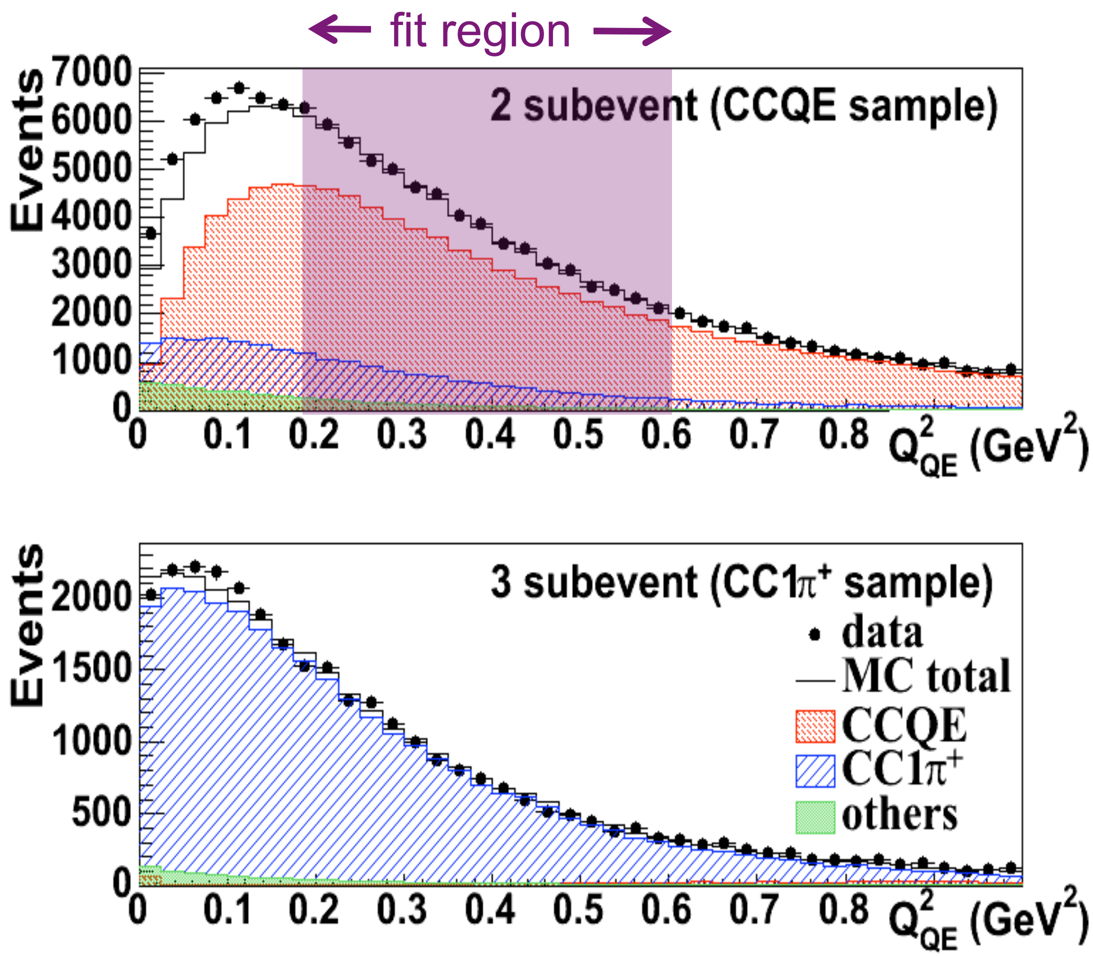

3. CC1π background constraint

This data driven MC tuning is based on 2 assumptions.

1. Kinematics measurement consistency between 2 and 3 subevent sample

Since 3 subevent has an additional particle (=pion), light profile is different. ~9% of events are misreconstructed to high Q^2 in 3 subevent, but majority of them are Q^2>0.5GeV^2, so they don't join the background subtraction.

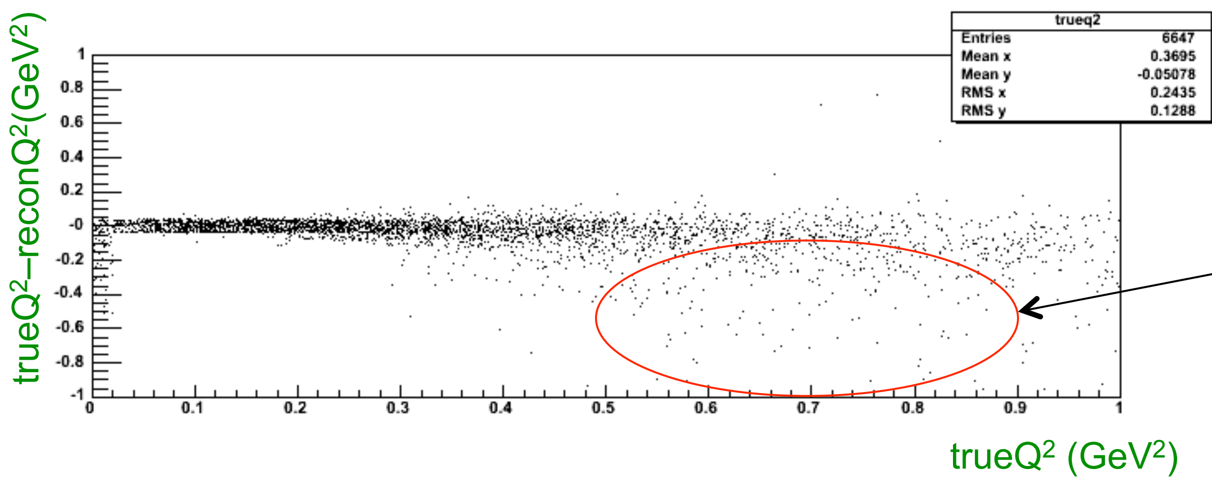

~9% of events are misreconstructed to high Q^2 (mostly >0.5GeV^2)

3. CC1π background constraint

This data driven MC tuning is based on 2 assumptions.

2. Pion absorption

The background subtraction is based on the assumption that our pion absorption model in the MC is right. To study this, we change the amount of pion absorption by a single number. Since pion absorption is the function of pion momentum, this is justified if pion momentum has week correlation with muon kinematics in CCπ event.

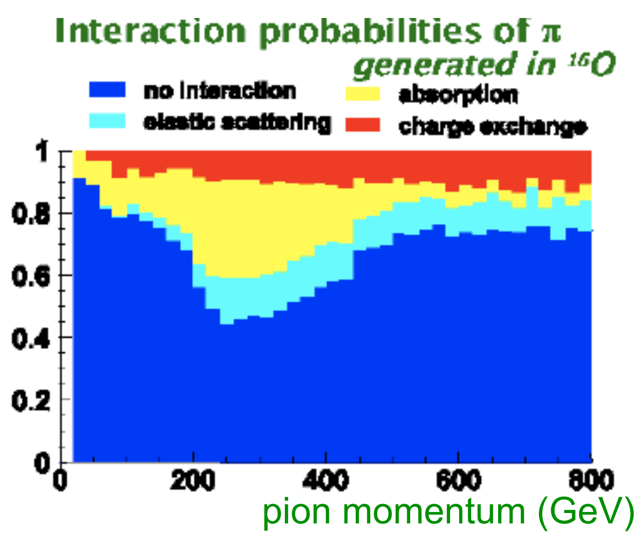

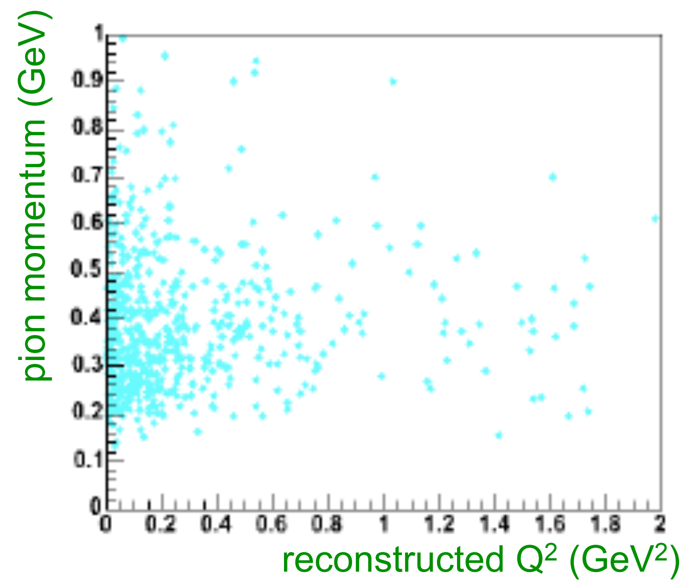

3. CC1π background constraint

This data driven MC tuning is based on 2 assumptions.

2. Pion absorption

The background subtraction is based on the assumption that our pion absorption model in the MC is right. To study this, we change the fraction of pion absorption.

Pion absorption is increased 0%, 15%, and 30%, meantime coherent fraction is decreased 0%, 50%, and 100%.

Any new xs models can provide good fit in 3 subevent sample in Q^2.

data-MC Q^2 ratio in 3 subevent

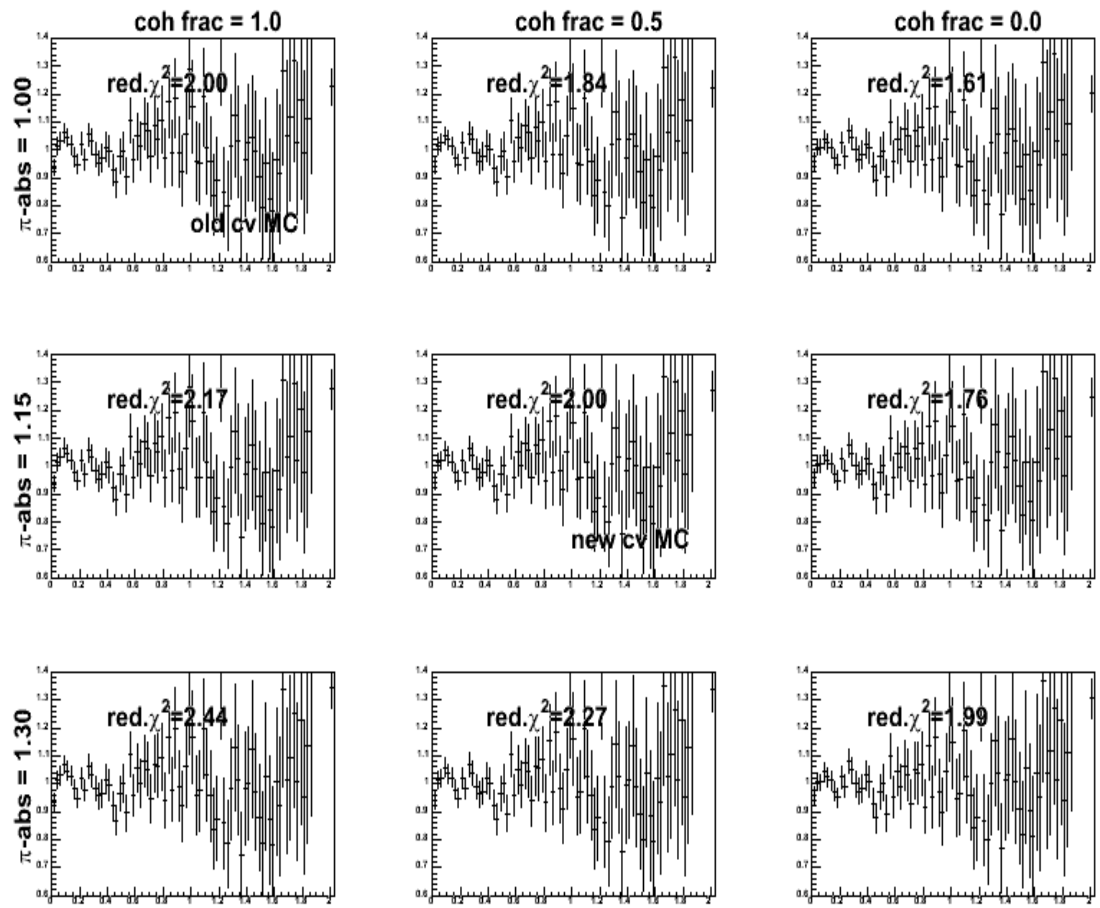

3. CC1π background constraint

This data driven MC tuning is based on 2 assumptions.

2. Pion absorption

However, we can differentiate xs models in T_μ-$\cos\theta_\mu$ plane.15% increase of piabs and 0% of coherent fraction gives the best fit.

We chose 15% for piabs, and 50% for cohfrac as new cv MC which will be used to estimate background from all kinematic distribution. This changes are well within our error (pion absorption 25%, charge exchange 30%). The rest of models go to make a new error matrix.

data-MC T_μ-$\cos\theta_\mu$ ratio in 3 subevent

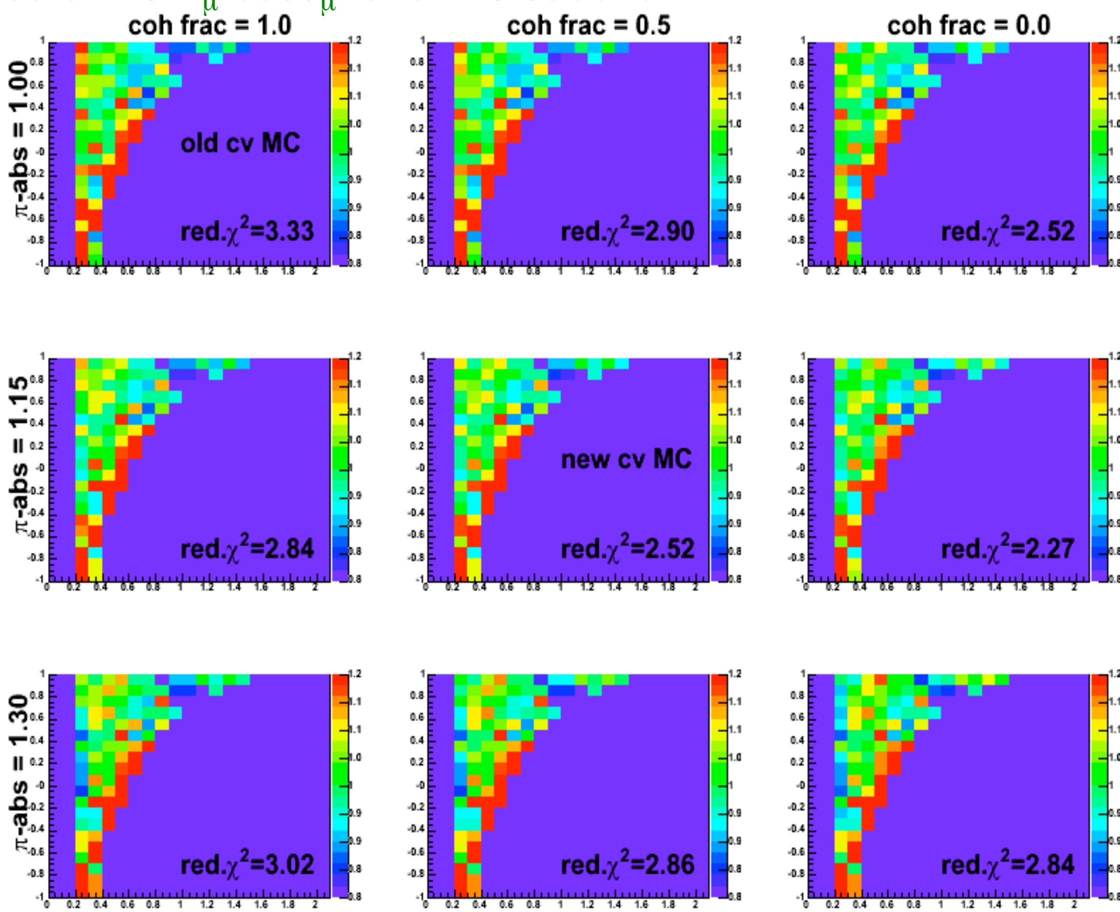

4. M_A-κ fit

Least χ^2 fit for Q^2 distribution

χ^2 = (data - MC)T $(M_{total})^{-1}$ (data - MC)

χ^2 minimum is found by global scan of shape only fit with $0.0<Q^2(GeV^2)<1.0$

Input error matrices

keep the correlation of systematics

dependent

independent

π+ production	(8 parameters)
π- production	(8 parameters)
K+ production	(7 parameters)
K0 production	(9 parameters)
beam model	(8 parameters)
cross section	(20 parameters)
detector model	(39 parameters)

The total output error matrix

keep the correlation of Q2 bins

M_{total} = M(π+ production)
+ M(π- production)
+ M(K+ production)
+ M(K0 production)
+ M(beam model)
+ M(cross section model)
+ M(detector model)
+ M(data statistics)

4. CCQE absolute cross section

Absolute flux-averaged differential cross section formula

i :true index
j : reconstructed index

The cross section is function of true value, for example, $d\sigma^2/T_\mu/\cos\theta_\mu$, $d\sigma/dQ^2_{QE}$, etc

Integrated flux is removed, so it is called flux-averaged cross section

- U_{ij} :unsmearing matrix
- d_j :data vector
- b_j :predicted background

$$\sigma_i = \frac{\sum_j U_{ij}(d_j - b_j)}{\varepsilon_i(\Phi T)}$$

- T :integrated target number
- ε_i :efficiency
- Φ :integrated ν-flux

4. CCQE absolute cross section

Absolute flux-unfolded total cross section formula

i :true index
j : reconstructed index

The cross section is function of true neutrino energy, $\sigma[E_\nu^{QE}]$

Flux shape is removed bin by bin, so it is called flux-unfolded cross section

U_{ij} :unsmearing matrix

d_j :data vector

$$\sigma_i = \frac{\sum_j U_{ij}(d_j - b_j)}{\varepsilon_i\,(\Phi T)}$$

b_j :predicted background

T :integrated target number

ε_i :efficiency

Φ_i :ν-flux vector

5. CCQE double differential cross section

Flux-averaged double differential cross section (T_μ-$\cos\theta$)

This is the most complete information about neutrino cross section based on muon kinematic measurement.

The error shown here is total error.

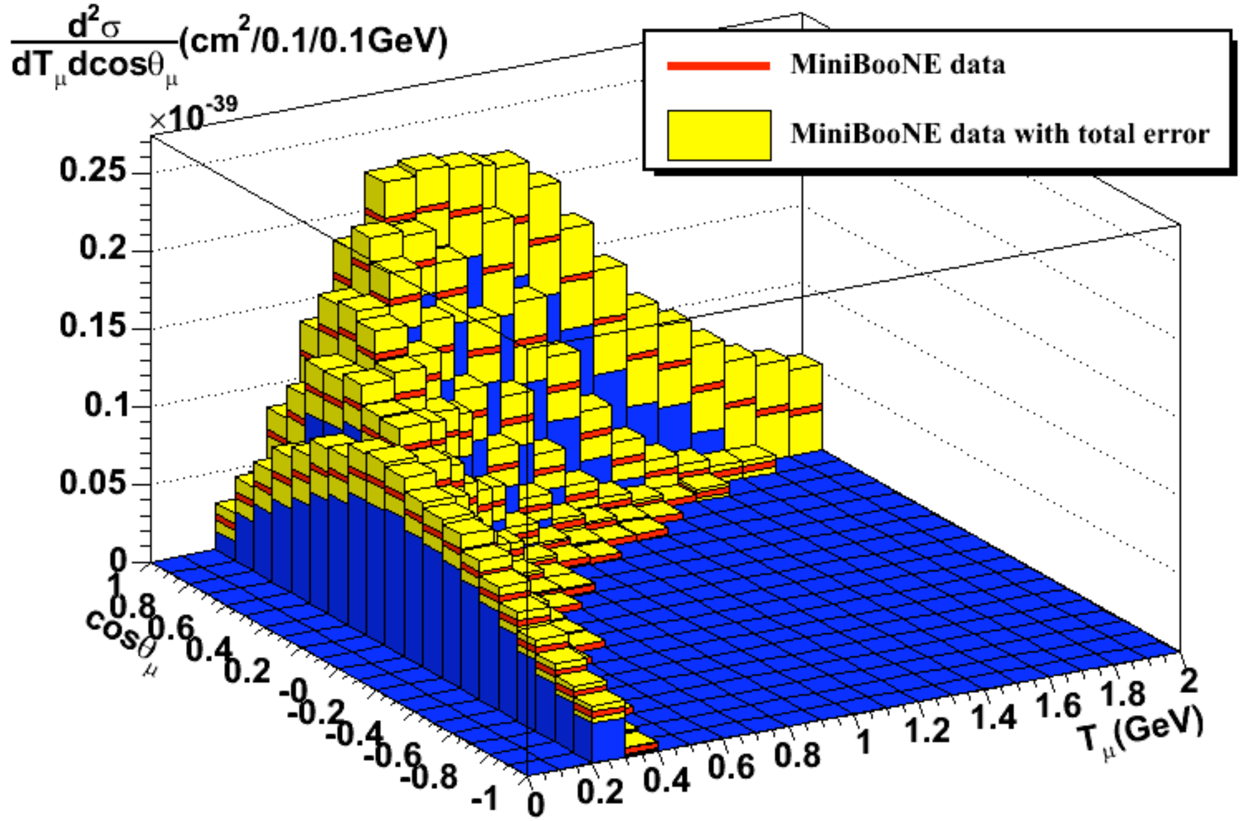

5. CCQE double differential cross section

Flux-averaged double differential cross section (T_μ-cosθ)

This is the most complete information about neutrino cross section based on muon kinematic measurement.

The error shown here is total error.

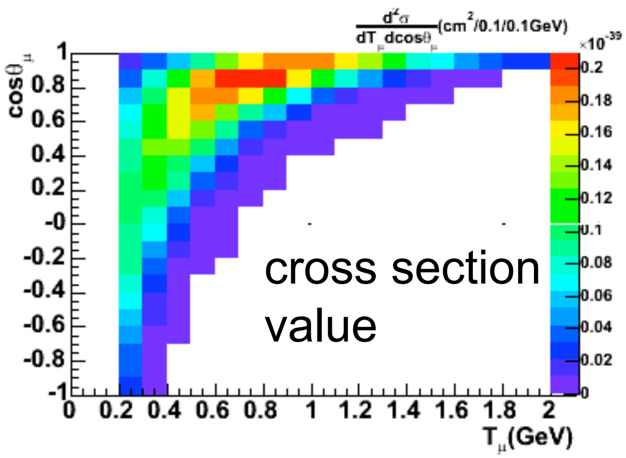

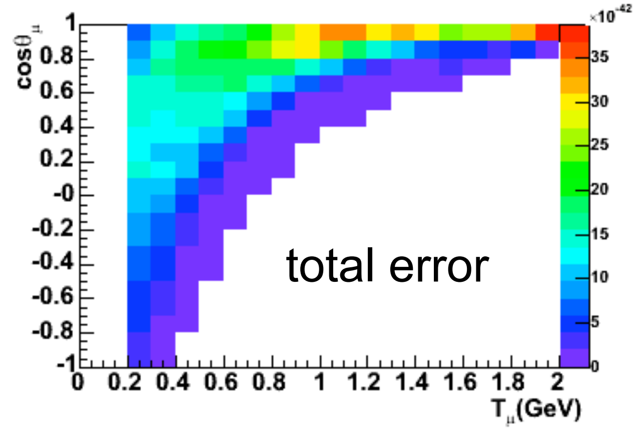

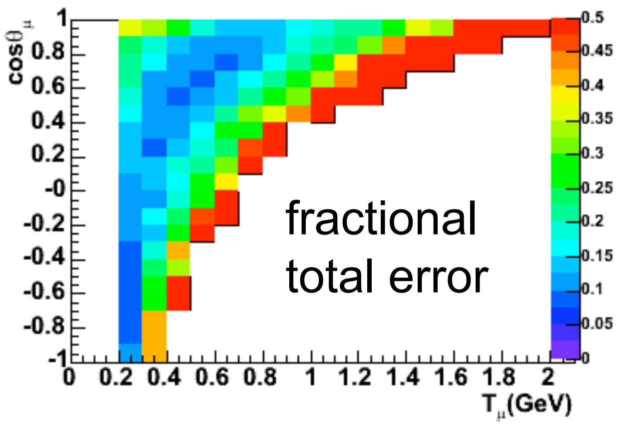

5. CCQE flux error

Flux error

The flux error dominates total normalization error.

The shape error is weak, except high energy region, where HARP measurement has large error and skin effect of horn has large error.

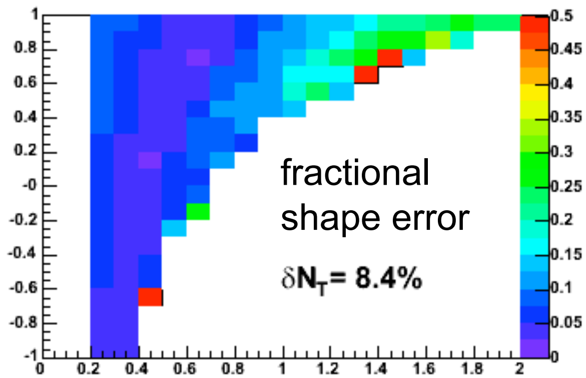

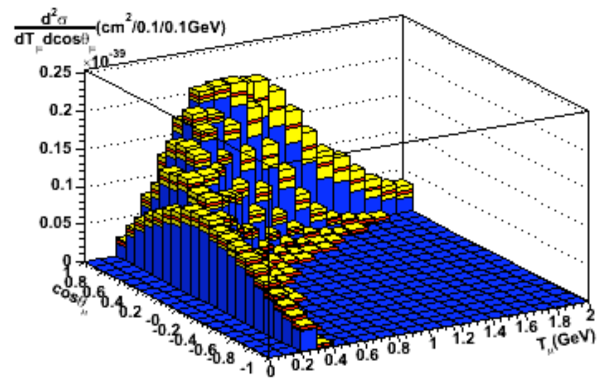

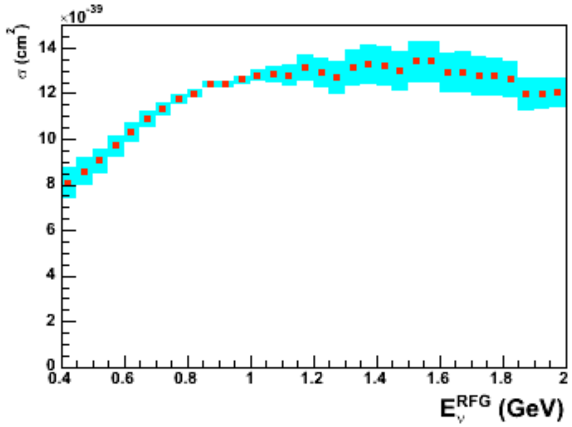

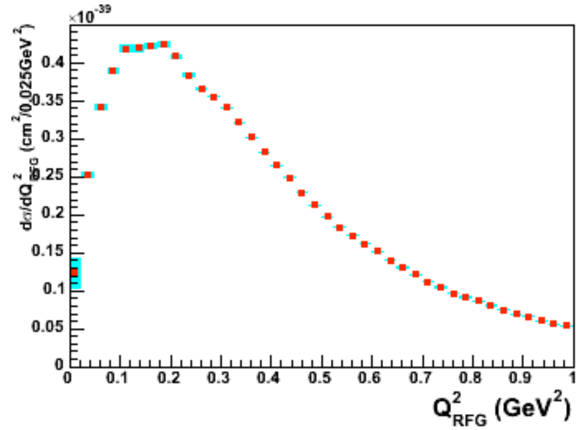

5. CCQE background cross section error

Background cross section error

The background cross section error is small, because of high purity and in situ background constraint.

The large error comes from pion absorption, so the kinematic space of CC1π events has large error

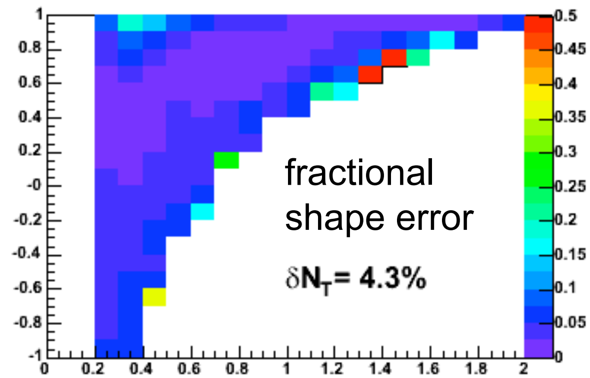

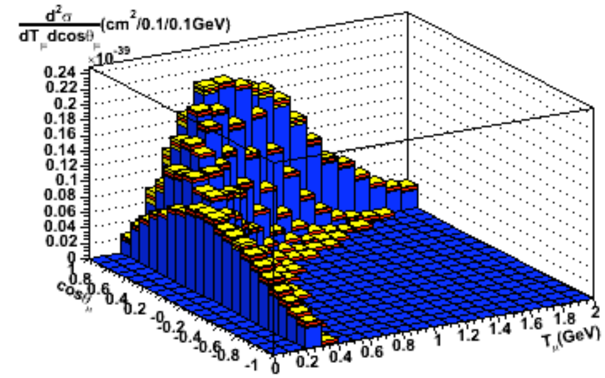

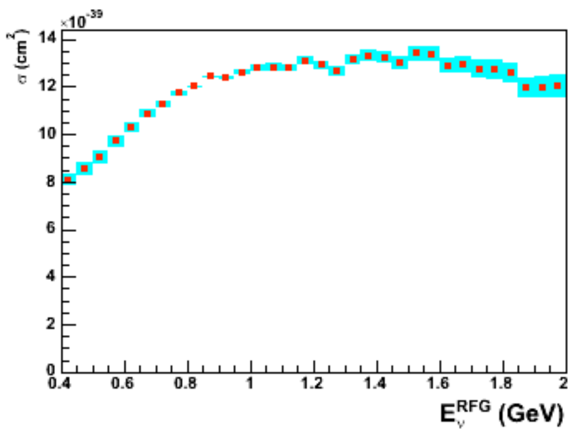

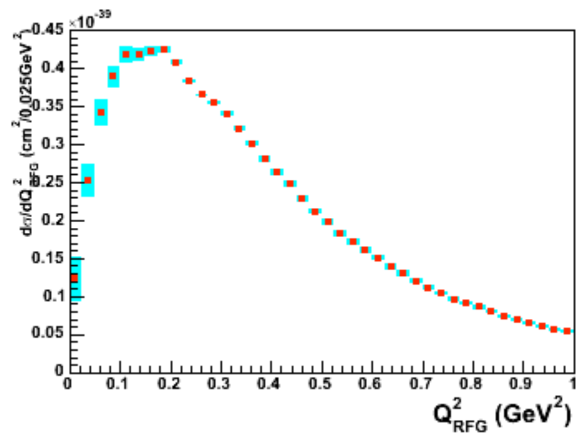

5. CCQE detector error

Detector error

The detector error has the largest contribution to the shape error because it is related with the energy scale of muon.

However the contribution to the total normalization error is not so large.

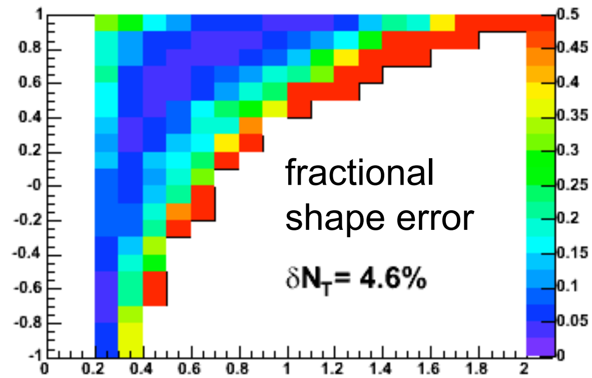

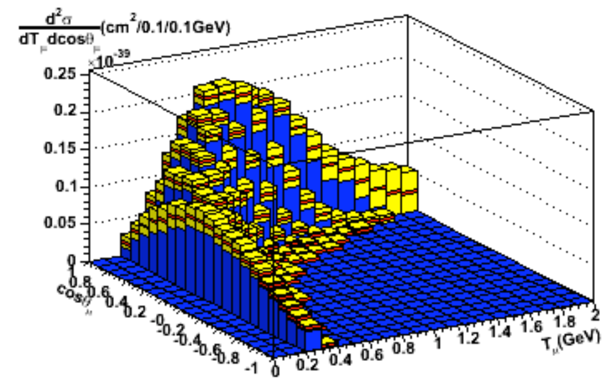

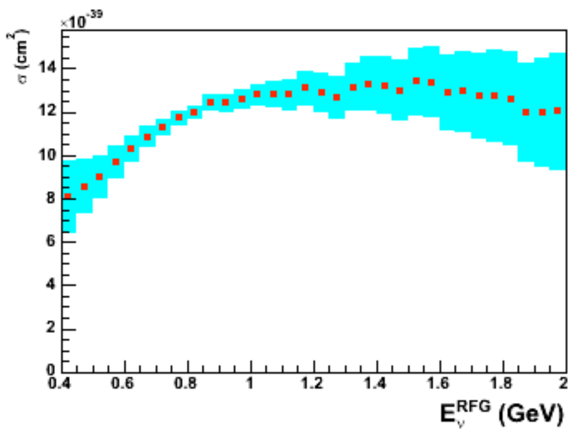

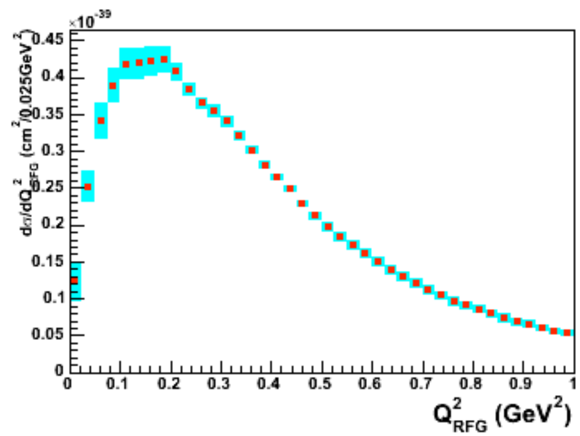

Jon Link, Nov. 18, 2005
Fermilab Wine & Cheese seminar

E 23, NUMBER 11 1 JUNE 1981

Quasielastic neutrino scattering: A measurement of the weak nucleon axial-vector form factor

N. J. Baker, A. M. Cnops,* P. L. Connolly, S. A. Kahn, H. G. Kirk, M. J. Murtagh, R. B. Palmer, N. P. Samios, and M. Tanaka
Brookhaven National Laboratory, Upton, New York 11973
(Received 12 February 1981)

Brookhaven AGS
7ft D_2 Bubble Chamber

The quasielastic reaction $\nu_\mu n \to \mu^- p$ was studied in an experiment using the BNL 7-foot deuterium bubble chamber exposed to the wide-band neutrino beam with an average energy of 1.6 GeV. A total of 1138 quasielastic events in the momentum-transfer range $Q^2 = 0.06-3.00$ (GeV/c)^2 were selected by kinematic fitting and particle identification and were used to extract the axial-vector form factor $F_A(Q^2)$ from the Q^2 distribution. In the framework of the conventional $V-A$ theory, we find that the dipole parametrization is favored over the monopole. The value of the axial-vector mass M_A in the dipole parametrization is 1.07 ± 0.06 GeV, which is in good agreement with both recent neutrino and electroproduction experiments. In addition, the standard assumptions of conserved vector current and no second-class currents are checked.

We have used a maximum likelihood method to extract M_A from the shape of the Q^2 distribution for each observed neutrino energy. This likelihood function $\mathcal{L}^I$ is independent of the shape of the neutrino spectrum ...

They didn't even try to determine their ν flux from pion production and beam dynamics.

Phys. Rev. D **25**, 617 (1982)

The distribution of events in neutrino energy for the 3C $\nu d \to \mu^- p p_s$ events is shown in Fig. 4 together with the quasielastic cross section $\sigma(\nu n \to \mu^- p)$ calculated using the standard $V-A$ theory with $M_A = 1.05 \pm 0.05$ GeV and $M_V = 0.84$ GeV. The absolute cross sections for the CC interactions have been measured using the quasielastic events and its known cross section.[4]

In subsequent cross section analyses the theoretical ("known") quas-ielastic cross section and observed quasi-elastic events were used to determine the flux.

Jon Link, Nov. 18, 2005
Fermilab Wine & Cheese seminar

Fermilab
15ft D_2 Bubble Chamber

REVIEW LETTERS 12 JULY 1982

Neutrino Flux and Total Charged-Current Cross Sections in High-Energy Neutrino-Deuterium Interactions

T. Kitagaki, S. Tanaka, H. Yuta, K. Abe, K. Hasegawa, A. Yamaguchi, K. Tamai, T. Hayashino, Y. Ohtani, and H. Hayano
Tohoku University, Sendai 980, Japan

To obtain the total cross section from the number of events, the neutrino flux has to be measured on an absolute scale. In this analysis, we determine the neutrino flux using 362 quasielastic events identified in our data[10] and the cross section for reaction (2) derived from the $V-A$ theory.

Again, they use QE events and theoretical cross section to calculate the ν.

When they try to get the flux from meson (π and K) production and decay kinematics they fail miserably for E_ν<30 GeV.

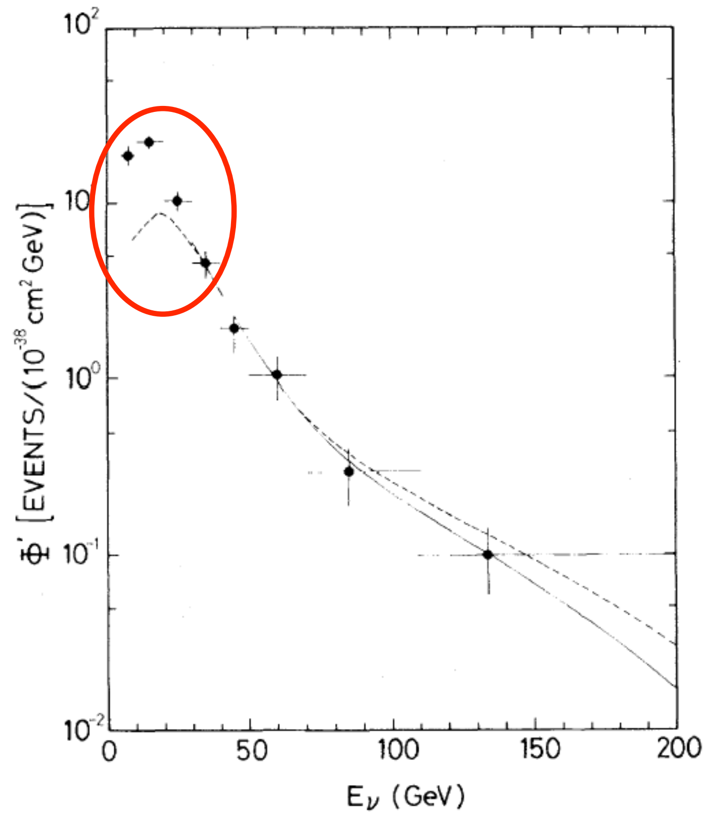

FIG. 2. Neutrino flux distribution obtained from the quasielastic events and the predicted cross section with M_A = 1.05 GeV. The solid curve is obtained from the best fit to the flux data for E_ν > 30 GeV. The dashed curve is taken from the Monte Carlo simulation of the flux.

Jon Link, Nov. 18, 2005
Fermilab Wine & Cheese seminar

ME 34, NUMBER 1 1 JULY 1986

Determination of the neutrino fluxes in the Brookhaven wide-band beams

L. A. Ahrens, S. H. Aronson, P. L. Connolly,* B. G. Gibbard, M. J. Murtagh, S. J. Murtagh,†
S. Terada, and D. H. White
Physics Department, Brookhaven National Laboratory, Upton, New York 11973

Brookhaven AGS
Liquid Scintillator

The beam calculations described here were based on the Grote, Hagedorn, and Ranft (GHR) (Ref. 11) parametrization; that of Sanford and Wang was used for comparison. An estimate was made of pion production by reinteracting protons guided by the shape of the observed ν_μ spectrum and the observed angular distribution of muons from quasielastic events. The procedure is described[12] in the Appendix.

The Procedure

- Pion production cross sections in some low momentum bins are scaled up by 18 to 79%.
- The K^+ to π^+ ratio is increased by 25%.
- Overall neutrino (anti-neutrino) flux is increased by 10% (30%).

All driven by the neutrino events observed in the detector!

Jon Link, Nov. 18, 2005
Fermilab Wine & Cheese seminar

16, NUMBER 11 1 DECEMBER 1977

Study of neutrino interactions in hydrogen and deuterium: Description of the experiment and study of the reaction $\nu + d \rightarrow \mu^- + p + p_s$†

S. J. Barish,* J. Campbell,‡ G. Charlton,§ Y. Cho, M. Derrick, R. Engelmann,‖ L. G. Hyman, D. Jankowski, A. Mann,¶ B. Musgrave, P. Schreiner, P. F. Schultz, R. Singer, M. Szczekowski,** T. Wangler, and H. Yuta††
Argonne National Laboratory, Argonne, Illinois 60439

Argonne ZGS
12ft D_2 Bubble Chamber

Flux derived from pion production data. Were able to test assumptions about the form of the cross section using absolute rate and shape information.

TABLE IV. Results of axial-form-factor fits.

Likelihood function	M_A^{Dipole} (GeV)	M_A^{Monopole} (GeV)	M_A^{Tripole} (GeV)
Rate	$0.75^{+0.13}_{-0.11}$	$0.45^{+0.11}_{-0.07}$	$0.96^{+0.17}_{-0.14}$
Shape	1.010 ± 0.09	0.56 ± 0.08	1.32 ± 0.11
Rate and shape	0.95 ± 0.09	0.52 ± 0.08	1.25 ± 0.11
Flux independent	0.95 ± 0.09	0.53 ± 0.08	1.25 ± 0.11

- Pion production measured in ZGS beams were used in this analysis
- A very careful job was done to normalize the beam.
- Yet they have a 25% inconsistency between the axial mass they measure considering only rate information verses considering only spectral information.

Interpretation: Their normalization is wrong.